Hydraulic Resistance of Biofilms

in Membrane Filtration Systems

Claudia Dreszer

Cover image:
Scanning electron micrograph showing the cross-section of a membrane (bottom) and biofilm (top) on the membrane surface (10000 x magnification).

Design and lay-out: Ubel Smid Vormgeving, Roden, the Netherlands.
Printing: GVO drukkers & vormgevers BV, Ponsen & Looijen, Ede, the Netherlands.

Dreszer, C., 2014
Hydraulic Resistance of Biofilms in Membrane Filtration Systems
ISBN: 978-90-6464-793-2

PhD thesis Wetsus centre of excellence for sustainable water technology in cooperation with University Duisburg-Essen, Essen, Germany - with references - with summary in English and German

Hydraulic Resistance of Biofilms

in Membrane Filtration Systems

Dissertation

zur Erlangung des akademischen Grades eines
Doktors der Naturwissenschaften
– Dr. rer. nat. –

vorgelegt von

Claudia Dreszer

geboren in Bochum

Biofilm Centre
der
Universität Duisburg-Essen
In Kooperation mit
Wetsus centre of excellence for sustainable water technology, The Netherlands

2014

Die vorliegende Arbeit wurde im Zeitraum von April 2009 bis Oktober 2013 im Arbeitskreis von Prof. Dr. Hans-Curt Flemming am Biofilm Centre der Universität Duisburg-Essen und Wetsus centre of excellence for sustainable water technology durchgeführt.

Tag der Disputation: 03.09.2014

Gutachter:	Prof. Dr. Hans-Curt Flemming
	Prof. Dr. Johannes Simon Vrouwenvelder
Vorsitzender:	Prof. Dr. Thomas Schrader

'When someone makes a decision, he is really diving into a strong current that will carry him to places he had never dreamed of when he first made the decision.'

Paulo Coelho

Für Oma und Mama

Abstract

The demand for drinking water in the world is increasing and water quality regulations become more stringent. High quality water can be produced with membrane filtration processes such as nanofiltration and reverse osmosis systems. A serious limitation in the application of these membrane processes for water treatment is biofouling. Biofouling occurs when the growth of biofilms negatively impacts membrane performance parameters like feed channel pressure drop and transmembrane pressure drop leading to a reduced water production (permeate flux). Biofouling increases the costs of plant operation strongly, and may even be prohibitive for the application of membrane filtration in water treatment. A biofilm acts like a secondary membrane on top of the filtration membrane adding an additional hydraulic resistance to the filtration system requiring an increase in transmembrane pressure to keep the production rate constant. Biofilms also lower the crossflow velocity inside a membrane module due to a high friction resistance. In order to maintain a steady transport of water throughout the whole filtration system higher feed pressures have to be applied. An increase in pressure always increases the operational costs. Concentration polarization, the accumulation of a solute at the membrane surface which is caused by the solute rejection of the membrane, can be influenced by the presence of biofilms as well. The lack of crossflow inside the biofilm enhances the accumulation of salts which leads to concentration polarization and decreases the performance. Regarding the importance of biofilms it is surprising that at the start of this PhD study, no data was available on the intrinsic hydraulic resistance of biofilms and its impact on membrane performance.

The main objective of this thesis was to determine the hydraulic resistance of biofilms and how it was affected by (operational) parameters such as permeate flux, crossflow velocity, biodegradable substrate content, and feed spacer presence.

A monitor was developed to assess the (i) hydraulic biofilm resistance and (ii) performance parameters feed channel pressure drop and transmembrane pressure drop (Chapter 2). By using a microfiltration membrane (pore size 0.05 µm) salt concentration polarization was avoided, allowing operation at low pressures enabling accurate measurement of the hydraulic biofilm resistance. Extensive validation tests showed that the small-sized monitor is a suitable tool to study the hydraulic biofilm resistance under controlled conditions.

With the developed monitor system studies were performed at two fluxes (20 and 100 L m^{-2} h^{-1}) and constant crossflow velocity (0.1 m s^{-1}) (Chapter 3). The biofilm resistance reached values up to 50×10^{12} m^{-1} at a flux of 20 L m^{-2} h^{-1}. An increased permeate flux (rate of water production) caused a higher resistance. The resistance was not caused by bacterial cells but by the extracellular polymeric substances (EPS) matrix. The biofilm resistance was (i) high compared to the resistance of the employed microfiltration membrane but (ii) low compared to the resistance of nanofiltration (20%) and reverse osmosis (2%) membranes. Nevertheless, biofouling is an important topic for nanofiltration and reverse osmosis membrane systems due to biofilm enhanced concentration polarization. The presence of a biofilm on the membrane surface enhances the accumulation of salts which requires increased pressure operation or causes a decreased water production rate.

Biofilm accumulation, transmembrane (biofilm) resistance and feed-channel pressure drop were studied as a function of crossflow velocity (0.05 and 0.20 m s^{-1}) and feed spacer presence at a permeate flux of 20 L m^{-2} h^{-1} (Chapter 4). As biodegradable nutrient, acetate was dosed to the feed water (0.25 and 1.0 mg L^{-1} carbon) to enhance biofilm accumulation in the monitors. This study showed that biofilm formation in membrane systems increased both the feed-channel and transmembrane pressure drop. The hydraulic biofilm resistance was increased by a (i) high biodegradable substrate load, (ii) high crossflow velocity, and (iii) feed spacer presence. Current membrane practice (high crossflow velocity and feed spacer presence) increased the impact of biofouling on membrane performance.

The results obtained by the studies described in this thesis are discussed in Chapter 5 and suggestions for future research are given. Nutrient limitation, low flux operation, and low crossflow velocity delay the transformation from biofilm into biofouling. Concentration polarization may be increased by a lower crossflow velocity but reduced by a lower permeate flux. The nutrient load in the membrane system will be reduced by the application of low crossflow velocities. Biofouling prohibition by nutrient limitation is nothing new but still one of the most effective ways to slow down the problem. The impact of modified operation conditions and design (e.g. spacers, membrane module) on membrane performance, cleanability, and concentration polarization in full scale membrane systems should be part of future biofouling research.

Zusammenfassung

Die weltweit steigende Nachfrage nach Trinkwasser geht mit immer strengeren Anforderungen an die Trinkwasserqualität einher. Membranfiltrationsprozesse (z.b. Nanofiltration und Umkehrosmose) bieten eine Möglichkeit, den strengen Anforderungen gerecht zu werden. Durch das Auftreten von Biofouling können membrangestützte Trinkwasseraufbereitungssysteme eine erhebliche Einschränkung ihrer Produktivität erfahren. Biofouling tritt ein, wenn das Biofilmwachstum auf der Membranoberfläche einen Toleranzwert überschreitet. Dies beeinflusst die Förderkanaldruckdifferenz und die transmembrane Druckdifferenz negativ, wodurch die Wasserproduktion (Permeatfluss) verringert wird. Dies erhöht die Betriebskosten der Membranfiltrationsanlage immens und kann die Wasseraufbereitung mit Membranfiltration unter wirtschaftlichen aspekten untragbar machen. In Membranfiltrationsanlagen verhalten sich Biofilme wie eine zusätzliche Membran und fügen einen weiteren hydraulischen Widerstand zu dem der Membran hinzu. Um die Wasserproduktionsrate dennoch konstant zu halten, muss die transmembrane Druckdifferenz erhöht werden. Aufgrund ihres hohen Reibungswiderstands verringern Biofilme die Querstromgeschwindigkeit in der Filtrationseinheit. Um dem entgegen zu wirken, muss der Wasserdruck am Eingang der Filtrationseinheit erhöht werden. Eine Druckerhöhung im Membranfiltrationssystem geht immer mit einer Erhöhung der Betriebskosten einher. Biofilme können auch Auswirkungen auf die Konzentrationspolarisation in einer Membranfiltrationsanlage haben. Konzentrationspolarisation ist die Anreichung von gelösten Substanzen auf der Membranoberfläche, welche durch die Membran zurückgehalten werden. Durch den fehlenden Querstromfluss innerhalb eines Biofilms wird die Akkumulation von Salzen begünstigt und damit die Konzentrationspolarisation verstärkt, was einen negativen Einfluss auf die Filtrationsleistung hat. Hinsichtlich der großen Bedeutung, die Biofilme für die Membranfiltration haben, war es überraschend, dass zu Beginn dieser Arbeit keine Daten über den hydraulischen Widerstand von Biofilmen und deren Einfluss auf die Membranleistung verfügbar waren.

Das Ziel dieser Arbeit war die Bestimmung des hydraulischen Widerstandes von Biofilmen und die Untersuchung, wie diese von Permeatfluss, Durchflussgeschwindigkeit, Nährstoffangebot und Feed Spacer beeinflusst werden.

Um den hydraulischen Widerstand von Biofilmen, die Förderkanaldruckdifferenz und die transmembrane Druckdifferenz zu messen, wurde ein kleinformatiges Membranfiltrationssystem entwickelt (Kapitel 2). Die Verwendung einer Mikrofiltrationsmembran (Porengröße 0,05 µm) verhinderte die Konzentrationspolarisation von Salzen an der Membranoberfläche, wodurch der Betrieb bei niedrigem Druck sowie die exakte Messung des hydraulischen Widerstandes der Biofilme ermöglicht wurde. Eine umfangreiche Validierung des Systems zeigte, dass dieses Filtrationssystem geeignet ist, den hydraulischen Widerstand von Biofilmen unter kontrollierten Bedingungen zu untersuchen.

Die Untersuchungen in dem oben beschriebenen System wurden bei zwei Permeatflussgeschwindigkeiten (20 und 100 L m^{-2} h^{-1}) und einer konstanten Querstromgeschwindigkeit (0.1 m s^{-1}) durchgeführt (Kapitel 3). Der hydraulische Widerstand der Biofilme erreichte Werte von bis zu 50×10^{12} m^{-1}, bei einem Permeatfluss von 20 L m^{-2} h^{-1}. Ein höherer Permeatfluss hatte einen vergrößerten Biofilmwiderstand zur Folge. Der Widerstand wurde nicht durch Bakterienzellen, sondern durch extrazelluläre polymere Substanzen (EPS) verursacht. Der Biofilmwiderstand war hoch im Vergleich zu dem Widerstand der verwendeten Mikrofiltrationsmembran, jedoch niedrig im Vergleich zu dem Widerstand von Nanofiltrations- (20%) und Umkehrosmosemembranen (2%). Dennoch spielt Biofouling aufgrund einer durch Biofilme verstärkten Konzentrationspolarisation, für Nanofiltration und Umkehrosmose eine große Rolle. Ein Biofilm auf der Membranoberfläche begünstigt die Akkumulation von Salzen, was wiederum die Filtrationsleistung beeinträchtigt.

Bei einem konstanten Permeatfluss von 20 L m^{-2} h^{-1} wurden die Biofilmakkumulation, der transmembrane (Biofilm-) Widerstand und die Förderkanaldruckdifferenz in Abhängigkeit von der Querstromgeschwindigkeit (0.05 und 0.20 m s^{-1}) und dem Einsatz von Feed Spacern untersucht (Kapitel 4). Durch die Zugabe von Azetat als biologisch abbaubaren Nährstoff im Zuflusswasser (0.25 und 1.0 mg L^{-1} Kohlenstoff) konnte eine beschleunigte Biofilmakkumulation erreicht werden. Die Untersuchungen zeigten, dass die Entstehung von Biofilmen in Membransystemen sowohl die Förderkanaldruckdifferenz als auch die transmembrane Druckdifferenz ansteigen lässt. Der hydraulische Widerstand des Biofilms stieg durch (i) erhöhtes Nährstoffangebot, (ii) erhöhte Querstromgeschwindigkeit und (iii) die Verwendung eines Feed Spacers. Die häufig in der Praxis angewendeten Produktionsparameter

in Membranfiltrationsanlagen (hohe Querstromgeschwindigkeiten und Feed Spacer Anwendung) verstärken die Auswirkungen von Biofouling auf die Membraneffizienz.

Die Ergebnisse dieser Arbeit sowie mögliche zukünftige Forschungsansätze für Biofouling-Untersuchungen werden in Kapitel 5 diskutiert. Die Transformation von Biofilmen zu einem Biofouling Problem kann durch die Senkung des Nährstoffgehalts im Zuflusswasser, einen niedrigen Permaetfluss und eine niedrige Querstromgeschwindigkeit hinausgezögert werden. Die Konzentrationspolarisation könnte einerseits durch eine niedrigere Querstromgeschwindigkeit erhöht, andererseits durch einen niedrigeren Permeatfluss wieder verringert werden. Der Nährstoffgehalt innerhalb der Filtrationseinheit wird jedoch durch eine niedrige Querstromgeschwindigkeit verringert. Biofouling-Hemmung durch Reduzierung der Nährstoffe ist keine neue Erfindung, aber dennoch eine der effektivsten Lösungen des Biofouling-Problems. Zukünftige Studien sollten sich mit den Auswirkungen von modifizierten Betriebsparametern und angepassten Feed Spacern auf die Effizienz der Membransysteme, die Konzentrationspolarisation und die nötige Reinigungsfrequenz beschäftigen. Eine Anwendung und Erforschung in „real life" Umgebungen wäre wünschenswert.

Contents

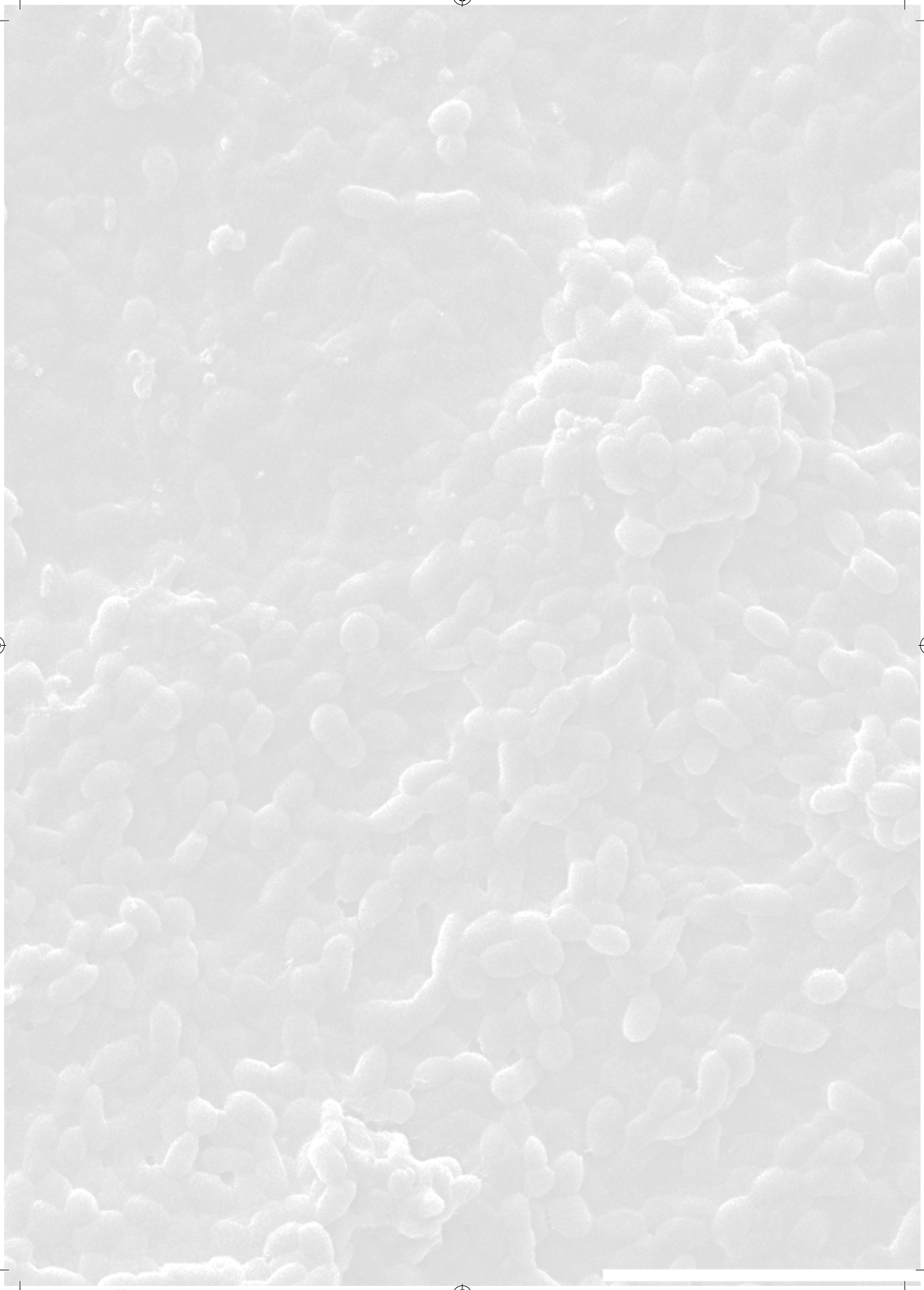

Chapter 1

Introduction

1.1 Freshwater scarcity

Today, around 700 million people in 42 countries suffer from water scarcity (United Nations, 2013). Projections show that this number will increase and even industrialized nations such as Australia will be threatened (Figure 1.1). Even Europe is not exempt from this problem since Spain suffered from fresh water shortage not long ago (Martin-Rosales et al., 2007). It is projected that 1.8 billion people will be living in absolute water scarcity conditions by 2025 and almost half of the world's population will be living in high water stress conditions by 2030 (United Nations, 2013). Absolute scarcity is defined as: annual water supply below 500 m^3 per person. Water stress is defined as: annual water supply below 1700 m^3 per person. More than 97% of the global water resources is salt water, less than 3% is fresh water. Almost 70% of this fresh water is present as glaciers and permanent snow and therefore not available for usage (UNESCO & WWAP, 2006) (Figure 1.2).

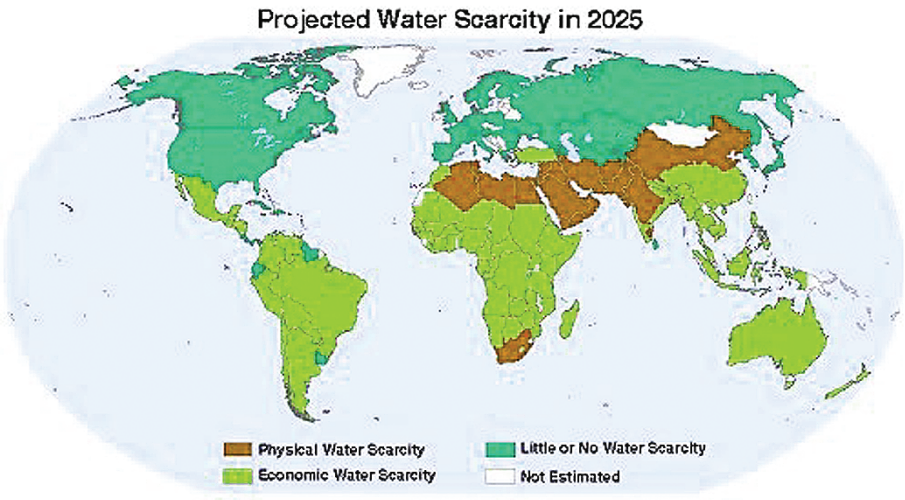

Figure 1.1: Projected water scarcity in 2025, showing areas for physical and economic water scarcity (International Water Management Institute, 2000).

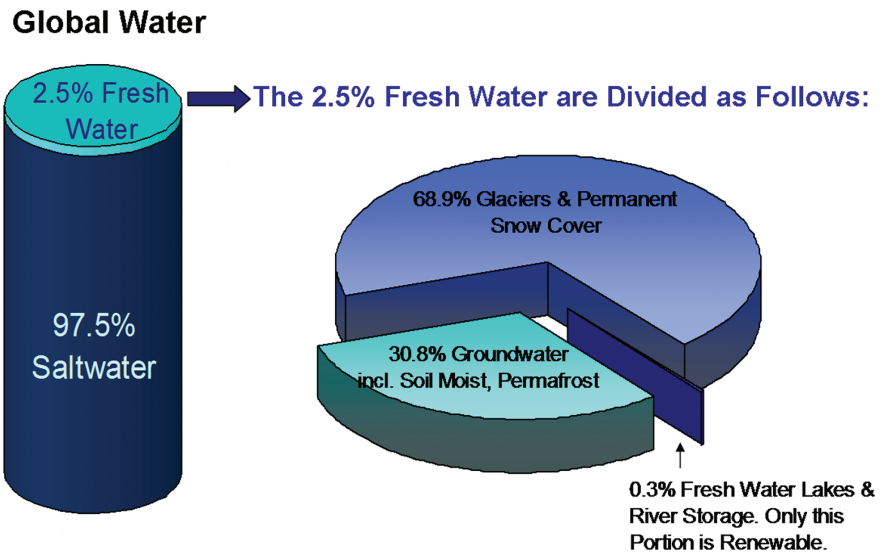

Figure 1.2: Global water resource. Fresh water has a global volume of 35.2 million km^3 only (data taken from Shiklomanov, 2000).

The fresh water is unevenly distributed, depending on geographical regions and season. The lack of access to clean, fresh water is not the only problem. An additional problem is the lack of a good sanitation. While 1.1 billion people don't have access to safe drinking water, around 2.4 billion people don't have access to proper sanitation (World Health Organization, 2013). Water born diseases caused the death of 2 million people and episodes of illness of 4 billion people in 2011 (World Health Organization, 2012).The problem is expected to get stronger due to the increasing world population and environmental pollution (United Nations, 2013).

Membrane filtration processes are employed to meet drinking water demand as well as water regulations. They can be applied to provide safe drinking water from various water sources such as groundwater, surface water and sea water. Because a broad variety of priority compounds are removed by membrane filtration, all types of contaminated water sources as well as waste water can be treated, producing safe fresh water.

However membrane filtration also has its limitations as well, the largest drawback being membrane fouling. From the different fouling types, biofouling causes the most serious problems.
In the introduction of this thesis a short overview on membrane technologies is given. Spiral wound membrane systems and the four membrane fouling types are introduced with special attention to biofilm formation and biofouling. In the last paragraph of the introduction the scope and outline of the thesis is addressed.

1.2 Membrane filtration

1.2.1 Membrane technology

In membrane filtration a driving force across the membrane is used to separate water from various substances in water. Microfiltration, ultrafiltration, nanofiltration, and reverse osmosis are pressure driven membrane processes. For microfiltration and ultrafiltration, pressures below 7 bar are commonly applied, while for nanofiltration and reverse osmosis a pressure of up to 70 bar is required. A commonly applied pressure range for reverse osmosis is 50 to 60 bar (Baker, 2012a). Semi-permeable membranes act as a selective physical barrier, allowing water and certain solutes to pass; depending on the feed water characteristics, membrane pore-size, plant design and operational conditions. Microfiltration causes the lowest rejection of solutes whilst by reverse osmosis the highest rejection is achieved (Figure 1.3).

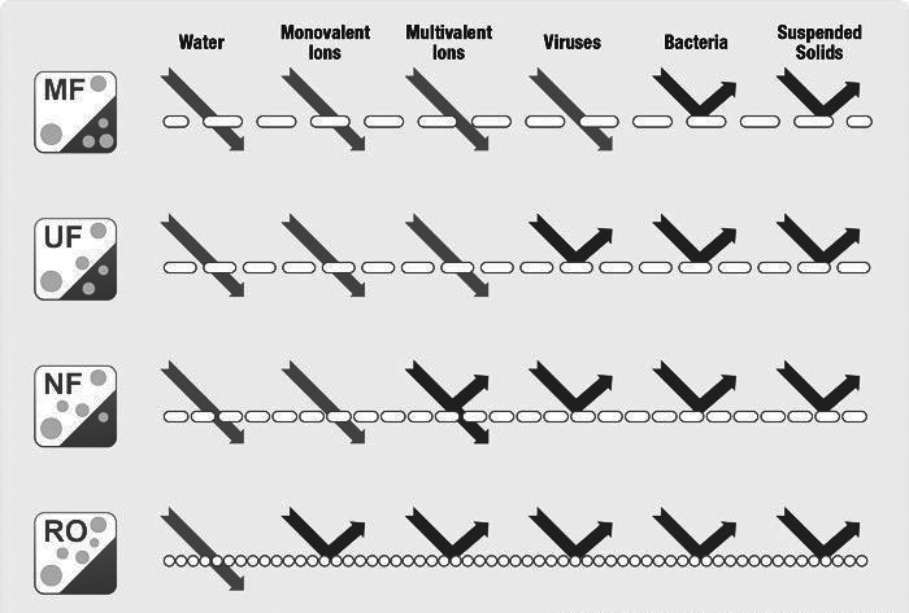

Figure 1.3: Rejection capabilities of MF (microfiltration), UF (ultrafiltration), NF (nanofiltration), and RO (reverse osmosis) membranes (Koch Membrane Systems, 2013a).

The two basic membrane filtration principles are dead-end and crossflow filtration (Figure 1.4). In dead-end filtration the feed water passes a semi-permeable membrane while the rejected material accumulates on the membrane surface. Dead-end filtration is commonly applied for micro- and ultrafiltration processes (Koch Membrane Systems, 2013b). One of the drawbacks of dead-end filtration is the built up of a filter cake at the membrane surface. To reduce concentration polarization on the membrane surface, crossflow filtration can be applied. In crossflow filtration the feed is separated into two streams: permeate and concentrate. The permeate contains solutes passing the membrane, while the concentrate contains solutes and particles rejected by the membrane (Amjad, 1993; Mallevialle et al., 1996). Membrane systems are operated at constant flux or at constant transmembrane pressure. The flux is defined as the water flow through a membrane area in a certain time. The transmembrane pressure is defined as the pressure difference between the feed and permeate side of the membrane. The transmembrane pressure is the driving force for the filtration process (Figure 1.5). Membrane systems operated at constant flux show an increase of transmembrane pressure over time. In order to maintain a constant flux at an

increasing transmembrane pressure, it is necessary to compensate the resistance of the accumulated material on the membrane by increasing the feed pressure. Systems operated at constant transmembrane pressure show a flux decrease over time, due to the accumulation of solutes and particles on the membrane.

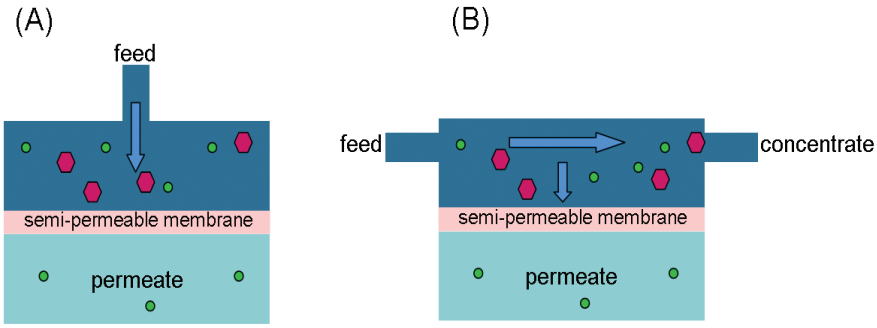

Figure 1.4: The concept of dead-end (A) and crossflow filtration (B).

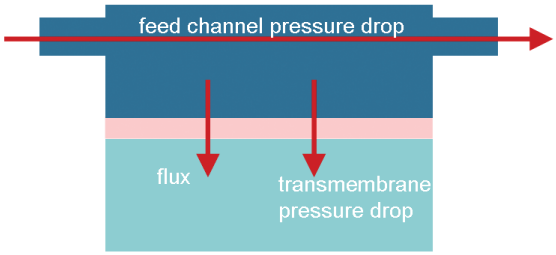

Figure 1.5: feed channel and transmembrane pressure drop and permeate flux in a crossflow filtration system.

1.2.2 Spiral wound membrane modules

Nanofiltration and reverse osmosis membranes are commonly applied in spiral wound modules in which membrane sheets are wrapped along a perforated central tube for permeate collection (Figure 1.6). The membrane sheets are present as envelopes in which two flat membrane sheets are glued together at three sides of the sheets, the remaining fourth side is connected with the perforated central permeate collection tube. Inside the envelope the two membrane sheets are separated by permeate spacers, consisting of a porous grid to facilitate the transport of the permeate to the central permeate collection tube. A membrane element contains several envelopes, separated from each other by feed spacers, placed at the feed side of the envelopes. A membrane element has a fiber glass casing. Typically four to eight membrane elements are present in a pressure vessel

(Baker, 2012b). A commonly applied pressure vessel with an internal diameter of 8 inches containing six membrane modules has a membrane surface area of 150-250 m^2 (Baker, 2012b). Recently, larger membrane modules with an internal diameter of 16 inches have become available (Baker, 2012b).

In a spiral wound membrane element the feed water flows through the feed channel, containing a feed spacer, towards the concentrate side. Only a small part of the water (7-15%) passes through the membrane and is collected in the central permeate collection tube, the rest ends up in the concentrate stream (Baker, 2012 b).

In the past the most commonly applied membrane material was cellulose acetate, because this type of membranes is chlorine resistant. Nowadays, the use of cellulose acetate membranes is restricted due to their low salt rejection properties, low pH and temperature requirements, high biofouling potential as well as a low permeability (Mallevialle et al., 1996; Vrouwenvelder et al., 2009). Currently, the most commonly applied nanofiltration and reverse osmosis membranes are polyamide thin film composite membranes. They consist of a dense, thin polyamide top layer, supported by an asymmetric, strong membrane structure. Polyamide thin film composite membranes have a high permeability and can be applied at a broader pH range and at higher temperatures than cellulose acetate membranes. However, polyamide thin film composite membranes are not chlorine resistant (Vrouwenvelder et al., 2009).

Feed spacers used in spiral wound membrane systems have a thickness between 660 µm and 810 µm (Bartels et al., 2007). A commonly applied feed spacer for water treatment in the Netherlands is a 787 µm thick diamond-shape spacer with a porosity of 0.85. The spacer consists of polypropylene strings, arranged in a net structure with 90° angles (Vrouwenvelder et al., 2011).

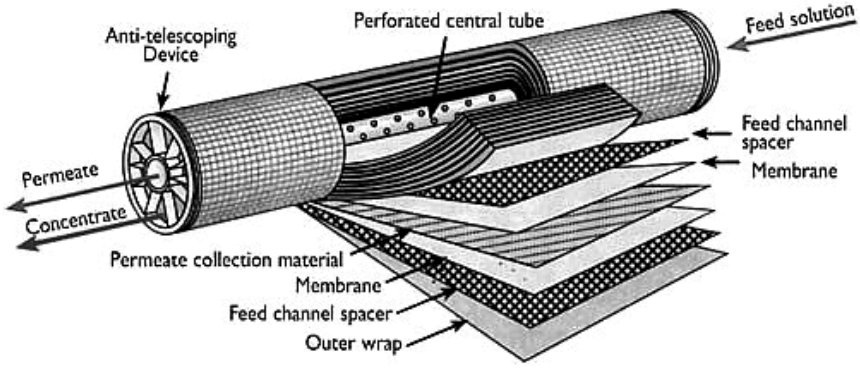

Figure 1.6: Scheme of a spiral wound membrane element (cmt-membranes, 2013).

1.2.3 Drawbacks of membrane filtration

Rejected material accumulates on the membrane over time causing membrane fouling, which is the major drawback of membrane filtration. Fouling decreases membrane performance and requires frequent cleaning and eventually early replacement of the membrane elements. Membrane fouling increases the overall operational costs strongly. Membrane fouling causes an increase in transmembrane pressure as well as feed channel pressure drop, causing a decrease in permeate flux. The three main parameters impacted by biofouling in membrane filtration systems are the mass transfer coefficient (MTC), the salt passage and the normalized pressure drop (NPD). The MTC describes the permeate flux normalized for temperature and net driving pressure (Nederlof et al., 2000; Schrader, 2006). If the MTC is decreased by 10% (Lenntech, 2013) or 15% (Huiting et al., 2001; Nederlof et al., 2000; Vrouwenvelder et al., 2008) the membrane element must be cleaned to restore original performance. An increase in salt passage of 5 – 10% requires a membrane cleaning as well (Lenntech, 2013). The NPD describes the feed channel pressure drop normalized for temperature and feed flow (Nederlof et al., 2000; Vrouwenvelder et al., 2008). When the NPD is increased by 10 – 15% a cleaning is necessary (Huiting et al., 2001; Lenntech, 2013; Nederlof et al., 2000; Vrouwenvelder et al., 2008). Membrane manufacturers restrict guarantees when the change in performance (MTC, salt passage and NPD) exceeds 15%.

Fouling can be classified into four types:

- Particulate fouling
- Inorganic fouling
- Organic fouling
- Biofouling

Particulate fouling is caused by suspended particles accumulating on the membrane surface or causing feed spacer plugging. Typically, suspended particles are precipitated salts, hydroxides, silica, organic colloids, iron corrosion products, and algae (Baker, 2012c). The most commonly reported inorganic fouling is scaling. Scaling occurs when in the feed water the solubility product of a specific salt is exceeded, causing precipitation on the membrane surface (Baker, 2012d). Organic fouling due to oil and grease is common to industrial applications, but also happens in drinking water treatment. Several types of fouling may take place at a membrane filtration plant at the same time. Commonly, particulate and organic fouling are present in the first modules, while inorganic fouling, especially scaling, is present in the last modules (Baker, 2012d). Pretreatment is the most efficient

way to minimize particulate and organic fouling (Baker, 2012e). The application of antiscalants in the feed water is a way to prevent scaling in the membrane modules (Baker, 2012d). Pretreatment and chemical dosage (e.g. scale inhibitors) are able to eliminate all membrane fouling types except biofouling. Biofouling causes major problems in membrane systems (Baker & Dudley, 1998; Ridgway & Flemming, 1996; Ridgway et al., 1983; Schneider et al., 2005; Tasaka et al., 1994; Vrouwenvelder et al., 2008). Since biofouling is the central topic of this study it is described in a separate section (1.3).

1.3 From biofilm to biofouling

1.3.1 Biofilms

Biofilms are defined as bacterial cells embedded in a highly hydrated matrix called extracellular polymeric substances (EPS). EPS consist of proteins, polysaccharides, nucleic acids, lipids and other biopolymers (Flemming & Wingender, 2010). Biofilms are one of the oldest and most efficient forms of life on earth, living in a biofilm brings a lot of advantages for the bacteria (Flemming, 2002; Flemming & Wingender, 2010; Schopf et al., 1983). Inside the biofilm EPS provide a protective barrier for bacteria against disinfectants and chemicals. EPS also provides bacteria with nutrients (C, N, and P containing compounds) (Flemming & Wingender, 2010). Bacteria profit from being in a biofilm by e.g. resistance against and survival of harsh conditions, horizontal gene transfer and reuse of metabolic byproducts (Flemming & Wingender, 2010; Wimpenny, 2000). An oxygen gradient may exist within the biofilm in which the part closest to the interface has the lowest oxygen content. Due to this oxygen gradient the same biofilm can provide space for aerobic as well as anaerobic bacteria (Babauta et al., 2013; Siegrist & Gujer, 1987).
Nearly all microorganisms are capable of biofilm formation (Flemming, 2002) and the bacterial number on a surface is always higher than the number of bacterial cells in the water phase (Madigan et al., 2001). Bacteria may attach to any surface and form a biofilm at any water interface. Biofilms can exist in many different places, such as marine environment (Kirchman & Mitchell, 1981; Meier et al., 2013), nuclear power plants (Satpathy, 1999), space stations (Koenig & Pierson, 1997) and in ultrapure water systems (Chicote et al., 2004; McFeters et al., 1993). Biofilm can have detrimental and beneficial properties. Biofilms are responsible for the self-cleaning of sediments, soil, and water by mineralizing organic matter (Wingender

& Flemming, 2011). Biofilms are used in biological waste water treatment (Wuertz et al., 2003), as well as in biofilters for drinking water production (Gimbel et al., 2006).

Biofilms can be smooth and flat or rough and fluffy and have different porosities (Flemming & Wingender, 2010). A mushroom-like morphology with macrocolonies surrounded by water filled voids represents a higher porosity than a smooth and flat morphology (Figure 1.7). Biofilm formation takes place in three stages; attachment, growth, and detachment (Figure 1.8). The detached bacteria and biofilm are transported with the water stream and can form a new biofilm wherever they attach again; for example downstream the membrane element.

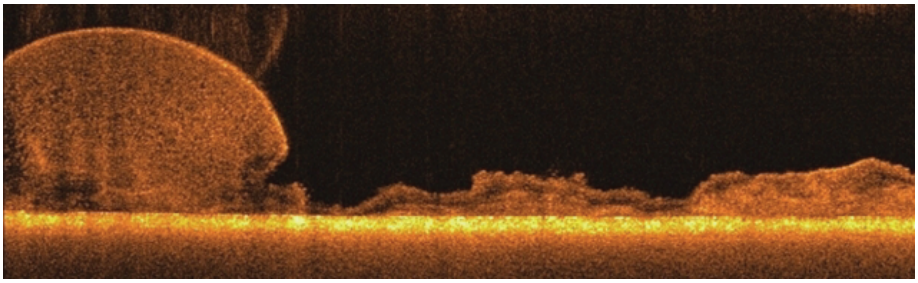

Figure 1.7: Optical coherence tomography image of a biofilm showing a mushroom-like shape as well as a smooth and flat morphology (picture taken from own database).

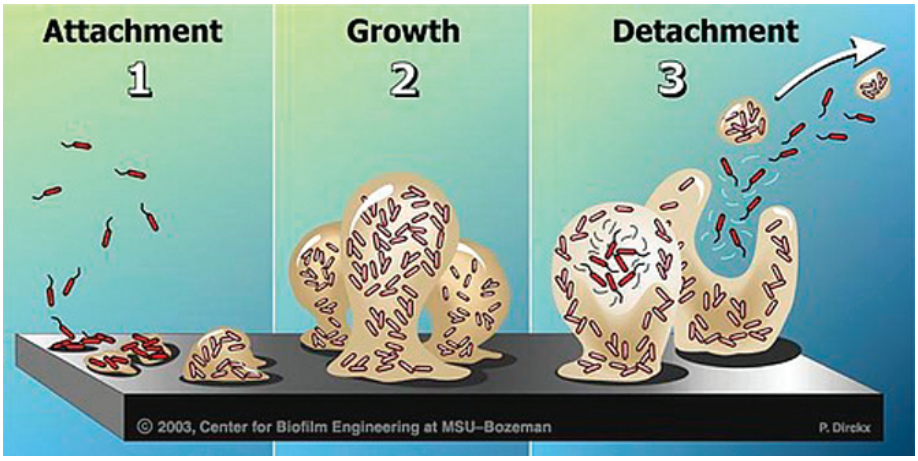

Figure 1.8: Biofilm formation: attachment, growth, and detachment (Center for Biofilm Engineering MSU-Bozeman, 2003).

1.3.2 Biofouling in membrane filtration systems

In membrane filtration systems a biofilm acts as a secondary membrane, causing an increase in feed channel pressure drop, transmembrane pressure drop, and hydraulic resistance of the system (Flemming et al., 1997). It has been shown that biofilms already develop during the first hours of operation of a spiral wound membrane system (Flemming, 1994). However, biofilm formation on the membrane presents problems only when the biofilm formation exceeds a threshold of interference, after which the biofilm formation is defined as biofouling (Figure 1.9) (Flemming, 2002; Flemming et al., 1997; Griebe & Flemming, 1998). Therefore, biofouling is an operationally defined parameter and commonly specified with a feed channel pressure drop increase of 10 - 15%, and/or an increase in salt passage of 5 - 10%, and/or a decrease in MTC of 10 – 15% (Huiting et al., 2001; Lenntech, 2013; Nederlof et al., 2000; Vrouwenvelder et al., 2008). The first modules of a membrane filtration system are most affected by biofouling due to the high load of biodegradable substrate which is consumed by bacteria as the water passes the membrane installation (Baker, 2012f).

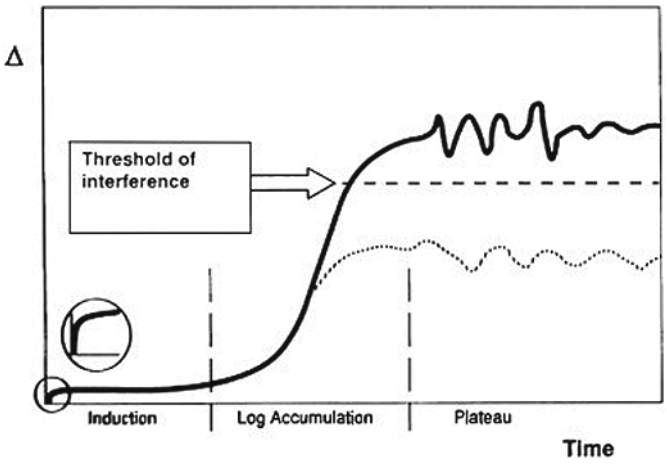

Figure 1.9: Growth curve of a biofilm showing the threshold of interference (Flemming, 2002).

Bacteria, causing biofouling by growth in a membrane filtration system, enter the membrane system with the feed water or are already present in the membrane elements at the start of the water production process. The feed water supplies the bacteria with biodegradable nutrients. Plastic and rubber connectors or seals (Kilb et al., 2003), and even the membrane itself are nutrient sources for the bacteria (Baker, 2012f). Due to nutrient rich conditions biofilm accumulation may turn into

biofouling. High water temperatures and high fluxes have a biofouling enhancing effect (Radu et al., 2012; Sim et al., 2011; Vrouwenvelder et al., 2011). Operational conditions such as permeate flux (Radu et al., 2010; Suwarno et al., 2012) and crossflow velocity (Choi et al., 2005; Radu et al., 2012; Vrouwenvelder et al., 2010), or spacer design and presence (Suwarno et al., 2012; Vrouwenvelder et al., 2009a; Yun et al., 2011) have a strong influence on biofouling. High shear forces can cause the bacteria to increase their EPS production and therefore form more biomass and further increase the hydraulic resistance (Percival et al., 1999).
Biofilms increase the pressure demand of a membrane filtration system in two ways. They increase the transmembrane pressure and the feed channel pressure drop which leads to performance losses and flux decline (Baker & Dudely, 1998). The increase of transmembrane pressure is related to the additional hydraulic resistance formed by the biofilm. In order to overcome the biofilm resistance an increased transmembrane pressure has to be applied to maintain a constant permeate flux rate (Flemming et al., 1997). Biofilm accumulation on the membrane blocks the narrow feed channel which increases the feed channel pressure drop and decreases the crossflow velocity (Vrouwenvelder et al., 2009b). Biofilm accumulation also decreases the crossflow velocity by increasing the friction resistance in the feed channel. Aquatic biofilms have viscoelastic properties therefore absorbing the kinetic energy of the water which results in an increase in friction resistance (Roeske, 2007). The EPS matrix is responsible for the viscoelasticity of the biofilm which leads to an increased friction resistance in piping systems as well as on ship hulls (Flemming & Wingender, 2001). One of the mechanisms for this behavior is the three-dimensional vibration of biofilms under influence of flow velocity which causes additional energy dissipation on the system (Andrewartha et al., 2010). Another reason for performance losses due to biofilm friction resistance is the surface roughness of the biofilm; it increases the frictional drag in a direct relation (Andrewartha et al., 2010; Picologlou et al., 1980).

To prevent or remove biofouling, biocides and cleaning agents are applied in membrane filtration systems (Flemming, 2002; Flemming et al., 1996). Bacteria inside the biofilm are protected by the surrounding EPS, which can restrict diffusion of the biocides through the biofilm (Flemming & Wingender, 2010; Nichols et al., 1988; Norwood & Gilmour, 2000). Also, adaptation of the bacteria to biocides is possible (Farr & Kogoma, 1991; Maira-Litran et al., 2000). In addition, killing is not cleaning (Flemming, 2002; Flemming et al., 1996). Dead biomass is still present

as a layer on the membrane, disturbing the filtration process (Flemming, 2002). Bacterial cells surviving the biocide dosage utilize the dead biomass as nutrient (Kappelhof et al., 2003).

An alternative approach to reduce the biofouling rate is the removal of biodegradable substrate from the feed water by pretreatment. A large number of research articles (Flemming et al., 1997; Griebe & Flemming, 1998; Flemming, 2002; Vrouwenvelder et al., 2009; Vrouwenvelder et al., 2010; Chen et al., 2013) show that nutrient limitation slows down the biofouling rate. Pretreatment by biofiltration is a commonly applied approach (Chinu et al., 2009; Hallé et al., 2009; Mosqueda-Jimenez & Huck, 2009; Huck et al., 2011; Peldszus et al., 2012; Bar-Zeev et al., 2013).

Modifications of membrane and feed spacer surfaces have been suggested as an approach to prevent biofouling. A large variety of membrane and spacer surface modifications and surface coatings have been proposed in order to prevent biofouling (Araujo et al., 2012a; Araujo et al., 2012b; Golbandi et al., 2013; Meng et al., 2014; Miller et al., 2012; Nikkola et al., 2014). But as soon as an initial layer of bacteria or particles is attached to the membrane or spacer surface a biofilm starts to grow, eventually causing biofouling (Araujo et al., 2012b; Miller et al., 2012). Despite chemical use, pretreatment and material modification biofouling is still a major problem in spiral wound NF and RO membrane systems.

So far it is not possible to get rid of biofilms in membrane filtration systems and therefore a way must be found to live with them. It is essential to investigate the intrinsic hydraulic biofilm resistance and to determine the contribution of biofilms to performance losses since surprisingly nothing is known about it. To measure the intrinsic biofilm resistance the influence of other fouling types and concentration polarization should be avoided. Concentration polarization is the accumulation of a solute in a thin layer at the membrane surface, caused by the crossflow operation and the membrane solute rejection properties (Baker, 2012d). Biodegradable substrate concentration polarization (higher food concentration at the membrane surface) enhances biofilm formation due to nutrient supply even close to the membrane surface, further away from the water phase (Herzberg et al, 2010a). Concentration polarization of salts reduces membrane performance by increasing the transmembrane osmotic pressure which reduces the permeate flux. Biofilm formation on the membrane and feed spacer enhance the accumulation

of salts and increase concentration polarization. The lack of crossflow velocity and the hampered back diffusion of salt ions within the gel-like biofilm promote the accumulation of salts (Gutman et al., 2012; Herzberg, 2010b; Radu et al., 2010; Chong et al., 2008; Herzberg & Elimelech, 2007). In summary, concentration polarization can influence both biofilm formation and membrane performance. The focus of this thesis is on hydraulic biofilm resistance without concentration polarization in order to investigate pure biofilms.

1.4 Biofouling monitor

Biofouling is a very costly problem in membrane filtration processes. By the time the fouling problem is identified as biofouling cleaning will present a difficult task. Early warning systems and regular surface sampling helps to prevent turning biofilm formation into biofouling. Most of the membrane filtration systems are build in such a way that surface sampling is not possible without the destruction of the membrane element. For such systems a side arm with a fouling monitor can help for monitoring of fouling development (Flemming, 2011). In order to prevent biofouling modified membrane installation operation conditions can be applied. Such modifications cannot be applied in full scale operation without prior testing due to a potential risk for the consumer and increased operational costs (Flemming, 2011). Especially long tern studies have to be performed in a biofouling monitor. A monitor has to be easy to handle and has to have similar hydrodynamics as full scale membrane plants. Validation of the biofouling monitor is essential for the quality of the results. A number of tests have to be performed in order to confirm the hydrodynamic properties of the monitor. Vrouwenvelder et al developed a number of monitor devices with e.g. glass windows, high pressure operation, for use in NMR systems, with and without permeate production (Vrouwenvelder, 2009a). The development of a new transparent membrane biofouling monitor is described in chapter 2. The developed monitor is based on the original MFS (Vrouwenvelder et al., 2006).

1.5 Flux enhancer

Since biofouling represents one of the biggest issues in membrane filtration countermeasures are needed. A flux enhancing substance that could be added to the feed water and does not require a back-flush or shut down of the installation is desired by the operators. In literature some approaches can be found (Hwang et al., 2007; Iversen et al., 2009; Koseoglu et al., 2008; Lee et al., 2007). In theory the flux enhancer should open the dense structure of the fouling layer in order to enhance membrane performance. Enzymes and detergents are most commonly used as flux enhancers during research approaches (McDonogh et al., 1994; Argüello et al., 2005, 2003; Kim et al., 2013). Typically, the target is to break up the EPS binding forces: hydrogen bonds, van der Waals bonds and electrostatical interactions (Flemming et al., 1997). If it is possible to disconnect the EPS binding forces its structure should become loose and therefore more permeable. In order to find such a substance which could be applied easily in full scale it is necessary to perform detailed tests in lab scale on different kinds of fouling layers. The complexity of fouling layers represents a big problem for the flux enhancer research because each fouling layer is different, depending on the feed water and the operational conditions. Enzymes that might target one kind of biofilm might not be effective on a different kind of biofilm in which a different bacterial community is present and therefore a different composition of EPS. The EPS is influenced by microorganisms, nutrient availability and source, shear force, and temperature (Flemming & Wingender, 2010). A flux enhancer might work only very specific for a small niche of fouling, while another is needed for another fouling layer. An overall solution which is applicable for every fouling layer is not very likely.

McDonogh et al. (1994) found an significant increase in relative biofilm permeability when conditioning the fouling layer with Ultrasil P 53 (Henkel) (Figure 1.10). This flux enhancing effect was observed on artificial biofilms consisting of an agar gel but could not be transferred to real biofilms completely. The observations of McDonogh et al. (1994) were the foundation of the initial research performed during this thesis. The experiments in which agar gels were conditioned with Ultrasil P53 were repeated at the same operational conditions defined by McDonogh et al. (1994) but the flux enhancing effect could not be observed. After an initial increase in permeability the flux decreased again after about 10 minutes of operation. An explanation might be a change in composition of Ultrasil P53 due to a time lag of 15 years in between the experiments. Since

the principal of flux enhancers represents an important topic other substances were tested for their flux increasing effect as well. The following substances were tested in a dead-end filtration system on artificial biofilms which consisted of agar, lipase, and latex beads: Urea (6 molar), guanidinium chloride (2 molar), and lithium bromide (6 molar). Urea and lithium bromide showed an initial flux increase after its application but the flux decreased again after about 10 minutes of operation. A fungus extract (supplied by the Karlsruhe Institute for Technology) was tested in a crossflow membrane filtration system on a biofilm grown on nutrient enriched drinking water. The flux enhancing effect found in these experiments was related to the shear stress which occurred when the feed water was replaced by the fungus extract and then again replaced by water.

Unfortunately, none of the tested substances showed the desired effect and it became obvious that more research on fouling layers is necessary beforehand. In order to be able to apply a substance which can decrease the hydraulic resistance of biofilms it is essential to learn more about the intrinsic hydraulic resistance of biofilms and its relation to biofilm composition. Therefore the impact of hydraulic biofilm resistance on membrane processes and the effect of operational parameters on biofilm formation and biofilm composition were investigated during this thesis.

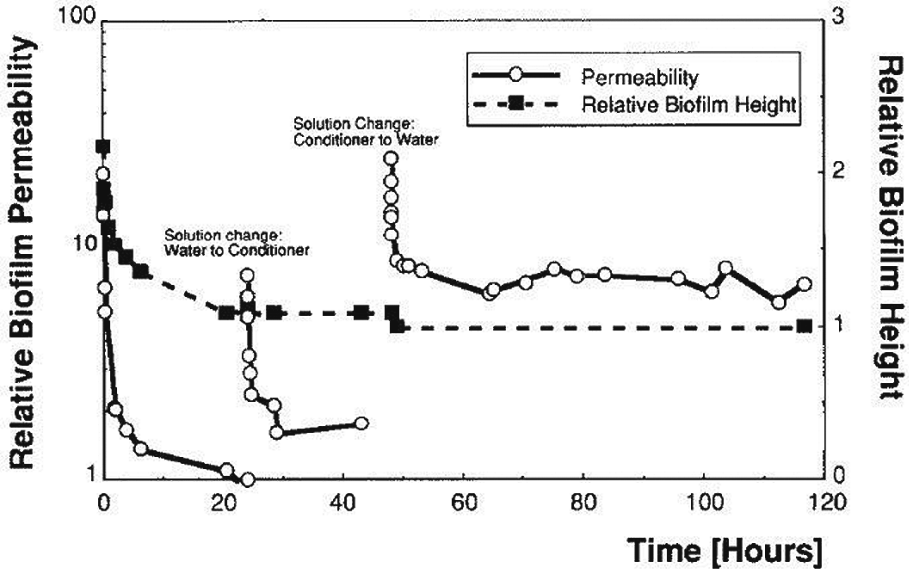

Figure 1.10: Impact of Ultrasil P53 (conditioner) on the relative biofilm permeability and height of an artificial biofilm consisting of agar (McDonogh et al., 1994).

1.6 Objectives

Hydraulic biofilm resistance is related to the increase of transmembrane pressure and decrease in permeate flux which is caused by biofilm formation on the membrane surface. The main objective of this thesis was to investigate the intrinsic hydraulic resistance of biofilms and how it is affected by various operational parameters such as: permeate flux, crossflow velocity, biodegradable substrate content, and feed spacer presence.

1.7 Outline of this thesis

Many of the existing monitors to study membrane fouling are not representative for practice and not comparable to spiral wound membrane module conditions. In order to pursue the mentioned objectives, a lab scale membrane filtration system with permeate production was developed, simulating practical hydrodynamic conditions: The transparent membrane biofouling monitor. Validation tests were performed to ensure that the monitor was representative for spiral wound membrane elements. The designed system was easy to use due to the application of microfiltration membranes which enabled low pressure operation and avoided concentration polarization (Chapter 2).

The experimental set-up enabled to determine the intrinsic biofilm resistance and to study the effect of permeate flux and feed spacer presence on biofilm resistance as well as the relation between biofilm resistance and biofilm parameters (Chapter 3).

The effect of crossflow velocity and feed spacer on biofilm resistance, feed channel pressure drop and biofilm parameters was studied in more detail. Different crossflow velocities were applied in combination with different biodegradable substrate concentrations in the feed water. All experiments were performed in the presence and absence of a feed spacer (Chapter 4).

So far methods to control biofouling have not been very successful. Based on insights obtained by the studies described in this thesis, an outlook is given of recommended research directions and potential approaches to control biofouling (Chapter 5).

This thesis is structured as a cumulative dissertation. The Chapters 2 to 4 are published in peer-reviewed journals. In some cases small adaptations have been made to improve the context.

References:

Amjad, Z. (1993). *Reverse Osmosis: Membrane Technology, water chemistry and industrial applications*. New York: Van Nostrand Reinhold.

Andrewartha, J., Perkins, K., Sargison, J., Osborn, J., Walker, G., Henderson, A., & Hallegraeff, G. (2010). Drag force and surface roughness measurements on freshwater biofouled surfaces. *Biofouling, 26(4),* 487-496.

Araujo, P. A., Kruithof, J. C., Van Loosdrecht, M. C. M., & Vrouwenvelder, J. S. (2012a). The potential of standard and modified feed spacers for biofouling control. *Journal of Membrane Science, 403-404*(0), 58-70.

Araujo, P. A., Miller, D. J., Correia, P. B., van Loosdrecht, M. C. M., Kruithof, J. C., Freeman, B. D., & Vrouwenvelder, J. S. (2012b). Impact of feed spacer and membrane modification by hydrophilic, bactericidal and biocidal coating on biofouling control. *Desalination, 295*(0), 1-10.

Argüello, M.A., Alvarez, S., Riera, F.A., Alvarez, R. (2003). Enzymatic cleaning of inorganic ultrafiltration membranes used for whey protein fractionation. *Journal of Membrane Science,* 216(1-2), 121-134.

Argüello, M.A., Alvarez, S., Riera, F.A., Alvarez, R. (2005). Utilization of enzymatic detergents to clean inorganic membranes fouled by whey proteins. *Separation and Purification Technology,* 41(2), 147-154.

Babauta, J. T., Nguyen, H. D., Istanbullu, O., & Beyenal, H. (2013). Microscale gradients of oxygen, hydrogen peroxide, and pH in freshwater cathodic biofilms. *ChemSusChem, 6*(7), 1252-1261.

Baker, J. S., & Dudley, L. Y. (1998). Biofouling in membrane systems - A review. *Desalination, 118*(1-3), 81-89.

Baker, R. W. (2012a). Membranes and Materials *Membrane Technology and Applications* (3rd ed., pp. 213). West Sussex: John Wiley and Sons Ltd.

Baker, R. W. (2012b). Spiral-Wound Modules *Membrane Technology and Applications* (3rd ed., pp. 158-162). West Sussex: John Wiley and Sons Ltd.

Baker, R. W. (2012c). Silt *Membrane Technology and Applications* (3rd ed., pp. 233). West Sussex: John Wiley and Sons Ltd.

Baker, R. W. (2012d). Scale *Membrane Technology and Applications* (3rd ed., pp. 231-233). West Sussex: John Wiley and Sons Ltd.

Baker, R. W. (2012e). Membrane Fouling Control *Membrane Technology and Applications* (3rd ed., pp. 231). West Sussex: John Wiley and Sons Ltd.

Baker, R. W. (2012f). Biofouling *Membrane Technology and Applications* (3rd ed., pp. 233). West Sussex: John Wiley and Sons Ltd.

Bartels, C., Hirose, M., & Fujioka, H. (2007). *Performance advancement in the spiral wound RO/NF element design*. Paper presented at the EDS Conference, Halkidiki, Greece.

Bar-Zeev, E.,Belkin, N., Liberman, B., Berman-Frank, I., & Berman, T. (2013). Bioflocculation: Chemical free, pre-treatment technology for the desalination industry. *Water Research, 47(9), 3093-3102*.

Center for Biofilm Engineering MSU-Bozeman. (2003). 2013, from http://www.biofilm.montana.edu /

Chen, X., Suwarno, S. R., Chong, T. H., McDougald, D., Kjelleberg, S., Cohen, Y., Fane, A. G., & Rice, S. A. (2013). Dynamics of biofilm formation under different nutrient levels and the effect on biofouling of a reverse osmosis membrane system. *Biofouling, 29(3), 319-330.*

Chicote, E., Moreno, D. A., Garcia, A. M., Sarro, M. I., Lorenzo, P. I., & Montero, F. (2004). Biofouling on the walls of a spent nuclear fuel pool with radioactive ultrapure water. *Biofouling, 20(1),* 35-42.

Chinu, K. J., Johir, A. H., Vigneswaran, S., Shon, H. K., & Kandasamy.J. (2009). Biofilter as pretreatment to membrane based desalination: Evaluation in terms of fouling index. *Desalination, 247(1-3), 77-84.*

Choi, H., Zhang, K., Dionysiou, D. D., Oerther, D. B., & Sorial, G. A. (2005). Influence of cross-flow velocity on membrane performance during filtration of biological suspension. *Journal of Membrane Science, 248* (1-2), 189-199.

Chong, T. H., Wong, F. S., & Fane, A. G. (2008). The effect of imposed flux on biofouling in reverse osmosis: Role of concentration polarisation and biofilm enhanced osmotic pressure phenomena. *Journal of Membrane Science, 325*(2), 840-850. cmt-membranes. (2013). http://www.cmt-membranes.com

Farr, S. B., & Kogoma, T. (1991). Oxidative stress responses in Escherichia coli and Salmonella typhimurium. *Microbiological Reviews, 55*(4), 561-585.

Flemming, H.-C. (1994). Biofilme, Biofouling und mikrobielle Materialschaedigung. *Stuttgarter Siedlungswasserwirtschaftliche Berichte.* Munich: Oldenbourg Verlag.

Flemming, H. C. (2002). Biofouling in water systems - Cases, causes and countermeasures. *Applied Microbiology and Biotechnology, 59*(6), 629-640.

Flemming, H. C., Griebe, T., & Schaule, G. (1996). Antifouling strategies in technical systems - A short review *Water Science and Technology* (Vol. 34, pp. 517-524).

Flemming, H. C., Schaule, G., Griebe, T., Schmitt, J., & Tamachkiarowa, A. (1997). Biofouling - The Achilles heel of membrane processes. *Desalination, 113*(2-3), 215-225.

Flemming, H. C., & Wingender, J. (2001). Relevance of microbial extracellular polymeric substances (EPSs) – Part II: Technical aspects. *Water Science and Technology, 43(6),* 9-16.

Flemming, H. C., & Wingender, J. (2010). The biofilm matrix. *Nature Reviews Microbiology, 8*(9), 623-633.

Flemming, H.C. (2011). Biofilm Highlights. *Microbial biofouling: Unsolved problems, insufficient approaches, and possible solutions.* Berlin Heidelberg. Springer Verlag

Gimbel, R., Graham, N. J. D., & Collins, M. R. (2006). *Recent Progress in Slow Sand and Alternative Biofiltration Processes.* London: IWA Publ.

Golbandi, R., Abdi, M. A., Babaluo, A. A., Khoshfetrat, A. B., & Mohammadlou, T. (2013). Fouling study of TiO2-boehmite MF membrane in defatting of whey solution: Feed concentration and pH effects. *Journal of Membrane Science,* 448, 135-142.

Griebe, T., & Flemming, H. C. (1998). Biocide-free antifouling strategy to protect RO membranes from biofouling. *Desalination, 118*(1-3), 153-159.

Gutman, J., Fox, S., Gilron, J. (2012). Interactions between biofilms and NF/RO flux and their implications for control-A review of recent developments. *Jounal of Membrane Science,* 421-422, 1-7.

Halle, C., Huck, P. M., Peldszus, S., Haberkamp, J., & Jekel, M. (2009). Assessing the performance of biological filtration as pretreatment to low pressure membranes for drinking water. *Environmental Science and Technology,* 43(19), 3878-3884.

Herzberg, M., Berry, D., Raskin, L. (2010a). Impact of microfiltration treatment of secondary wastewater effluent on biofouling of reverse osmosis membranes. *Water Research,* 44(1), 167-176.

Herzberg, M. (2010b). Osmotic effects of biofouling in reverse osmosis (RO) processes: Physical and physiological measurements and mechanisms. *Desalination and Water Treatment, 15*(1-3), 287-291.

Herzberg, M., & Elimelech, M. (2007). Biofouling of reverse osmosis membranes: Role of biofilm-enhanced osmotic pressure. *Journal of Membrane Science, 295*(1-2), 11-20.

Huck, P. M., Peldszus, S., Halle, C., Ruiz, H., Jin, X., Van Dyke, M., Amy, G., Uhl, W., Theodoulou, M., & Mosqueda-Jimenez, D. B. (2011). Pilpt scale evaluation of biofiltration as an innovative pre-treatment for ultrafiltration membranes for drinking water treatment. *Water Science and Technology: Water Supply, 11(1), 23-29.*

Huiting, H., Kappelhof, J. W. N. M., & Bosklopper, T. G. J. (2001). Operation of NF/RO plants: From reactive to proactive. *Desalination, 139*(1-3), 183-189.

Hwang, B.K., Lee, W.N., Park, P.K., Lee, C.H., Chang, I.S. (2007). Effect of membrane fouling reducer on cake structure and membrane permeability in membrane bioreactor. *Journal of Membrane Science,* 288(1-2), 149-156.

International Water Management Institute. (2000). 2013, from http://www.iwmi.cgiar.org/

Iversen, V., Koseoglu, H., Yigit, N. O., Drews, A., Kitis, M., Lesjean, B., & Kraume, M. (2009). Impacts of membrane flux enhancers on activated sludge respiration and nutrient removal in MBRs. *Water Research, 43*(3), 822-830.

Kappelhof, J. W. N. M., Vrouwenvelder, H. S., Schaap, M., Kruithof, J. C., Van Der Kooij, D., & Schippers, J. C. (2003) An in situ biofouling monitor for membrane systems. *Vol. 3* (pp. 205-210).

Kilb, B., Lange, B., Schaule, G., Flemming, H. C., & Wingender, J. (2003). Contamination of drinking water by coliforms from biofilms grown on rubber-coated valves. *International Journal of Hygiene and Environmental Health, 206*(6), 563-573.

Kim, L.H., Kim, S.J., Kim, C.M., Shin, M.S., Kook, S., Kim, I.S. (2013). Effects of enzymatic treatment on the reduction of extracellular polymeric substances (EPS) from biofouled membranes. *Desalination and Water Treatment,* 51(31-33), 6355-6361.

Kirchman, D., & Mitchell, R. (1981). *BIOCHEMICAL MECHANISM FOR MARINE BIOFOULING.* Paper presented at the Oceans Conference Record (IEEE).

Koch Membrane Systems. (2013a). Membrane Technologies

Koch Membrane Systems. (2013b). An Overview of Membrane Technology and Theory *Application Bulletin.* 2013, from http://www.kochmembrane.com/PDFs/KMS-Membrane-Theory.aspx *Lerning Center.* 2013, from http://www.kochmembrane.com/Learning-Center/Technologies.aspx

Koenig, D. W., & Pierson, D. L. (1997). Microbiology of the space shuttle water system *Water Science and Technology* (Vol. 35, pp. 59-64).

Koseoglu, H., Yigit, N.O., Iversen, V., Drews, A., Kitis, M., Lesjean, B., Kraume, M. (2008). Effects of several different flux enhancing chemicals on filterability and fouling reduction of membrane bioreactor (MBR) mixed liquors. *Journal of Membrane Science,* 320(1-2), 57-64.

Lee, W.N., Chang, I.S., Hwang, B.K., Park, P.K., Lee, C.H. (2007).Changes in biofilm architecture with addition of membrane fouling reducer in a membrane bioreactor. *Process Biochemistry,* 42(4), 655-661.

Lenntech (Producer). (2013). Cleaening Procedures for DOW FILMTEC FT30 Elements. *Dow Filmtec Membranes.*

Madigan, M. T., Martinko, J. M., & Parker, J. (2001). 16.2 Mikroorganismen in der Natur. In W. Goebel (Ed.), *Brock Mikrobiologie.* Heidelberg Berlin: Spktrum.

Maira-Litran, T., Allison, D. G., & Gilbert, P. (2000). Expression of the multiple antibiotic resistance operon (mar) during growth of Escherichia coli as a biofilm. *Journal of Applied Microbiology, 88*(2), 243-247.

Mallevialle, J., Odendaal, P. E., & Wiesner, M. R. (1996). *Water Treatment Membrane Processes.* New York: Graw-Hill.

Martin-Rosales, W., Pulido-Bosch, A., Vallejos, A., Gisbert, J., Andreu, J. M., & Sanchez-Martos, F. (2007). Hydrological implications of desertification in southeastern Spain. *Hydrological Science Journal, 52(6), 1146-1161*.

McDonogh, R., Schaule, G., & Flemming, H.-C. (1994). The permeability of biofouling layers on membranes. *Journal of Membrane Science, 87*(1-2), 199-217.

McFeters, G. A., Broadaway, S. C., Pyle, B. H., & Egozy, Y. (1993). Distribution of bacteria within operating laboratory water purification systems. *Applied and Environmental Microbiology, 59*(5), 1410-1415.

Meier, A., Tsaloglou, N.-M., Mowlem, M. C., Keevil, C. W., & Connelly, D. P. (2013). Hyperbaric biofilms on engineering surfaces formed in the deep sea. *Biofouling, 29*(9), 1029-1042.

Meng, S., Mansouri, J., Ye, Y., & Chen, V. (2014). Effect of templating agents on the properties and membrane distillation performance of TiO2-coated PVDF membranes. *Journal of Membrane Science, 450*, 48-59.

Miller, D. J., Araujo, P. A., Correia, P. B., Ramsey, M. M., Kruithof, J. C., van Loosdrecht, M. C. M., Vrouwenvelder, J. S. (2012). Short-term adhesion and long-term biofouling testing of polydopamine and poly(ethylene glycol) surface modifications of membranes and feed spacers for biofouling control. *Water Research, 46*(12), 3737-3753.

Mosqueda-Jimenez, D. B. & Huck, P. M. (2009). Effect of biofiltration as pretreatment on the fouling of nanofiltration membtranes. *Desalination, 245(1-3), 60-72.*

Nederlof, M. M., Kruithof, J. C., Taylor, J. S., Van Der Kooij, D., & Schippers, J. C. (2000). Comparison of NF/RO membrane performance in integrated membrane systems. *Desalination, 131*(1-3), 257-269.

Nichols, W. W., Dorrington, S. M., Slack, M. P. E., & Walmsley, H. L. (1988). Inhibition of tobramycin diffusion by binding to alginate. *Antimicrobial Agents and Chemotherapy, 32*(4), 518-523.

Nikkola, J., Sievänen, J., Raulio, M., Wei, J., Vuorinen, J., & Tang, C. Y. (2014). Surface modification of thin film composite polyamide membrane using atomic layer deposition method. *Journal of Membrane Science, 450,* 174-180.

Norwood, D. E., & Gilmour, A. (2000). The growth and resistance to sodium hypochlorite of Listeria monocytogenes in a steady-state multispecies biofilm. *Journal of Applied Microbiology, 88*(3), 512-520.

Peldszus, S., Benecke, J., Jekel, M., & Huck, P. M. (2012). Direkt biofiltration pretreatment for fouling control of ultrafiltration membranes. *American Water Works Association, 104(7), E430-E445.*

Percival, S. L., Knapp, J. S., Wales, D. S., & Edyvean, R. G. J. (1999). The effect of turbulent flow and surface roughness on biofilm formation in drinking water. *Journal of Industrial Microbiology and Biotechnology, 22*(3), 152-159.

Picologlou, B. F., Zelver, N., & Characklis, W. G. (1980). Biofilm growth and hydraulic performance. *Journal of Hydraulics Division, 106(5),* 733-746.

Radu, A. I., Vrouwenvelder, J. S., van Loosdrecht, M. C. M., & Picioreanu, C. (2010). Modeling the effect of biofilm formation on reverse osmosis performance: Flux, feed channel pressure drop and solute passage. *Journal of Membrane Science, 365*(1-2), 1-15.

Radu, A. I., Vrouwenvelder, J. S., van Loosdrecht, M. C. M., & Picioreanu, C. (2012). Effect of flow velocity, substrate concentration and hydraulic cleaning on biofouling of reverse osmosis feed channels. *Chemical Engineering Journal, 188,* 30-39.

Ridgway, H. F., Flemming, H. C. (1996). Biofouling of membranes. In J. Mallevialle, Odendaal, P. E., Wiesner, M. R. (Ed.), *Water treatment membrane processes* (pp. 629 - 640). New York: McGraw-Hill.

Ridgway, H. F., Kelly, A., Justice, C., & Olson, B. H. (1983). Microbial fouling of reverse-osmosis membranes used in advanced wastewater treatment technology: Chemical, bacteriological, and ultrastructural analyses. *Applied and Environmental Microbiology, 45*(3), 1066-1084.

Roeske, W. (2007). Trinkwasserdesinfektion. (2nd. ed). München, Oldenbourg Industrieverlag.

Satpathy, K. K. (1999). Effects of biofouling on the cooling water quality of a nuclear power plant. *Bulletin of Electrochemistry, 15*(3-4), 143-147.

Schneider, R. P., Ferreira, L. M., Binder, P., Bejarano, E. M., Góes, K. P., Slongo, E., . . . Rosa, G. M. Z. (2005). Dynamics of organic carbon and of bacterial populations in a conventional pretreatment train of a reverse osmosis unit experiencing severe biofouling. *Journal of Membrane Science, 266*(1-2), 18-29.

Schopf, J. W., Hayes, J. M., & Walter, M. R. (1983). Evolution on earth's earliest ecosystems: recent progress and unsolved problems. In J. W. Schopf (Ed.), *Earth's earliest biosphere* (pp. 361-384). New Jersey: Princeton University Press.

Schrader, G. A. (2006). *Direct Nanofiltration of Waste Water Treatment Plant Effluent*. (PhD thesis), University of Twente, Twente, The Netherlands.

Shiklomanov, I. A. (2000). Appraisal and Assessment of World Water Resources. *Water International, 25*(1), 11-32.

Siegrist, H., & Gujer, W. (1987). Demonstration of mass transfer and pH effects in a nitrifying biofilm. *Water Research, 21*(12), 1481-1487.

Sim, L. N., Ye, Y., Chen, V., & Fane, A. G. (2011). Comparison of MFI-UF constant pressure, MFI-UF constant flux and Crossflow Sampler-Modified Fouling Index Ultrafiltration (CFS-MFIUF). *Water Research, 45*(4), 1639-1650.

Suwarno, S.R., Chen, X., Chong, T.H., Puspitasari, V.L., McDougald, D., Cohen, Y., Rice, S.A. & Fane, A.G. (2012) The impact of flux and spacers on biofilm development on reverse osmosis membranes. *Journal of Membrane Science* 405-406(0), 219-232.

Tasaka, K., Katsura, T., Iwahori, H., & Kamiyama, Y. (1994). Analysis of RO elements operated at more than 80 plants in Japan. *Desalination, 96*(1-3), 259-272.

UNESCO & WWAP. (2006). Water a shared responsibility; The United Nations World Water Development Report 2. *World Water Development Report 2, Berghahn Books, NY, USA.*

United Nations. (2013). Water scarcity. *International Decade for Action 'Water for Life' 2005-2015*. 2013, from https://www.un.org/waterforlifedecade/scarcity.shtml

Vrouwenvelder, J. S., van Paassen, J. A. M., Wessels, L. P., van Dam, A. F., & Bakker, S. M. (2006). The Membrane Fouling Simulator: A practical tool for fouling prediction and control. *Journal of Membrane Science, 281*(1-2), 316-324.

Vrouwenvelder, H. (2009a). *Biofouling of Spiral Wound Membrane Systems.* (PhD thesis), Delft University of Technology, Delft, The Netherlands.

Vrouwenvelder, J. S., van Paassen, J. A. M., Kruithof, J. C., & van Loosdrecht, M. C. M. (2009b). Sensitive pressure drop measurements of individual lead membrane elements for accurate early biofouling detection. *Journal of Membrane Science, 338*(1-2), 92-99.

Vrouwenvelder, J. S., Buiter, J., Riviere, M., van der Meer, W. G. J., van Loosdrecht, M. C. M., & Kruithof, J. C. (2010). Impact of flow regime on pressure drop increase and biomass accumulation and morphology in membrane systems. *Water Research, 44*(3), 689-702.

Vrouwenvelder, J. S., Manolarakis, S. A., van der Hoek, J. P., van Paassen, J. A. M., van der Meer, W. G. J., van Agtmaal, J. M. C., van Loosdrecht, M. C. M. (2008). Quantitative biofouling diagnosis in full scale nanofiltration and reverse osmosis installations. *Water Research, 42*(19), 4856-4868.

Vrouwenvelder, J. S., Van Loosdrecht, M. C. M., & Kruithof, J. C. (2011). A novel scenario for biofouling control of spiral wound membrane systems. *Water Research, 45*(13), 3890-3898.

Wimpenny, J. (2000). An overview of biofilms as functional communities. In D. Allison, P. Gilbert, H. Lappin-Scott & M. Wilson (Eds.), *Community structure and co-operation in biofilms.* (pp. 1-24). Cambridge: Cambridge University Press.

Wingender, J., & Flemming, H. C. (2011). Biofilms in drinking water and their role as reservoir for pathogens. *International Journal of Hygiene and Environmental Health, 214*(6), 417-423.

World Health Organization. (2012). UN-water global annual assessment of sanitation and drinking-water (GLAAS) 2012 report: the challenge of extending and sustaining services. Geneva, Switzerland: World Health Organization UN water.

World Health Organization (Producer). (2013). Water supply, sanitation and hygiene development. *Water Sanitation Health* Retrieved from http://www.who.int/water_sanitation_health/hygiene/en/

Wuertz, S., Bishop, P., & Wilderer, P. A. (2003). *Biofilms in Wastewater Treatment.* London: IWA Publ.

Yun, Y., Wang, J., Ma, R., & Fane, A. G. (2011). Effects of channel spacers on direct contact membrane distillation. *Desalination and Water Treatment, 34*(1-3), 63-69.

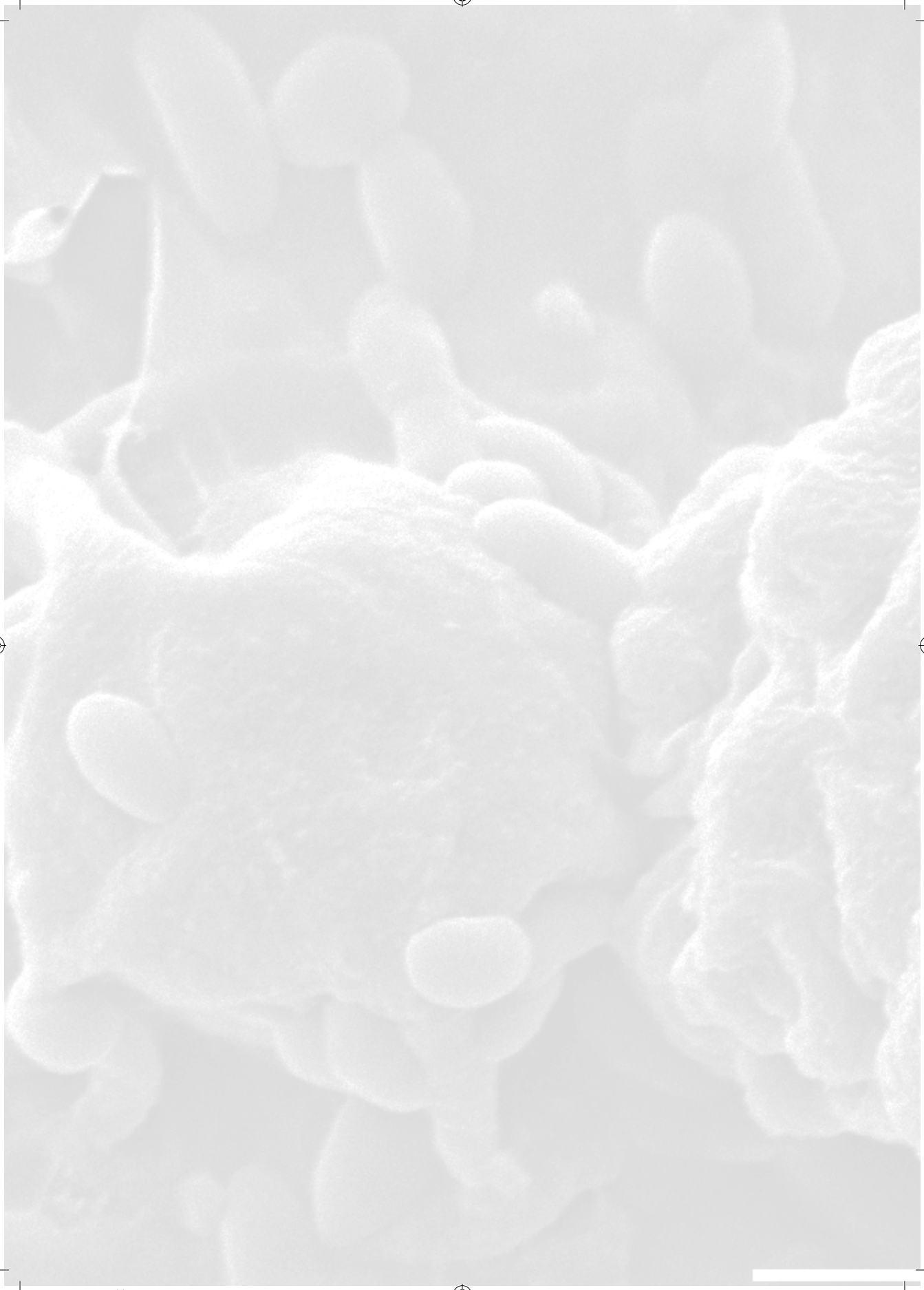

Chapter 2

Development and testing of a transparent membrane biofouling monitor

This chapter is published as:
C. Dreszer, H.-C. Flemming, A.D. Wexler,
A. Zwijnenburg, J.C. Kruithof, J.S. Vrouwenvelder
Development and testing of a transparent membrane biofouling monitor,
Desalination and Water Treatment 52 (2014) 1807-1819.

Abstract

A modified version of the membrane fouling simulator (MFS) was developed for assessment of (i) hydraulic biofilm resistance, (ii) performance parameters feed-channel pressure drop and transmembrane pressure drop, and (iii) *in situ* spatial visual and optical observations of the biofilm in the transparent monitor, e.g. using optical coherence tomography. The flow channel height equals the feed spacer thickness enabling operation with and without feed spacer. The effective membrane surface area was enlarged from 80 to 200 cm^2 by increasing the monitor width compared to the standard MFS, resulting in larger biomass amounts for analysis. By use of a microfiltration membrane (pore size 0.05 µm) in the monitor salt concentration polarization is avoided, allowing operation at low pressures enabling accurate measurement of the intrinsic hydraulic biofilm resistance. Validation tests on e.g. hydrodynamic behavior, flow field distribution, and reproducibility showed that the small-sized monitor was a representative tool for membranes used in practice under the same operating conditions, such as spiral-wound nanofiltration and reverse osmosis membranes. Monitor studies with and without feed spacer use at a flux of 20 L m^{-2} h^{-1} and a crossflow velocity of 0.1 m s^{-1} clearly showed the suitability of the monitor to determine hydraulic biofilm resistance and for controlled biofouling studies.

2.1 Introduction

High quality water from water sources including seawater and sewage can be produced with membrane filtration processes like nanofiltration (NF) and reverse osmosis (RO). Because the global demand for clean fresh water is growing, the application of these membrane technologies has increased strongly (Shannon et al., 2008). One of the most serious problems in NF and RO applications is biofouling - biofilm formation causing unacceptable operational problems (Baker & Dudley, 1998; Ridgway & Flemming, 1996; Ridgway et al., 1983; Schneider et al., 2005; Shannon et al., 2008; Tasaka et al., 1994; Vrouwenvelder et al., 2008). Biofilms may interfere with membrane performance in three ways: (i) increase of transmembrane pressure drop (TMP), (ii) increase of feed-channel (feed-concentrate) pressure drop (FCP), and (iii) decrease of salt rejection. According to manufacturer's specifications an operational problem of a membrane installation is defined when the transmembrane and/or feed-channel pressure drop (FCP) increase and/or salt rejection decrease exceed 15% of the start-up values (Huiting et al., 2001; Nederlof et al., 2000; Vrouwenvelder et al., 2008). When these parameters change by more than 15%, corrective actions must be taken and guarantees are restricted by the manufacturers of membrane elements. Biofouling, excessive growth of biomass, is an operationally defined problem affecting the performance of these membrane systems, influencing the amount and quality of the produced fresh water and costs.

In view of the relevance of biofouling, it is surprising how few data exist about the hydraulic resistance of biofilms that may affect the TMP and membrane passage. To investigate the effect of biofilm formation on a membrane system, it is essential to differentiate between the hydraulic resistance of the membrane and the fouling layer. Furthermore, intrinsic biofilms need to be obtained without disturbances by other fouling types, which is often not possible in NF and RO membrane systems. Therefore, a measurement of the clean water permeability of a fouled membrane module compared to a virgin module would not provide the pure biofilm resistance (since different fouling types and the module fouling distribution may play a role). Until now, there is no fouling simulation system available which allows the study of the intrinsic biofilm resistance without the influence of salt concentration polarization.

The objective of this study was to develop a transparent representative monitor with permeate production. The monitor should be suitable for assessment of (i) intrinsic hydraulic biofilm resistance, (ii) performance parameters: FCP and TMP, and (iii) *in situ* visual and optical spatial observations of the biofilm in the monitor. The boundary conditions for accurate and sensitive assessment of the intrinsic hydraulic biofilm resistance are exclusion of salt concentration polarization effects and operation at low pressures, resulting in the selection of a membrane with a pore size of 0.05 µm. The membrane fouling simulator (MFS), the monitor used in many research efforts (Araujo et al., 2012; Creber et al., 2010; Miller et al., 2012; Prest et al., 2012; Vrouwenvelder et al., 2010; Vrouwenvelder et al., 2009), has shown to be representative for spiral-wound membrane modules used in practice. The MFS operated under crossflow conditions without permeate production, gives identical results for fouling in a full-scale membrane module (Vrouwenvelder et al., 2007a; Vrouwenvelder et al., 2007b; Vrouwenvelder et al., 2006) The original MFS was used as the prototype for the design of a monitor with permeate production to study the intrinsic hydraulic biofilm resistance.

2.2 Material and methods

2.2.1 Transparent membrane biofouling monitor (tMBM)

The tMBM is made of polymethylmethacrylate (PMMA). This transparent material offers the possibility to study biofilm growth *in situ*. The tMBM is suitable for crossflow operation. Spatial dimensions and hydrodynamics are similar to spiral-wound NF and RO membrane elements. The external dimensions of the tMBM are 300 × 170 × 0.787 mm, with 200 cm of permeate producing membrane area. The feed channel dimensions are 200 × 100 × 0.787 mm (Figure 1). The height of the feed channel (0.787 mm) and the product spacer channel (0.25 mm) are based on reported data of spiral-wound membrane modules (Schock & Miquel, 1987; van der Meer, 2003). The height of the feed channel is equivalent to the height of a 31 mil (787 µm) thick feed spacer enabling operating the system with or without feed spacer presence. The membrane is fixed in place by a frame on the edge of the feed channel and is sealed by an O-ring. This construction prevents shifting of the membrane even without feed spacer presence. The large membrane area allows harvesting of a sufficient amount of biomass for analyses. The tMBM is equipped with one feed, one concentrate, and two permeate connections and can withstand pressures up to 5 bar. The pressure

development over the feed channel and the membrane can be measured via external connections at the feed, concentrate, and permeate inlets. During operation, the monitors are placed in opaque boxes to prevent growth of phototrophic organisms.

2.2.2 Membrane and spacer

The membranes used in this system were PES (polyethersulfone) microfiltration membranes (Nadir MP 005, Microdyn-Nadir GmbH Wiesbaden, Germany) with a pore size of 0.05 µm to enable operation at low pressure and prevent concentration polarization by salts. The 787 µm thick feed spacer consisted of polypropylene strings, arranged as a net structure with 90º angles and a porosity of about 0.85. This feed spacer is commonly used in spiral-wound NF and RO modules for water treatment in The Netherlands (Vrouwenvelder et al., 2011).

2.2.3 Setup configuration for operation of the transparent MBM

The test system (Dreszer et al., 2013) comprised four identical tMBMs which were installed as shown in Figure 2.1. Feed water (see Section 2.2.4) was filtered through two 10 µm pore size cartridge filters and was kept constant at a temperature of 20˚C. A pressure reducer (V782, Vink Kunststoffen B.V., Didam, The Netherlands) enabled a stable feed pressure of 1.7 bar for all experiments performed during the studies described in this paper. Before water entered the filtration cell, nutrients were added using a peristaltic pump (Masterflex L/S pumps, Cole-Palmer Instrument Company, Vernon Hills, Illinois, USA). The linear flow velocity of the feed water was monitored by a flow controller for each tMBM (8805/8905, Brooks Instrument, Hatfield, PA, USA) which was installed at the outlet of each monitor. The permeate rate was maintained by a peristaltic pump (Masterflex L/S pumps, Cole-Palmer Instrument Company, Vernon Hills, Illinois, USA). The fouling development was monitored by measuring the pressure drop over the feed channel and over the membrane, using a differential pressure transmitter (Deltabar S PMD70, Endress + Hauser, Maulburg, Germany; (Vrouwenvelder et al., 2009)). The pressures were measured at the monitor inlet, permeate outlet, and concentrate outlet. Temperature, flow velocity, flux, FCP, TMP, and nutrient supply were measured twice a day.

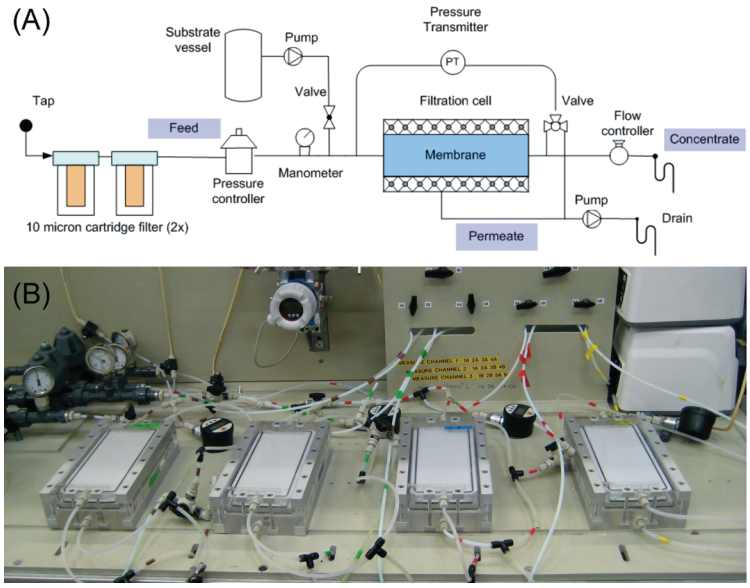

Figure 2.1: (A) configuration of the filtration setup and (B) picture of four monitors in parallel.

2.2.4 Feed water for the transparent MBM experiments

Drinking water prepared from anaerobic ground water (subsequently treated by aeration, rapid sand filtration deacidification, softening, and rapid sand filtration at treatment plant Spannenburg in The Netherlands) is distributed without primary chemical disinfection and without a disinfectant residual. This drinking water was used as feed water source for the crossflow filtration system experiments. The TCN in the feed water was 3×10^5 cells mL^{-1}. The number of colony forming units on R2A media (Reasoner & Geldreich, 1985) after 10 d incubation at 25˚C was 2×10^3 CFU mL^{-1}. There are significantly more microbial cells in water than can be cultured on growth media (Hammes et al., 2008; Lautenschlager et al., 2013).
As nutrients for the tMBM experiments, a solution of sodium acetate (NaCH3COO), sodium nitrate (NaNO3), and sodium di-hydrogen orthophosphate (NaH2PO4) in the mass ratio for C:N:P of 100:20:10, respectively, was employed at a final concentration of 1 mg L^{-1} of organic carbon. This nutrient composition has been used in several previous studies on biofilm formation and biofouling (Araujo et al., 2012; Miller et al., 2012; Vrouwenvelder et al., 2009). All chemicals were purchased in analytical grade from Boom B.V. (Meppel, The Netherlands). All chemicals were dissolved in milliQ water. The concentrated substrate solution (10 L) was dosed into the feed water prior to the filtration cell at a flow of 0.12

$L\,h^{-1}$ using a peristaltic pump (Masterflex). The dosage of the nutrient solution was tested periodically by measuring the weight of the dosing container. To restrict bacterial growth in the substrate dosage bottle, the pH value was adjusted to 11 by NaOH addition. Fresh substrate solutions were prepared every 2 d. The chemical dosage flow rate (0.12 L h^{-1}) was low compared to the feed water flow rate (28.2 L h^{-1}). So, the effect of the chemical dosage on the pH of the feed water was insignificant. The monitor was fed with 28.3 L per hour, requiring 28.3 mg acetate-C in the hourly dosed volume (0.12 L) of the concentrated acetate solution. The acetate-C stock solution concentration was 236 mg L^{-1} (28.3 mg/0.12 L), 236 times higher than the monitor feed water acetate-C concentration. The feed water before and after dosage of substrate and the concentrate had a pH value of 7.8. The nutrients were handled the same way as in previous research (Araujo et al., 2012; Dreszer et al., 2013; Miller et al., 2012; Vrouwenvelder et al., 2009).

2.2.5 Biofilm characterization

The procedures for biofilm characterization were described in (Dreszer et al., 2013). After the defined operation time, the transparent MBMs were opened and the biofilm was harvested with a cell scraper (TPP, St. Louis, MO, USA) and suspended in phosphate buffered saline; the solution was shaken for 30 min. Then, the biofilm sample was subjected to ultrasonic treatment (Bransonic, Berlin, Germany: model 5510E-DTH, output 135 W, 42 kHz), for 2 min. Afterwards, it was homogenized using an ultrasonic probe (Brandson Sonifier 250, G. Heinemann Ultraschall- und Labortechnik, Schwäbisch Gmü nd, Germany) in pulsating mode (20% sonification per time-unit) for 10 pulses with an output of 45 W. The obtained biofilm suspension was used for total organic carbon (TOC) and total cell number (TCN) determination.

2.2.5.1 Resistance

Prior to biofilm analysis and during operation, the resistance (R) was determined on the basis of the following calculations:

$$R = TMP / (\eta \times J)\ [m^{-1}] \qquad (1)$$

where TMP [Pa] is the transmembrane pressure, J [$m^3\ m^{-2}\ s^{-1}$] is the permeate flux, and η [Pa s] is the dynamic viscosity of the water at a given temperature, in this study 20˚C.

The TMP is the driving force for filtration. It is the average pressure difference between the feed and permeate:

$TMP = (P_{inlet} + P_{outlet}) / 2) - P_{permeate}$ [bar] (2)

The flux J of water passing a membrane is expressed as the amount of water V [L] flowing through a certain membrane area A [m^2] in time t [h]:

$J = V / (A \times t)$ [$Lm^{-2}h^{-1}$] (3)

The resistance in Eq. (1) is the sum of the membrane resistance and the resistance due to biofilm formation:

$R_{total} = R_{membrane} + R_{biofilm}$ [m^{-1}] (4)

The resistance measurement at t = 0 gives the virgin membrane resistance which is used to calculate the biofilm resistance:

$R_{biofilm} = R_{total} - R_{membrane} = R_{total} - R_{total(t=0)}$ [m^{-1}] (5)

2.2.5.2 TOC

To determine the TOC content of the biofilm (the sum of intra and extracellular organic carbon), an aliquot of the biofilm sample was placed in a TOC-free glass tube. The sample was treated with the ultrasonic probe (Brandson Sonifier 250, G. Heinemann Ultraschall- und Labortechnik, Schwäbisch Gmünd, Germany) in pulsating mode (20% sonication per time-unit) for 30 pulses with an output of 45 W. During the ultrasonic treatment, the sample was kept on ice for sample temperature control. The TOC was measured with a Shimadzu TOC analyzer (Shimadzu Scientific instruments, Kyoto, Japan).

2.2.5.3 TCN

A Neubauer Improved Counting Chamber was used for TCN determination of the biofilm sample. Bacterial cells were counted at 400× magnification with phase contrast using a Leica microscope (DM750, Leica, Wetzlar, Germany). Two times 5 squares were counted and the average value for 5 squares was taken for the calculation of the TCN by the following equation:

TCN = counted bacterial cells / (counted area [mm^2] x chamber depth [mm] x dilution) [cells/µL] (6)

2.2.5.4 Scanning electron microscopy (SEM)

Pieces of membrane (~1 cm^2) were used for SEM of the biofilms. The samples were fixed in 3% glutaraldehyde (Sigma–Aldrich, Steinheim, Germany) at 4˚C for 24 h, then washed twice in phosphate buffered saline and dehydrated in

increasing concentrations of ethanol (30, 50, 70, 90% for 20 min each; 96% for 30 min, twice). Finally, the samples were air dried in a drying chamber (45˚C, 30–60 min) and stored in a desiccator until microscopic investigation. To obtain the cross-section images, the pretreated membrane samples were placed in liquid nitrogen for shock freezing. At such low temperatures, the polymeric membrane and the organic biofilm became brittle. By breaking the frozen samples, sharp cross-sections without artifacts were obtained. The samples were sputtered with gold (Jeol JFC-1200 Fine Coater, Tokyo, Japan). SEM was performed with a JEOL JSM 6480 LV microscope (JEOL Technics Ltd., Tokyo, Japan) in high vacuum mode (emission electrons detection, acceleration voltage 6–10 kV, operating distance 10 mm).

2.2.5.5 Optical coherence tomography (OCT)

Imaging of the feed channel surface of the membrane was conducted *in situ* using a spectral domain optical coherence tomograph (Thorlabs Ganymede OCT System) fitted with a 5X telecentric scan lens (Thorlabs LSM03BB) which provides a maximum scan area of 100 mm^2. The OCT engine was configured to provide high resolution images with a sensitivity of 106 dB at 1.25 kHz A-scan rate. Volumetric images were created using the maximum intensity profile algorithm included in the instrument software (Thorlabs SD-OCT system software version 3.2.1) for a rectangular area 2 × 5 mm from 200 B-scans and 500 A-scans of 619 pixels corresponding to a physical depth of 1.1 mm. The axial resolution for the instrument is below 5.8 µm and the lateral resolution is 8 µm.

2.2.6 Experiments and operational conditions

Temperature, flow velocity, feed pressure, flux, nutrient concentration, and operation time were constant throughout each set of experiments. FCP and TMP varied during operation time in response to biofilm formation. Flux and nutrient concentration differed from experiment to experiment to study the relation with biofilm permeability and operational parameters. Furthermore, the applicability of the tMBM as an essential research tool for biofilm studies was pursued. Table 2.1 gives an overview of the experiments.

Table 2.1: Schematic setup of studies

Studies[a]	Feed spacer presence	Permeate production	Cross-flow velocity (m s^{-1})	Substrate dosage (1 mg/L acetate) C)	Section
Validation studies					2.3.1
Hydraulic characterization of monitor	yes	no	0–0.37	no	2.3.1.1
Flow field distribution	yes	no	0.1	no	2.3.1.2
Microfiltration use: internal fouling	no	yes	0.1	yes	2.3.1.3
Reproducibility	no/yes	yes	0.1	yes/no	2.3.1.4
Visual and optical observations	no	yes	0.1	yes/no	2.3.1.5
Application aspects of monitor					2.3.2
Biofilm characterization without feed spacer	no	yes	0.1	yes/no	2.3.2.1
Biofilm resistance with and without feed spacer	no/yes	yes	0.1	yes/no	2.3.2.2
FCP and biofilm resistance	yes	yes	0.1	yes/no	2.3.2.3

[a]All studies were carried out with 0.05 µm pore size membranes. The feed spacer was a 31 mil (787 µm) thick spacer as applied in practice. All studies with permeate production were performed at 20 L m^{-2} h^{-1}, except the reproducibility test (100 and 20 L m^{-2} h^{-1}). Nutrient dosage comprised 1 mg L^{-1} acetate C in the feed water.

2.3 Results

In this study, the tMBM was tested on suitability to study the hydraulic biofilm resistance (Section 2.3.1) and a number of monitor studies are presented to evaluate potential monitor applications (Section 2.3.2, Table 2.1).

2.3.1 Validation studies

2.3.1.1 Hydraulic characterization of the monitor

The relationship between linear flow velocity and FCP of the tMBM was calculated, using the methodology developed for spiral-wound membrane modules as applied in practice (Schock & Miquel, 1987). Mathematically, the pressure drop is expressed by:

$$\Delta P = \lambda \times ((\rho \times v^2)/2) \times L / dh \quad (7)$$

where λ is the friction coefficient, ρ the specific liquid density, *v* the linear velocity,

L the length of the membrane or MBM, and *d*h the hydraulic diameter. The friction coefficient is given by the correlation function (Schock & Miquel, 1987):

$\lambda = 6.23 \times Re^{-0.3}$ (8)

where Re is the Reynolds number. The measured relation between the linear flow velocity and pressure drop for the tMBM fitted very well with the calculated data using the formula for spiral-wound membrane elements (Figure 2.2). Evidently, the tMBM had similar spatial dimensions (height of the feed spacer channel) as spiral-wound membrane elements applied in practice, resulting in an identical relation between linear flow velocity and pressure drop.

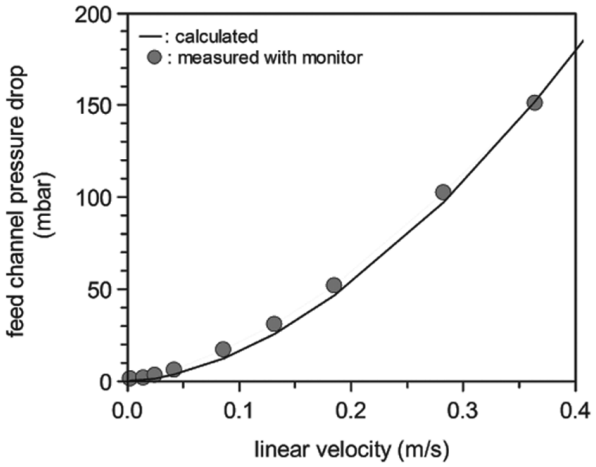

Figure 2.2: Linear flow velocity (m s^{-1}) and FCP (mbar) in the tMBM containing a feed spacer. The dots represent measured data and the line represents calculated data using the formula for spiral-wound membrane elements of Schock and Miquel (1987).

2.3.1.2 ***Flow field distribution***

The flow field distribution in the tMBM was determined by injecting a pulse of a colored solution (blue ink) into the feed water. The front of the colored solution was equally distributed over the width of the tMBM (Figure 2.3). The same flow regime was observed in the original MFS (Vrouwenvelder et al., 2007a) and in spiral-wound membrane elements (Van Gauwbergen & Baeyens, 1997).

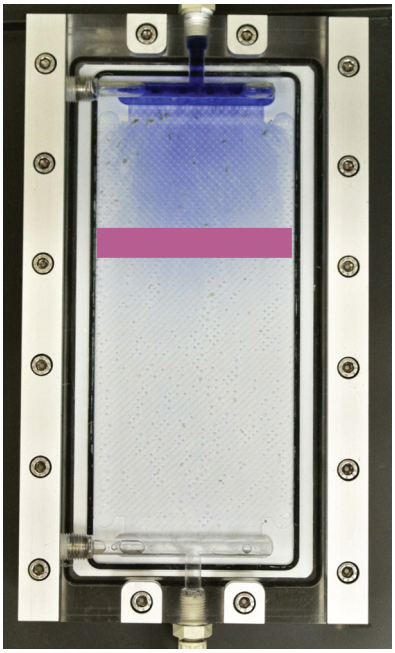

Figure 2.3: The front of the blue dye spiked to the water equally distributed over the width during transport through the monitor, as illustrated with the purple bar.

2.3.1.3 Microfiltration membrane use: internal fouling

SEM observations. In order to operate the tMBM under low pressure conditions and to exclude salt concentration polarization effects, a 0.05 µm pore size membrane was selected. The hydraulic resistance of this membrane was expected to be significantly lower than the resistance of biofilms, enabling accurate and sensitive measurement of the hydraulic biofilm resistance. It is important to determine whether internal membrane fouling occurs, adding to the TMP. To evaluate this, a tMBM was operated at constant flux (20 L m^{-2} h^{-1}) and linear flow velocity (0.1 m s^{-1}), fed with tap water supplemented with a biodegradable nutrient (1 mg L^{-1} acetate C). During 4 d of operation accumulation of biomass on the membrane was observed visually through the transparent monitors. SEM examination (up to 10,000× magnification) of membrane samples taken from the tMBM, after that period of operation, showed that fouling accumulated only on the membrane surface and not in the membrane pores (Figure 2.4). Clearly, the microorganisms (≥~1 µm, Figure 2.4) were retained by the membrane due to the pore size of the membrane (0.05 µm). No apparent fouling could be visually observed in the pores of the membrane (Dreszer et al., 2013).

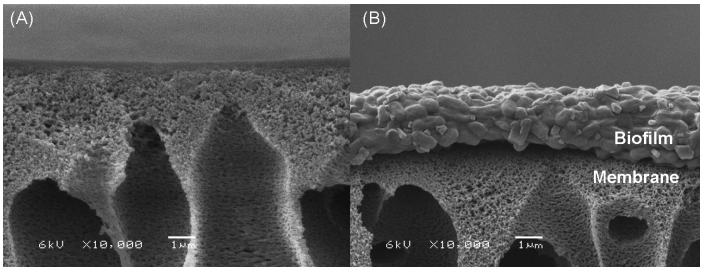

Figure 2.4: Scanning electron micrograph of a membrane cross-section. (A) original membrane, (B) membrane with biofilm after 4 d of operation (Dreszer et al., 2013).

Resistance of virgin and mechanically cleaned membranes. In addition to the SEM analyses, the possibility of adsorption of macromolecules in the pores of the membrane affecting the resistance was determined by experiments performed under the same conditions (substrate, flux, and crossflow velocity) as the SEM observations. The total resistance was determined before (virgin membrane), after fouling and after subsequent cleaning by removal of the biofilm. Experiments were performed in triplicate and biomass was removed by scraping. Scraping off the fouled membrane reduced the resistance to values similar to the virgin membrane resistance (Figure 2.5). The scraped membrane had a resistance up to 5% higher than the virgin membrane probably caused by residual biofilm on the membrane surface. The effect of internal membrane fouling on the resistance is therefore negligible compared to the effect of fouling on the membrane surface (Figure 2.5).

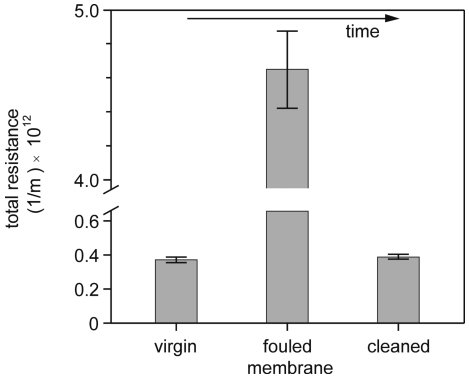

Figure 2.5: Resistance prior to fouling (virgin membrane), after fouling, and after subsequent cleaning by scraping of the fouled membrane surface to remove the accumulated biofilm. A similar resistance of the virgin and cleaned membrane indicates that fouling predominantly occurred on the membrane surface (Dreszer et al., 2013).

2.3.1.4 ***Reproducibility***

The reproducibility of the results obtained from the monitor experiments was examined. An experiment without feed spacer was repeated six times at the same flux (100 L m^{-2} h^{-1}), linear flow velocity (0.1 m s^{-1}), and substrate concentration (1 mg L^{-1} acetate C) for 4 d. The same development of total resistance and biomass accumulation (measured as TOC) was observed (Figure 2.6). The average TOC concentration was 0.101 ± 0.005 mg cm^{-2}, showing a 5% standard deviation.

Experiments conducted with feed spacer at a flux of 20 L m^{-2} h^{-1} showed the same development of resistance and biomass (data not shown). Both reproducibility and comparability of results obtained with this test system and configuration were verified.

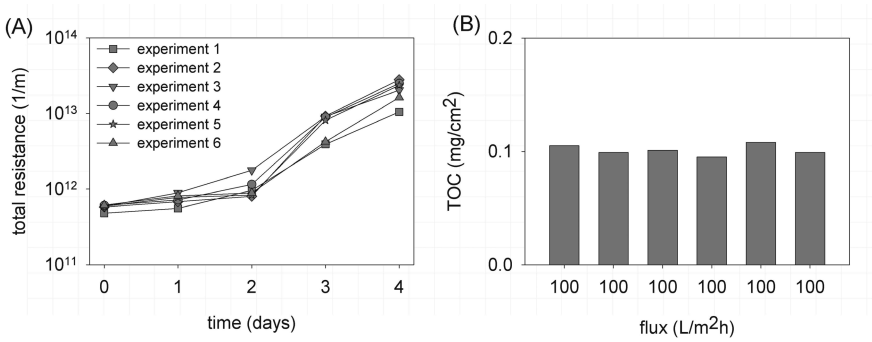

Figure 2.6: Development of the total resistance for six experiments operated at a flux of 100 L m^{-2} h^{-1} at a crossflow velocity of 0.1 m s^{-1} with a substrate dosage of 1 mg L^{-1} acetate C in the feed water (A) and the amount of accumulated biomass at the end of the operational period (B).

2.3.1.5 ***Visual and optical observations***

The choice of PMMA as material for the tMBM enables visual and optical observations of biofilm development in time and spatial distribution over the membrane surface during tMBM operation (Figure 2.7). To investigate the visual appearance of the biofilm, two tMBMs were operated in parallel for 4 d at a constant flux and crossflow velocity without feed spacer. For one tMBM, the feed water was supplemented with additional nutrients (1 mg L^{-1} acetate C), while the other monitor had no nutrient dosage (blank).

With nutrient dosage a more rapid accumulation of material on the membrane was observed. The material seemed to be equally distributed over the membrane surface area by visual inspection during tMBM operation. The material

accumulated gradually in time. A distinct difference in color was detected between the tMBM with and without substrate dosage (Figure 2.7). With nutrient dosage the accumulated material had a darker color. *In situ* OCT imaging confirmed biofilm formation throughout the feed-channel of the monitor supplied with substrate (Figure 2.7 C and D). The scanned rectangular area of 2 × 5 mm showed a heterogeneous biofilm structure on the membrane, varying in thickness from a few µm to ~200 µm. The structure of the biofilm growing on the window differed from the structure growing on the membrane. Biochemical analysis after 4 d tMBM operation confirmed that biomass had accumulated on the membrane with substrate dosage. The transparent MBM is suitable to study biofouling development using *in situ* non-destructive visual and optical observations.

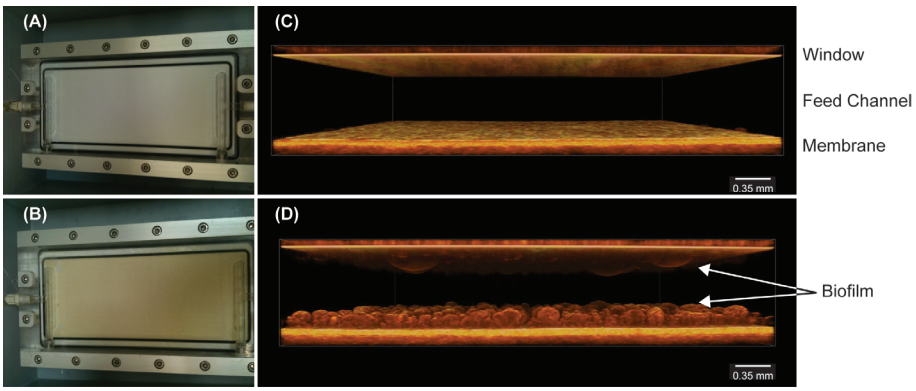

Figure 2.7: Visual observations and OCT images for the feed channel in the tMBM after 4 d operation without (A, C) and with dosage (B, D) of a biodegradable substrate to the feed water.

2.3.2 Application aspects of monitor

Application aspects of the transparent MBM were tested in a series of experiments to evaluate the suitability of the monitor.

2.3.2.1 Biofilm characterization without feed spacer

The development of transmembrane resistance and biofilm amount was determined using tMBMs without feed spacer at a flux of 20 L m^{-2} h^{-1}. In a parallel study, four tMBMs were operated without nutrient dosage and four tMBMs with nutrients dosage (1 mg L^{-1} acetate C). After day 1, 2, 3, and 4 of operation, a tMBM with and a tMBM without nutrient dosage were opened for biomass quantification.

With nutrient supply, a strong increase of total resistance (Figure 2.8 A) and biomass amount (Figure 2.8 B and C) in time was found. After 4 d of operation, the total resistance was about 50 times higher than the intrinsic resistance of the 0.05 µm pore membrane (Figure 2.8 A). This difference in resistance enables distinguishing the resistance of the biofilm from that of the membrane. After 4 d of operation, the bacterial cell number and TOC concentration on the membrane were several log-units higher in the nutrient supplied system (Figure 2.8 B and C), indicating that biomass accumulated predominantly as a growing biofilm.

It can be concluded that the monitor enables to study biofilm development and the hydraulic biofilm resistance.

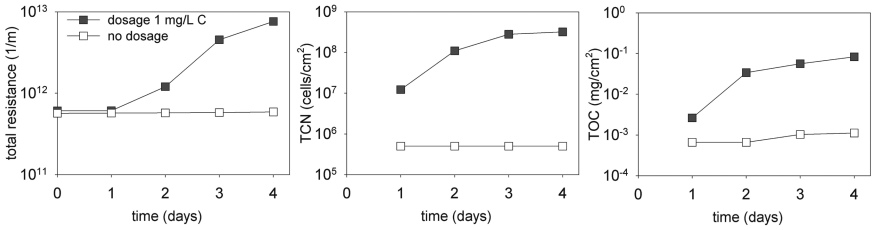

Figure 2.8: Development of total resistance (A), TCN (total bacterial cell number: B) and TOC (total organic carbon: C) without feed spacer presence during 4 d of operation at a flux of 20 L m^{-2} h^{-1} and crossflow velocity of 0.1 m s^{-1} with and without nutrient dosage (1 mg L^{-1} acetate C). The increase in resistance is caused by the biofilm formation.

2.3.2.2 ***Biofilm resistance with and without feed spacer***

Feed spacers have been shown to play an important part in fouling (Bakeret al., 1995; Suwarno et al., 2012; Tran et al., 2007; van Paassen et al., 1998; Vrouwenvelder etal.,2009). In the present study, the effect of spacer presence on transmembrane hydraulic biofilm resistance was evaluated. The development of total resistance was studied using monitors with and without feed spacer and with and without nutrient dosage.

Regardless of feed spacer presence, the same initial transmembrane resistance and the same increase of total resistance was observed with nutrient supply (Figure 2.9), at operating conditions (flux and crossflow) as applied in practice for spiral-wound NF and RO membrane elements. The monitor can be used to evaluate the effect of a feed spacer on hydraulic biofilm resistance.

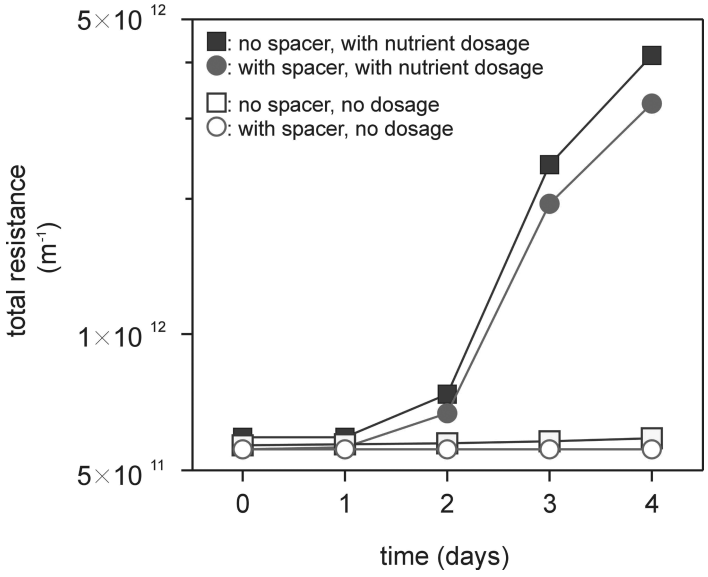

Figure 2.9: Development of total resistance in monitors with and without feed spacer during 4 d at a flux of 20 L m^{-2} h^{-1} and crossflow velocity of 0.1 m s^{-1} with and without nutrient dosage (1 mg L^{-1} acetate C) (Dreszer et al., 2013).

2.3.2.3 FCP and transmembrane resistance

Biofilm formation can have a negative impact on NF and RO membrane performance by increasing the TMP and the FCP. Past and current monitors used for membrane biofouling research are suitable only to study either the TMP or the FCP. The increase of both, total transmembrane resistance and FCP could be determined using the newly developed tMBM. tMBMs containing a feed spacer were operated at a flux of 20 L m^{-2} h^{-1} and a crossflow velocity of 0.1 m s^{-1} without and with nutrient dosage (1 mg L^{-1} acetate C). With nutrient supply, both the transmembrane biofilm resistance and the FCP increased in time (Figure 2.10).

The tMBM enables the assessment of biofilm formation effects on both the TMP and FCP. The presence of elevated nutrient concentrations in the feed water speeds up the biofilm formation, enabling to perform short-term biofouling studies.

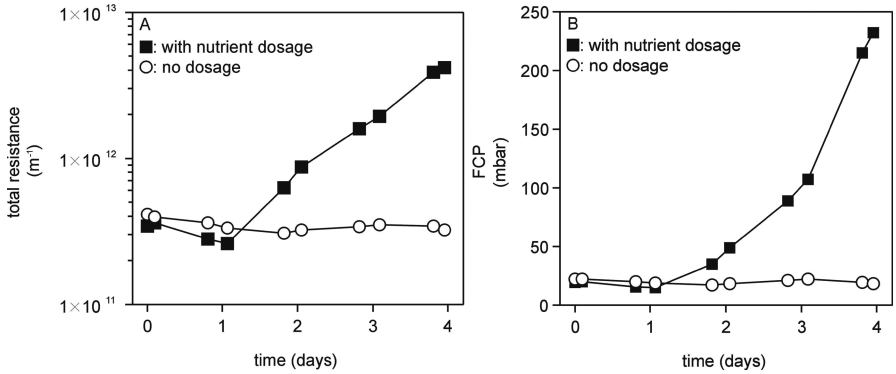

Figure 2.10: Total resistance (A) and FCP (B) development over time at a flux of 20 L m^{-2} h^{-1} and crossflow velocity of 0.1 m s^{-1} with and without nutrient dosage (1 mg L^{-1} acetate C). The experiment was performed with feed spacer.

2.4 Discussion

2.4.1 Evaluation of the tMBM

A transparent MBM is developed, enabling to study the hydraulic biofilm resistance and the direct impact of biofilm formation on the TMP and FCP. The tMBM is representative for spiral-wound membrane elements used in practice with regard to the materials used (membranes and spacers), spatial dimensions (height of feed and product spacer channels), hydraulics (FCP and flow distribution), and operational conditions (transmembrane flux and crossflow velocity range: e.g. a flux of 20 L m^{-2} h^{-1} and a crossflow velocity of 0.1 m s^{-1}). Using the tMBM, fouling can be quantified and characterized by: (i) the increase of transmembrane resistance and FCP; (ii) *in situ*, real-time, and non-destructive observations; and (iii) analysis of membrane and spacer sampled from the tMBM. The scale of the tMBM makes handling easy, minimizes equipment and operation costs, and reduces chemical and water consumption. Compared to the description of an ideal monitor (Flemming et al., 1998; Flemming, 2003; Vrouwenvelder et al., 2007a), the tMBM fulfills most requirements making it a well-suited tool for biofouling prediction and control research.

The microfiltration membrane (pore size 0.05 µm) used in the tMBM prevents salt concentration polarization and allows operation at low pressures, thus permitting accurate measurement of the intrinsic hydraulic biofilm resistance. The contribution of the membrane resistance to the total resistance is much

smaller than the contribution of the hydraulic biofilm resistance (see Figures 2.8-2.10) allowing more accurate measurements using standard pressure transducers. TMP and FCP measurements are sufficiently sensitive to allow the study of hydraulic biofilm resistance and development.

2.4.2 Application of the tMBM

Unique aspects of the tMBM, as illustrated in Section 2.3.1, are the possibilities to study and monitor the (i) hydraulic biofilm resistance, (ii) performance parameters FCP and TMP, and (iii) *in situ* spatially resolved observations of the biofilm thickness in the transparent MBM. The tMBM is suitable as a simulator for spiral-wound modules as previously discussed (Schock & Miquel, 1987) and integrates well into the laboratory environment. Such biofouling studies can be performed with and without a feed spacer and the tMBM is adaptable to various spacer designs (thickness, geometry, and porosity) operated under varying conditions.

OCT was developed in 1991 by Huang et al. (1991) as a tool for medical imaging. This relatively new optical method has the ability to non-destructively provide volumetric imaging of the biofilm with micron resolution (Derlon et al., 2013; Derlon et al., 2012; Haisch & Niessner, 2007; Janjaroen et al., 2013; Wagner et al., 2010; Xi et al., 2006). Since 2006, the OCT has been used to study biofilm structures in water systems: degradation by a disinfectant (Haisch & Niessner, 2007), impact of flow conditions (Wagner et al., 2010), mechanisms of *Escherichia coli* attachment on biofilms (Janjaroen et al., 2013), and metazoan activity in relation to biofilm structure and flux in ultrafiltration membranes (Derlon et al., 2013; Derlon et al., 2012). The tMBM is ideally suited for OCT studies of *in situ* biofilm development in membrane systems (Figure 2.7). The OCT instrument axial resolution is less than 6 µm and the lateral resolution 8 µm. OCT images provide a quantitative high-resolution spatially-resolved means to characterize biofilm thickness, structural heterogeneity, growth, and detachment over large areas of membrane and spacer. Examples of studies could be the influence of operational parameters (flux and crossflow velocity), spacer design (spacer geometry), and control strategies on biofilm development and removal. Such detailed biofilm studies may lead to novel and more effective strategies to control membrane biofouling.

Additional tools needed to complement current research techniques for gaining insight into membrane (bio)fouling characterization and control are: (i) a monitor with the length of a membrane module enabling direct visual observations of

accumulated fouling and monitoring of all performance parameters (FCP, flux, and salt passage) during operation at pressures and conditions as applied in practice and (ii) a high pressure miniature monitor to unravel the relationship between concentration polarization, biofouling, and membrane performance. Since the low-pressure tMBM showed to be suitable for biofilm studies in membrane systems, a high-pressure version of tMBM is being developed.

2.4.3 Representativeness and validation of membrane biofouling monitors

In membrane conference papers and peer reviewed journals membrane biofouling monitors have been presented as suitable tools for biofouling control studies. In commercial brochures, membrane biofouling monitors have been advertised by their suppliers. In general, no data on monitor validation is included, while a critical evaluation of the representativeness of the monitor results for practice hardly exists. For a comprehensive understanding of the state of the art in biofouling control, it is essential to address and report monitor validation tests in peer-reviewed papers.

Many membrane biofouling monitor studies have been described, from which the laboratory conditions are not representative for conditions of pilot and full scale membrane installations. However, a biofouling control approach effective under non-representative laboratory conditions is most probably not predictive for industrial practice.

The results reported in this paper present a versatile tool for biofilm research and biofouling control that has been validated (Sections 2.3.1.1–2.3.1.4) under laboratory conditions representative for the application of spiral-wound membrane modules.

2.5 Conclusions

The results showed that the newly developed tMBM is representative for spiral-wound membrane elements with regard to spacer channel height and hydrodynamic behavior. The monitor is suitable for (i) measuring the feed channel pressure drop and TMP (ii) *in situ,* real-time and non-destructive (visual and optical) observations of accumulated material, and (iii) analysis of membrane and spacer from the tMBM. The monitor proved to be easy to handle.

The results presented in this paper led to the following conclusions for the tMBM:

(1) The tMBM can be used to quantify the intrinsic hydraulic biofilm resistance.

(2) The tMBM can be operated:
   (a) with and without feed spacer;
   (b) with and without permeate production;
   (c) at crossflow and flux conditions as applied in practice;
   (d) with several water types such as surface water, brackish water, and seawater.

Acknowledgements

This work was performed at Wetsus, Centre of Excellence for Sustainable Water Technology (www.wetsus.nl). Wetsus is funded by the Dutch Ministry of Economic Affairs, the European Union European Regional Development Fund, the Province of Fryslân, the city of Leeuwarden, and by the EZ-KOMPAS Program of the "Samenwerkingsverband Noord-Nederland." The authors like to thank the par- ticipants of the research theme "Biofouling" and Evides waterbedrijf for the fruitful discussions and their financial support. In addition, the authors would especially like to thank the students Malgorzata Nowak, Stanislaw Wojciechowski, Judita Laurinonyte, Nathalie Juranek, and Zhen Xiang for their great support with the experimental work in the laboratory. The photographs of the tMBM were taken by Christina Kappel and her work is herewith gratefully acknowledged.

References

Araujo, P. A., Kruithof, J. C., Van Loosdrecht, M. C. M., & Vrouwenvelder, J. S. (2012). The potential of standard and modified feed spacers for biofouling control. *Journal of Membrane Science, 403-404*(0), 58-70.

Baker, J., Stephenson, T., Dard, S., & Côte, P. (1995). Characterisation of Fouling of Nanofiltration Membranes used to Treat Surface Waters. *Environmental Technology, 16*(10), 977-985.

Baker, J. S., & Dudley, L. Y. (1998). Biofouling in membrane systems - A review. *Desalination, 118*(1-3), 81-89.

Creber, S. A., Vrouwenvelder, J. S., van Loosdrecht, M. C. M., & Johns, M. L. (2010). Chemical cleaning of biofouling in reverse osmosis membranes evaluated using magnetic resonance imaging. *Journal of Membrane Science, 362*(1-2), 202-210.

Derlon, N., Koch, N., Eugster, B., Posch, T., Pernthaler, J., Pronk, W., & Morgenroth, E. (2013). Activity of metazoa governs biofilm structure formation and enhances permeate flux during Gravity-Driven Membrane (GDM) filtration. *Water Research, 47*(6), 2085-2095.

Derlon, N., Peter-Varbanets, M., Scheidegger, A., Pronk, W., & Morgenroth, E. (2012). Predation influences the structure of biofilm developed on ultrafiltration membranes. *Water Research, 46*(10), 3323-3333.

Dreszer, C., Vrouwenvelder, J. S., Paulitsch-Fuchs, A. H., Zwijnenburg, A., Kruithof, J. C., & Flemming, H. C. (2013). Hydraulic resistance of biofilms. *Journal of Membrane Science, 429*(0), 436-447.

Flemming, H.-C., Tamachkiarowa, A., Klahre, J., & Schmitt, J. (1998). Monitoring of fouling and biofouling in technical systems. *Water Science and Technology, 38*(8-9), 291-298.

Flemming, H. C. (2003). Role and levels of real-time monitoring for successful anti-fouling strategies - An overview *Water Science and Technology* (Vol. 47, pp. 1-8).

Haisch, C., & Niessner, R. (2007). Visualisation of transient processes in biofilms by optical coherence tomography. *Water Research, 41*(11), 2467-2472.

Hammes, F., Berney, M., Wang, Y., Vital, M., Köster, O., & Egli, T. (2008). Flow-cytometric total bacterial cell counts as a descriptive microbiological parameter for drinking water treatment processes. *Water Research, 42*(1-2), 269-277.

Huang, D., Swanson, E. A., Lin, C. P., Schuman, J. S., Stinson, W. G., Chang, W., Hee, M.R., Flotte, T., Gregory, K., Puliafito, C.A.,& Fujimoto, J. G. (1991). Optical Coherence Tomography. *Science, 254*(5035), 1178-1181.

Huiting, H., Kappelhof, J. W. N. M., & Bosklopper, T. G. J. (2001). Operation of NF/RO plants: From reactive to proactive. *Desalination, 139*(1-3), 183-189.

Janjaroen, D., Ling, F., Monroy, G., Derlon, N., Mogenroth, E., Boppart, S. A., Liu, W.-T., & Nguyen, T. H. (2013). Roles of ionic strength and biofilm roughness on adhesion kinetics of Escherichia coli onto groundwater biofilm grown on PVC surfaces. *Water Research, 47*(7), 2531-2542.

Lautenschlager, K., Hwang, C., Liu, W. T., Boon, N., Köster, O., Vrouwenvelder, H., Egli, T., & Hammes, F. (2013). A microbiology-based multi-parametric approach towards assessing biological stability in drinking water distribution networks. *Water Research, 47*(9), 3015-3025.

Miller, D. J., Araujo, P. A., Correia, P. B., Ramsey, M. M., Kruithof, J. C., van Loosdrecht, M. C. M., Freeman, B.D., Paul, D.R., Whiteley, M., & Vrouwenvelder, J. S. (2012). Short-term adhesion and long-term biofouling testing of polydopamine and poly(ethylene glycol) surface modifications of membranes and feed spacers for biofouling control. *Water Research, 46*(12), 3737-3753.

Nederlof, M. M., Kruithof, J. C., Taylor, J. S., Van Der Kooij, D., & Schippers, J. C. (2000). Comparison of NF/RO membrane performance in integrated membrane systems. *Desalination, 131*(1-3), 257-269.

Prest, E. I., Staal, M., Kuehl, M., van Loosdrecht, M. C. M., & Vrouwenvelder, J. S. (2012). Quantitative measurement and visualization of biofilm O2 consumption rates in membrane filtration systems. *Journal of Membrane Science, 392-393*(0), 66-75.

Reasoner, D. J., & Geldreich, E. E. (1985). A new medium for the enumeration and subculture of bacteria from potable water. *Applied and Environmental Microbiology, 49*(1), 1-7.

Ridgway, H. F., & Flemming, H. C. (1996). Biofouling of membranes. In J. Mallevialle, Odendaal, P. E., Wiesner, M. R. (Ed.), *Water treatment membrane processes* (pp. 629 - 640). New York: McGraw-Hill.

Ridgway, H. F., Kelly, A., Justice, C., & Olson, B. H. (1983). Microbial fouling of reverse-osmosis membranes used in advanced wastewater treatment technology: Chemical, bacteriological, and ultrastructural analyses. *Applied and Environmental Microbiology, 45*(3), 1066-1084.

Schneider, R. P., Ferreira, L. M., Binder, P., Bejarano, E. M., Góes, K. P., Slongo, E., Machado, C.R., & Rosa, G. M. Z. (2005). Dynamics of organic carbon and of bacterial populations in a conventional pretreatment train of a reverse osmosis unit experiencing severe biofouling. *Journal of Membrane Science, 266*(1-2), 18-29.

Schock, G., & Miquel, A. (1987). Mass transfer and pressure loss in spiral wound modules. *Desalination, 64*(0), 339-352.

Shannon, M. A., Bohn, P. W., Elimelech, M., Georgiadis, J. G., Marinas, B. J., & Mayes, A. M. (2008). Science and technology for water purification in the coming decades. *Nature, 452*(7185), 301-310.

Suwarno, S. R., Chen, X., Chong, T. H., Puspitasari, V. L., McDougald, D., Cohen, Y., Rice, S.A., & Fane, A. G. (2012). The impact of flux and spacers on biofilm development on reverse osmosis membranes. *Journal of Membrane Science, 405-406*, 219-232.

Tasaka, K., Katsura, T., Iwahori, H., & Kamiyama, Y. (1994). Analysis of RO elements operated at more than 80 plants in Japan. *Desalination, 96*(1-3), 259-272.

Tran, T., Bolto, B., Gray, S., Hoang, M., & Ostarcevic, E. (2007). An autopsy study of a fouled reverse osmosis membrane element used in a brackish water treatment plant. *Water Research, 41*(17), 3915-3923.

van der Meer, W. G. J. (2003). *Mathematical modeling of NF and RO membrane filtration plants and modules.* (PhD thesis). Retrieved from http://www.sciencedirect.com/science/article/pii/S0011916403003965

Van Gauwbergen, D., & Baeyens, J. (1997). Macroscopic fluid flow conditions in spiral-wound membrane elements. *Desalination, 110*(3), 287-299.

van Paassen, J. A. M., Kruithof, J. C., Bakker, S. M., & Kegel, F. S. (1998). Integrated multi-objective membrane systems for surface water treatment: pre-treatment of nanofiltration by riverbank filtration and conventional ground water treatment. *Desalination, 118*(1-3), 239-248.

Vrouwenvelder, J. S., Bakker, S. M., Cauchard, M., Le Grand, R., Apacandie, M., Idrissi, M., Lagrave, S., Wessel, L.P., van Passen, J.A.M., Kruithod, J.C., & van Loosdrecht, M. C. M. (2007a). The Membane Fouling Simulator: a suitable tool for prediction and characterisation of membrane fouling. *Water Sci Technology, 55*(55), 197 - 205.

Vrouwenvelder, J. S., Bakker, S. M., Wessels, L. P., & van Paassen, J. A. M. (2007b). The Membrane Fouling Simulator as a new tool for biofouling control of spiral-wound membranes. *Desalination, 204*(1-3), 170-174.

Vrouwenvelder, J. S., Buiter, J., Riviere, M., van der Meer, W. G. J., van Loosdrecht, M. C. M., & Kruithof, J. C. (2010). Impact of flow regime on pressure drop increase and biomass accumulation and morphology in membrane systems. *Water Research, 44*(3), 689-702.

Vrouwenvelder, J. S., Graf von der Schulenburg, D. A., Kruithof, J. C., Johns, M. L., & van Loosdrecht, M. C. M. (2009). Biofouling of spiral-wound nanofiltration and reverse osmosis membranes: A feed spacer problem. *Water Research, 43*(3), 583-594.

Vrouwenvelder, J. S., Hinrichs, C., Van der Meer, W. G. J., Van Loosdrecht, M. C. M., & Kruithof, J. C. (2009). Pressure drop increase by biofilm accumulation in spiral wound RO and NF membrane systems: role of substrate concentration, flow velocity, substrate load and flow direction. *Biofouling, 25*(6), 543-555.

Vrouwenvelder, J. S., Manolarakis, S. A., van der Hoek, J. P., van Paassen, J. A. M., van der Meer, W. G. J., van Agtmaal, J. M. C., Prummel, H.D.M., Kruithof, J.C., & van Loosdrecht, M. C. M. (2008). Quantitative biofouling diagnosis in full scale nanofiltration and reverse osmosis installations. *Water Research, 42*(19), 4856-4868.

Vrouwenvelder, J. S., Van Loosdrecht, M. C. M., & Kruithof, J. C. (2011). A novel scenario for biofouling control of spiral wound membrane systems. *Water Research, 45*(13), 3890-3898.

Vrouwenvelder, J. S., van Paassen, J. A. M., Wessels, L. P., van Dam, A. F., & Bakker, S. M. (2006). The Membrane Fouling Simulator: A practical tool for fouling prediction and control. *Journal of Membrane Science, 281*(1-2), 316-324.

Wagner, M., Taherzadeh, D., Haisch, C., & Horn, H. (2010). Investigation of the mesoscale structure and volumetric features of biofilms using optical coherence tomography. *Biotechnology and Bioengineering, 107*(5), 844-853.

Xi, C., Marks, D., Schlachter, S., Luo, W., & Boppart, S. A. (2006). High-resolution three-dimensional imaging of biofilm development using optical coherence tomography. *Journal of Biomedical Optics, 11*(3).

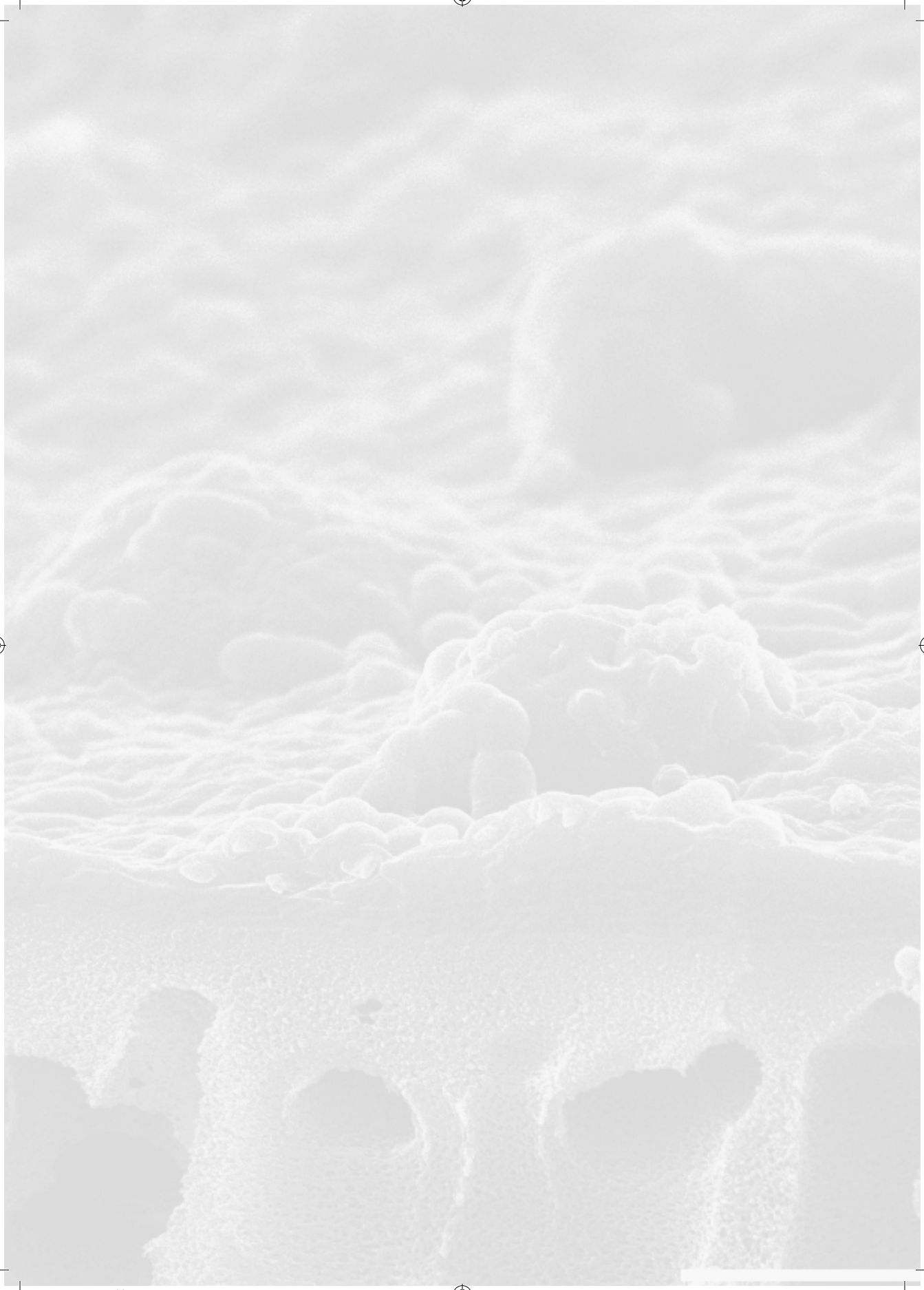

Chapter 3

Hydraulic Resistence of Biofilms

This chapter is published as:
C. Dreszer, J.S. Vrouwenvelder, A.H. Paulitsch-Fuchs, A. Zwijnenburg, J.C. Kruithof,
H.-C. Flemming, Hydraulic resistance of biofilms,
Journal of Membrane Science 429 (2013) 436-447.

Abstract

Biofilms may interfere with membrane performance in at least three ways: (i) increase of the transmembrane pressure drop, (ii) increase of feed channel (feed-concentrate) pressure drop, and (iii) increase of transmembrane passage. Given the relevance of biofouling, it is surprising how few data exist about the hydraulic resistance of biofilms that may affect the transmembrane pressure drop and membrane passage. In this study, biofilms were generated in a lab scale crossflow microfiltration system at two fluxes (20 and 100 L m^{-2} h^{-1}) and constant crossflow (0.1 m s^{-1}). As a nutrient source, acetate was added (1.0 mg L^{-1} acetate C) besides a control without nutrient supply. A microfiltration (MF) membrane was chosen because the MF membrane resistance is very low compared to the expected biofilm resistance and, thus, biofilm resistance can be determined accurately. Transmembrane pressure drop was monitored. As biofilm parameters, thickness, total cell number, TOC, and extracellular polymeric substances (EPS) were determined, it was demonstrated that no internal membrane fouling occurred and that the fouling layer actually consisted of a grown biofilm and was not a filter cake of accumulated bacterial cells. At 20 L m^{-2} h^{-1} flux with a nutrient dosage of 1 mg L^{-1} acetate C, the resistance after 4 days reached a value of 6 x 10^{12} m^{-1}. At 100 L m^{-2} h^{-1} flux under the same conditions, the resistance was 5 x 10^{13} m^{-1}. No correlation of biofilm resistance to biofilm thickness was found; Biofilms with similar thickness could have different resistance depending on the applied flux. The cell number in biofilms was between 4 x 10^{7} and 5 x 10^{8} cells cm^{-2}. At this number, bacterial cells make up less than a half percent of the overall biofilm volume and therefore did not hamper the water flow through the biofilm significantly. A flux of 100 L m^{-2} h^{-1} with nutrient supply caused higher cell numbers, more biomass, and higher biofilm resistance than a flux of 20 L m^{-2} h^{-1}. However, the biofilm thickness after 4 days at a flux of 100 L m^{-2} h^{-1} (97 mm) was in the same order of magnitude as the thickness of a biofilm at a flux of 20 L m^{-2} h^{-1} (114 mm). An increase of flux caused an increased biofilm resistance while a decrease of flux caused a decreased resistance. The effect was reversible. It is suggested that the biofilm resistance is mainly attributed to EPS, probably due to the tortuosity ("hair-in-sink-effect") of the biopolymers to water molecules travelling across the biofilm. The data show clearly that biofilm resistance (6 x 10^{12} m^{-1}) was high compared to the intrinsic resistance of the employed MF membrane (5 x 10^{11} m^{-1}). However, in nanofiltration (intrinsic membrane resistance ca. 2 x 10^{13} m^{-1}) and reverse osmosis membranes (intrinsic resistance ca. 9 x 10^{13} m^{-1}), the biofilm will not contribute significantly to the overall resistance.

3.1 Introduction

Membrane technology has developed into a very powerful process for water treatment and it experiences a steady increase in application, sophistication, and efficacy. At the same time, membrane systems have turned out to provide popular and ample living space for diverse feedwater-borne microorganisms, which can freely access, virtually all surfaces in these systems. The relationship between bacteria and membranes has been described poetically as "love at first sight" (Flemming, 2000): i.e., membrane systems are bound to be colonized by bacteria. Newly attached bacterial cells grow into biofilms as long as nutrients are supplied by the water and/or from the surfaces. The biofilm lifestyle is an extremely successful mode of life on Earth (Stoodley et al., 2002) with a high degree of physical, chemical, and biological heterogeneity (Stewart & Franklin, 2008). It is in biofilms where the processes for environmental self-purification occur, and microbiological processes are widely used for both drinking and waste water treatment (Flemming & Wingender, 2003). Exactly the same processes occur in membrane systems. Operators of membrane facilities are not especially happy about this love affair between membranes and bacteria because it can seriously impair the performance of membrane processes. This problem is called "biofouling", which is purely operationally defined and is generally referring to the interference of biofilms in membrane processes, causing reduced product quality/ quantity or biodeterioration of the membranes or module components. The acceptable level of interference usually represents an arbitrary threshold defined by the manufacturer or operator (Flemming, 2011). The use of biocides is perhaps the most commonly applied method for controlling biofilms and biofouling (Winters et al., 1983), but this strategy is based on the historically successful medical paradigm, which postulates that killing of the fouling bacteria solves the problem (Kim et al., 2009). This appears plausible, but it works only in living organisms, which possess an immune system that is able to dispose of the dead or injured microbial cells. In water-treatment systems, this is not the case because killing alone does not necessarily equate to cleaning, so dead biomass will remain in place and will support rapid regrowth. The lack of cleaning effectiveness by biocides is frequently observed in practice but rarely published (Klahre & Flemming, 2000). More efficacious approaches for biofouling control might involve limiting the extent of biofilm growth or a mitigation of the effects of biofouling. For example, limiting the extent of biofilm formation may be achieved by nutrient starvation (Flemming

& Ridgway, 2009; Griebe & Flemming, 1998). Indeed, nutrients are the driving force for biofilm growth in membrane systems and it is important not only to consider organic carbon but also phosphate (Vrouwenvelder et al., 2007a; Vrouwenvelder et al., 2010a; Vrouwenvelder et al., 2009a) as viable nutrient sources. Therefore, biodegradable substrates are eligible as potential biomass, but these are usually not addressed by biocide treatment per se. Such considerations suggest that it may be possible (or desirable) "to live with biofilms", i.e., to accept a tolerable extent of biofilm growth below the biofouling interference threshold. Thus, an important question is: how and when do biofilms interfere with membrane processes? Biofilms can affect membrane systems in various ways, ranging from an increase of transmembrane resistance, crossflow resistance, i.e., feed-concentrate pressure drop (Vrouwenvelder et al., 2010a), precipitation of mineral deposits, e.g., $CaCO_3$ scaling, accumulation of abiotic particles due to the adhesive properties of the biofilm matrix (Flemming, 2002), to even an enzymatic attack on the membrane or the glue lines (Ridgway & Flemming, 1996). Furthermore, biofilms can contribute to concentration polarization (Chong et al., 2008; Herzberg & Elimelech, 2008; Vrouwenvelder et al., 2007b).

Intuitively, one of the most plausible explanations for a decline of membrane performance may be the contribution of a biofilm (as a secondary membrane) to the overall transmembrane resistance. In that case, the hydraulic resistance of the biofilm is a crucial consideration. Chong et al. (2008) investigated biofouling of reverse osmosis (RO) membranes, identifying concentration polarization and not biofilm resistance per se as a key factor leading to flux loss. However, Chong and coworkers did not investigate the contribution of individual biofilm components to the flux decline. For a more complete understanding of the role of biofilms in membrane performance loss, the major components of biofilms and their relative contributions to flux decline should be considered. Biofilms mainly consist of (1) the bacterial cells and (2) the complex matrix of extracellular polymeric substances (EPS), which in turn consists of polysaccharides, proteins, extracellular DNA and lipids (Flemming & Wingender, 2010). The cell density in a drinking water biofilm of 100 mm thickness is usually in the range of 7–8 x 10^8 cells cm^{-2} (Wingender & Flemming, 2001), which represents less than 5% of the total biofilm volume. The major fraction is composed of EPS, strongly hydrated with water. Microorganisms form the EPS matrix, which holds the microbial cells together and attaches the biofilm to the membrane and spacer surface. The EPS, which has been postulated to contribute most to the hydraulic resistance of biofilms (Chong et al., 2008),

consist of highly hydrated biopolymers, forming a hydrogel with a water content of 95–99% (Wingender & Flemming, 2004).

The aim of the present study was to determine the resistance of biofilms grown under defined conditions at two constant fluxes, with and without an external supply of acetate as a nutrient source. MF membranes were chosen because their hydraulic resistance was expected to be significantly lower than that of the biofilms, allowing separation of biofilm resistance effects from those of the membrane. In addition, the apparent intrinsic biofilm resistance can be compared with the clean water resistances of ultrafiltration (UF), nanofiltration (NF), and RO membranes in order to evaluate the contribution of the biofilm as a secondary membrane for these types of membrane materials.

3.2 Materials and methods

3.1.2 Test system and configuration

The test system consisted of four identical crossflow filtration cells, each with a permeate producing membrane area of 200 cm^2 and a flow-channel height of 787 mm (31 mil: 1 mil = 25.4 mm; 31 mil = 787 mm). In essence, the design of the filtration cells was similar to the membrane fouling simulator (Vrouwenvelder et al., 2007b; Vrouwenvelder et al., 2006). Spatial dimensions and hydrodynamics were similar to spiral wound NF and RO membrane elements. Microfiltration membranes (Nadir MP 005, Microdyn-Nadir GmbH Wiesbaden, Germany) with a pore size of 0.05 µm were used. The 787 mm thick feed spacer consisted of polypropylene strings, arranged as a net structure with 90° angles and a porosity of about 0.85. This feed spacer is commonly used in spiral-wound NF and RO modules for water treatment in The Netherlands (Vrouwenvelderet al., 2011). The height of the flow-channel inside the filtration cell was equal to the spacer thickness: 787 mm. The four flow cells were produced from poly methyl methacrylate (PMMA). The transparent material offered the possibility for direct non-destructive visual observations of the biofilm growth. Figure 3.1 shows the flow sheet for one flow cell. Feed water (see Section 3.2.2) was filtered through two 10 mm pore size cartridge filters and kept constant at 20 °C. The pressure reducer (V782, Vink Kunststoffen B.V., Didam, The Netherlands) enabled a stable feed pressure of 1.7 bar for all experiments performed during the studies described in this paper. Before entering the filtration cell, nutrients were added using a peristaltic pump (Masterflex L/S pumps, Cole-Palmer Instrument Company, Vernon Hills, Illinois, USA). Linear flow velocity of the

feed water was monitored by a flow controller (8805/8905, Brooks Instrument, Hatfield, PA, USA), which was installed behind the outlet of the filtration cell. The permeation rate was maintained by a peristaltic pump (Masterflex L/S pumps, Cole-Palmer Instrument Company, Vernon Hills, Illinois, USA). Fouling development was monitored by measuring the pressure drop over the feed channel and over the membrane, using a differential pressure transmitter (Deltabar S PMD70, Endress þ Hauser, Maulburg, Germany; (Vrouwenvelder et al., 2009a)). The pressures were measured at the monitor inlet and permeate and concentrate outlet. Temperature, water flow velocity, flux, feed channel pressure drop (FCP), transmembrane pressure drop (TMP), and nutrient supply were measured twice a day.

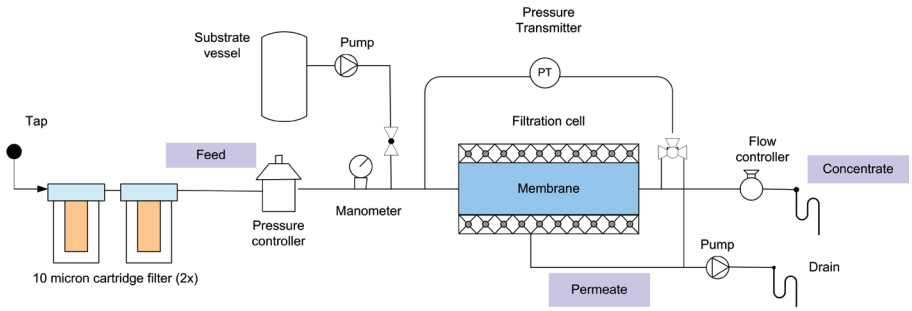

Figure 3.1: Configuration of test system.

3.2.2 Water and added nutrients

Drinking water prepared from anaerobic groundwater (subsequently treated by aeration, rapid sand filtration, deacidification, and softening at treatment plant Spannenburg in The Netherlands) is distributed without post disinfection and without disinfectant residual. So the water is treated and distributed without any chlorination step. This drinking water was used as feed water source for the crossflow filtration set up. The total bacterial cell number in the feed water was 3 x 10^5 cells mL^{-1}. The number of colony forming units on R2A media after 10 days incubation at 25 °C was 2 x 10^3 CFU mL^{-1}. As nutrients, a solution of sodium acetate ($NaCH_3COO$), sodium nitrate ($NaNO_3$) and sodium dihydrogen orthophosphate (NaH_2PO_4) in the mass ratio for C:N:P of 100:20:10, respectively. The final concentration of organic carbon was 1 mg L^{-1}. This nutrient composition has been used in several previous studies on biofilms and biofouling (Araújo et al., 2012; Miller et al., 2012; Vrouwenvelder et al., 2010a; Vrouwenvelder et al., 2009a). All chemicals were purchased in analytical grade from Boom B.V. (Meppel,

The Netherlands). All chemicals were dissolved in milliQ water. The concentrated substrate solution (10 L) was dosed into the feed water prior to the filtration cell using a peristaltic pump (Masterflex) at a flow of 0.12 L h^{-1}. The dosage of the nutrient solution was tested periodically by measuring the weight of the dosing container. To restrict bacterial growth in the substrate dosage bottle, the pH was set at 11 by NaOH dosage. Stock solutions were replaced every 2 days with freshly prepared solutions. The chemical dosage flow rate (0.12 L h^{-1}) was low compared to the feed water flow rate (28.2 L h^{-1}). The effect of the chemical dosage on the pH of the feed water was insignificant. The feed water before and after dosage of substrate and the concentrate had a pH of 7.8. Handling of the nutrients was applied as in the previous research (Araújo et al., 2012; Miller et al., 2012; Vrouwenvelder et al., 2010a).

For one experiment described in Section 3.3.2 a high-density bacterial suspension replaced the nutrient solution. This bacterial suspension contained a cell count of 6 x 10^9 cells mL^{-1} and was injected to the monitor feed system at a flow rate of 1.5 L h^{-1}. It was operated for 2 hours to create a bacterial cell layer on the membrane surface. The bacterial suspension was obtained by incubating tap water with a highly concentrated nutrient amount (same nutrient composition as described in this section) for 5 days at 25 °C.

3.2.3 Biofilm analysis

After the defined operation time the crossflow cells were opened and the biofilm was analyzed. The biofilm was removed from the membrane with a cell scraper (TPP, St. Louis, MO, USA) and suspended in phosphate buffered saline (PBS: NaCl 8 g L^{-1}, KCl 0.2 g L^{-1}, $Na_2HPO_4.7H_2O$ 1.15 g L^{-1} and KH_2PO_4 0.2 g L^{-1}; the pH was adjusted to 7.3) and the solution was shaken for 30 minutes. Then, the biofilm sample was subjected to ultrasonic treatment (Bransonic, Berlin, Germany: model 5510E-DTH, output 135 Watts, 42 kHz,) for 2 minutes. Afterwards, it was homogenized using an ultrasonic probe (Brandson Sonifier 250, G. Heinemann Ultraschall- und Labortechnik, Schwäbisch Gmünd, Germany) in pulsating mode (20% sonification per time-unit) for 10 pulses with an output of 45 Watt. Control experiments showed that this pretreatment was efficient for biomass removal from the membrane and the treatment did not lead to lower heterotrophic plate counts, suggesting that cell lysis did not occur (data shown in supplementary material, Figure S3.1).

The obtained biofilm suspension was used for all biofilm parameter analyses and is referred to as biofilm sample, obtained from a defined surface area of the membrane which was 200 cm^2.

3.2.4 Resistance

Prior to biofilm analysis and during operation, the permeability and resistance of the biofilms were assessed on basis of the following considerations:

The flux J of water through a membrane is expressed as the amount of water V [L] flowing through a certain membrane area A [m^2] in time t [h]

$$J = \frac{V}{A \cdot t} \quad [Lm^{-2}h^{-1}] \tag{1}$$

The permeability K of the membrane is defined as:

$$K = \frac{J}{TMP} \quad [Lm^{-2}h^{-1}bar^{-1}] \tag{2}$$

K is expressed in $Lm^{-2}h^{-1}bar^{-1}$. TMP is the driving force for filtration. It is the average pressure difference between the feed and permeate

$$TMP = \frac{P_{inlet} + P_{outlet}}{2} - P_{permeate} \quad [bar] \tag{3}$$

Flux and permeability are temperature dependent due to temperature influence on the viscosity of water. In these experiments the temperature was maintained at 20 °C.

Experiments were performed at constant flux. This leads to increasing transmembrane pressure (TMP) during the growth of the biofilm, resulting in a decrease in K. The resistance R is inversely related to the permeability K

$$R = \frac{TMP}{\eta \cdot J} \quad [m^{-1}] \tag{4}$$

where η [Pa s] is the dynamic viscosity of water at a given temperature.

The resistance in equation (4) is the sum of the membrane resistance and the extra resistance due to biofilm formation

$$R_{total} = R_{membrane} + R_{biofilm} \quad [m^{-1}] \tag{5}$$

The resistance measurement at t=0 gives the original membrane resistance which is used to calculate the biofilm resistance:

$$R_{biofilm} = R_{total} - R_{membrane} \quad [m^{-1}] \tag{6}$$

The calculated resistance of the biofilm can be used to calculate the biofilm permeability by inversing the resistance

$$K_{biofilm} = \frac{1}{R_{biofilm} \cdot \eta} \quad [Lm^{-2}h^{-1}bar^{-1}] \qquad (7)$$

3.2.5 Biofilm thickness

The thickness of the biofilm was obtained by calculation (equation 8) based on the biofilm weight per cm2. The membrane was taken from the flow cell after 4 days operation. The biofilm weight was determined by the weight difference of the (i) membrane including the biofilm and the (ii) membrane after mechanical biofilm removal using a cell scraper. Both weights were determined within 10 minutes after membrane removal from the flow cell to minimize liquid evaporation from the biofilm and membrane. For the calculation, a density equal to the density of water was assumed given that the water content within the analyzed biofilms was above 95%. Results gained with this method were verified by confocal laser scanning microscopy (confocal laser scanning microscope, Axiovert 100M, Zeiss, Jena, Germany).

$$\text{Biofilm thickness} = h = \frac{m}{\rho \cdot A} \quad [m] \qquad (8)$$

As a biofilm is composed mainly of water, the density was assumed in first approximation as 1 g cm^{-3}.

3.2.6 Scanning electron microscopy (SEM)

Pieces of membrane (~1 cm^2) were used for scanning electron microscopy of the biofilms. The samples were fixed in 3% glutaraldehyde (Sigma-Aldrich, Steinheim, Germany) at 4°C for 24 h, then washed twice in phosphate buffered saline (PBS) and dehydrated in increasing concentrations of ethanol (30, 50, 70, 90% for 20 minutes each; 96% for 30 minutes, twice). Finally, the samples were air dried in a drying chamber (45 °C, 30-60 minutes) and stored in a desiccator until microscopic investigation. The samples were sputtered with gold (Jeol JFC-1200 Fine Coater, Tokyo, Japan). SEM was performed with a JEOL JSM 6480 LV microscope (JEOL Technics Ltd., Tokyo, Japan) in high vacuum mode (emission electrons detection, acceleration voltage 6-10 kV, operating distance 10 mm).

Cross-section images of glutaraldehyde fixed samples were conducted from samples which underwent the following pretreatment. The membrane samples

were placed in liquid nitrogen for shock freezing; at such low temperatures the polymeric membrane and the organic biofilm became brittle. By breaking the frozen samples, sharp cross-sections without artifacts were obtained and these samples were observed under high vacuum conditions with the SEM.

3.2.7 Confocal laser scanning microscopy (CLSM)

Samples were stained with 100 ml of a DNA specific fluorescent stain, Syto9 (Invitrogen/Molecular Probes, Carlsbad, California, USA). It was used in a concentration of 5 µM and the stained samples were incubated in the dark for 20 min. A confocal laser scanning microscope Axiovert 100M (Zeiss, Jena, Germany) was employed. An argon laser was used with an excitation wavelength of 488 nm. The emission was detected with a bandpass-filter (505 and 530 nm).

3.2.8 Total organic carbon (TOC)

To determine the total organic carbon content of the total biofilm (the sum of intra and extracellular organic carbon), an aliquot of the biofilm sample (prepared as described in Section 3.2.3) was placed in a TOC-free glass tube. The sample was treated with the ultrasonic probe (Branson Sonifier 250, G. Heinemann Ultraschall- und Labortechnik, Schwäbisch Gmünd, Germany) in pulsating mode (20% sonication per time-unit) for 30 pulses with an output of 45 W. During the ultrasonic treatment, the sample was kept on ice for sample temperature control. The TOC was measured with a Shimadzu TOC analyzer (Shimadzu Scientific instruments, Kyoto, Japan).

3.2.9 Total cell number (TCN)

For TCN determination, a Neubauer Improved Counting Chamber was used and the sample was counted with a microscope (DM750, Leica, Wetzlar, Germany). Two times five squares were counted and the average value for five squares was taken. The following equation was used to determine the TCN.

3.2.10 EPS isolation

For EPS isolation, the biofilm sample was mixed with a cation exchange resin (CER) in the Na^+-form (Dowex, Sigma-Aldrich, Steinheim, Germany) in the ratio of 0.2 g resin per 1 mL sample (see section 3.2.3 for details of the sample) and shaken for 2 hours at room temperature (Wingender et al., 2001). During this reaction time the Na^+ of the CER was exchanged against Ca^{2+} which allowed the EPS to dissolve into the liquid. This suspension was centrifuged at 9000 *g* for 20 minutes at 4 ˚C to separate the bacterial cells from the supernatant (containing EPS) was used for further analyses (proteins and polysaccharides). The number of colony forming units (CFU) and TCN determination before and after cation exchange treatment was not influenced by the EPS isolation procedure. The CER method for EPS extraction has proven to be successful and mild for charged and non-charged biopolymers, avoiding cell lysis and still providing a good yield of EPS (Frølund et al., 1996).

3.2.11 Protein quantification in EPS

Protein concentration was determined using the bicinchoninic acid (BCA) method (Smith et al., 1985) in the Pierce BCA Protein Assay Kit 23225 (Thermo Scientific, Rockford, IL, USA).

3.2.12 Polysaccharide quantification in EPS

Polysaccharides were quantified by the phenol/sulfuric acid method (Dubois et al., 1956). Glucose was used as standard. 0.5 ml of sample/standard was mixed with 0.5 mL of 5% phenol solution and 2.5 mL of 96% sulfuric acid. The absorption was measured at 490 nm with a microtiterplate reader (1420 Multilable counter Victor^3, PerkinElmer, Waltham, MA, USA).

3.2.13 Experiments and operational conditions

Temperature, water flow velocity, feed pressure, flux, nutrient concentration and operation time were stable throughout each set of experiments. The feed channel pressure drop and TMP changed during operation time in response to biofilm formation. Flux and feed water nutrient concentration differed from experiment to experiment to investigate the relation of biofilm permeability and operational parameters. Table 3.1 gives an overview of the experiments.

Table 3.1: Scheme of the experimental conditions for the biofilm permeability studies.

Study	dosed substrate concentration in feed water	flux	linear cross flow velocity	feed spacer presence	section
	mg L^{-1} acetate C	L m^{-2} h^{-1}	m s^{-1}		
Intramembrane fouling	1.0	20	0.1	no	3.3.1
Biofouling layer formation: filtration or biofilm growth?	0 / 0.1# / 1.0	20/100	0.1	no	3.3.2#
Fouling effects	0 / 1.0	20/100	0.1	no	3.3.3
Effect of flux variation on biofilm resistance	1.0	20/100	0.1	no	3.3.4
Effect of spacer presence on biofilm resistance	0 / 1.0	20/100	0.1	no, yes	3.3.5

#: see fig. S3.2, in supplementary material.

3.3. Results

The reproducibility of the results obtained from the flow cell experiments was examined. Six flow cells were operated independently at the same flux (100 m^{-2} h^{-1}), linear flow velocity (0.1 m s^{-1}) and substrate concentration (1.0 mg L^{-1} acetate C, see section 3.2.2) for 4 days. The same development of total resistance and biomass accumulation (measured as TOC) was observed in the six monitors (Figure S3.3, supplementary material). With this, both reproducibility and comparability of results obtained with this test system and configuration were verified.

The experiments were carried out at constant flux conditions. This requires an increase of the pressure in order to overcome increasing resistance of fouling layers. The duration of the experiments was limited to 4 days because after that period the required pressure to maintain constant flux would have exceeded the pressure allowed for the flow cells.

3.3.1 Intramembrane fouling?

3.3.1.1 Scanning Electron Microscopy observations

The objective of this research effort was to determine the hydraulic resistance of biofilms. In order to do so, a microfiltration membrane was chosen with a hydraulic resistance significantly lower than the resistance of biofilms. It is important to find out if, in addition to biofilm formation on top of the membrane, internal membrane fouling occurs adding to the transmembrane pressure drop. To address this, a cell was operated with constant flux (20 L m^{-2} h^{-1}) and linear flow velocity (0.1 m s^{-1}),

fed with tap water supplemented with a nutrient source (1 mg L^{-1} acetate C). During 4 days of operation accumulation of biomass on the membrane was observed visually through the transparent monitors. SEM examination (up to 10000x magnification) of membrane samples taken from the monitors after that period of operation showed that fouling accumulated on the membrane surface and not in the membrane pores (Figure 3.2). Clearly, the microorganisms were retained by the membrane due to the small membrane pore size (0.05 µm). No apparent fouling could be visually detected in the pores of the membrane.

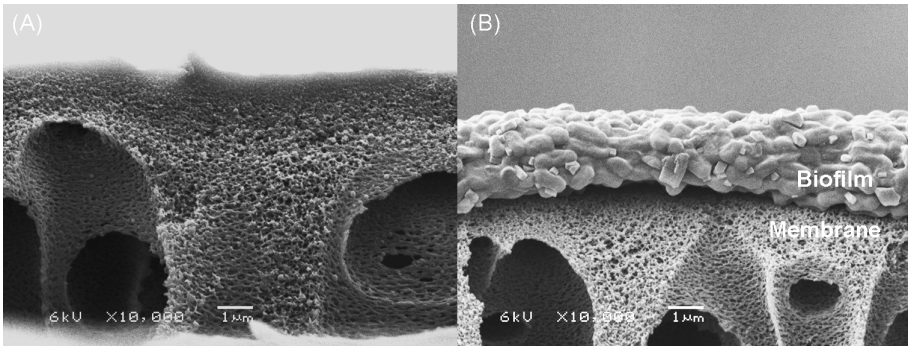

Figure 3.2: Scanning electron micrograph of a membrane cross-section. A: original membrane, B: membrane with biofilm after 4 days of operation.

3.3.1.2 ***Resistance of virgin and mechanically cleaned membranes***

In addition to the SEM analyses the possibility of adsorption of macromolecules to the pores of the membrane affecting the resistance was determined by experiments performed under the same conditions (substrate, flux and crossflow velocity) as the SEM observations. The total resistance was determined before (virgin membrane), after fouling and after subsequent cleaning by removal of the biofilm (see Table S3.1 in supplementary material). Experiments were performed in triplicate and biomass was removed by scraping.

Scraping off the fouled membrane reduced the resistance to values similar to the virgin membrane resistance (Figure 3.3 and Table S3.1 in supplementary material). The scraped membrane had a resistance up to 5% higher than the virgin membrane probably mainly caused by not-removed biofilm on the membrane surface.

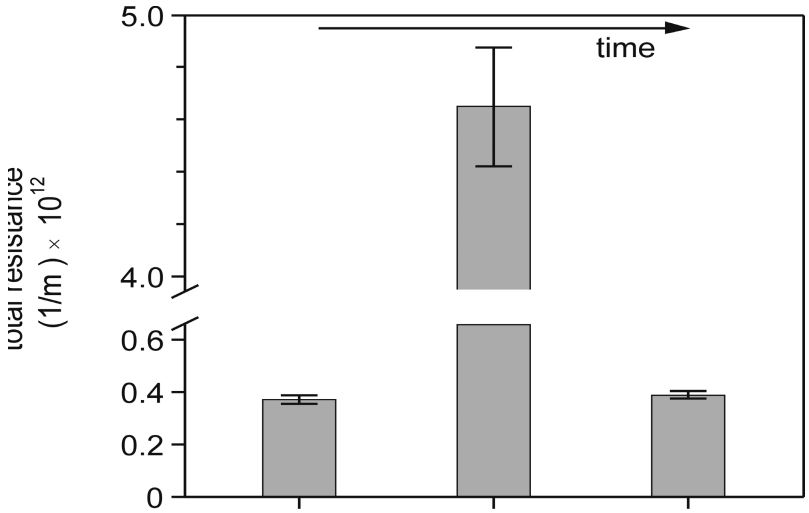

Figure 3.3: Resistance prior to fouling (virgin membrane), after fouling and after subsequent cleaning by scraping of the fouled membrane surface to remove the accumulated biofilm.

3.3.2 Biofouling layer formation: filtration or biofilm growth?

It has been hypothesized that the resistance properties of a grown biofilm are different from a cake layer generated by bacterial cells accumulated on the membrane surface by filtration. In order to distinguish both, experiments with and without addition of a nutrient source to feed water were carried out. Two flow cells were operated in parallel for 4 days at two fluxes (20 and 100 L m^{-2} h^{-1}), constant linear velocity, without and with acetate dosage. The contribution of total water volume throughput to biofilm growth was evaluated and found to be very small (see Figure S3.4 in supplementary material). Figure 3.4 shows that the addition of nutrients strongly increased the biofilm resistance by several orders of magnitude (Figure 3.4a), while the cell number (Figure 3.4b) and the TOC (Figure 3.4c) increased significantly as well. A higher substrate concentration in the feed water caused more rapid increase of the biofilm resistance and biofilm parameters (Figure S3.2 in supplementary material). The results indicate that biofilm growth and not accumulation of microbial cells imported by the feed water caused the fouling effect. The biofilm thickness was about the same height at 20 L m^{-2} h^{-1} and at 100 L m^{-2} h^{-1} (Figure 3.4d). This may indicate that a slightly higher concentration of EPS and microbial cells in the biofilm contributes to higher resistance. Obviously, thickness is not simply proportional to resistance.

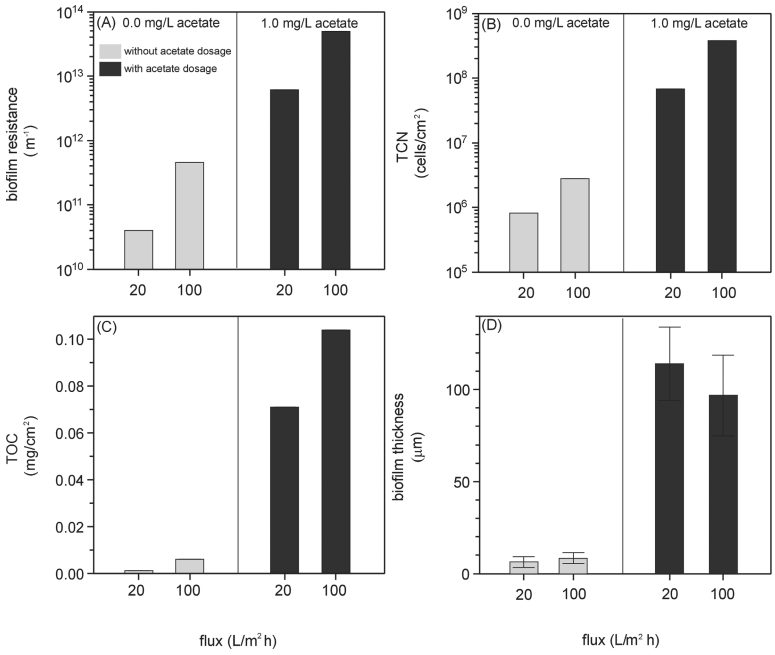

Figure 3.4: Parameters biofilm resistance (A), total cell numbers (B), TOC (C), and thickness (D) after 4 days of operation. Standard deviation of the thickness is shown by error bars (n = 23).

The impact of microbial cells without an EPS matrix was further investigated by comparison of a grown biofilm with a filter cake of similar cell number per cm^2. In this experiment, the filter cake was generated by accumulation of cells added to the feed water onto the membrane surface (Figure 3.5; see section 3.2.2 for filter cake preparation). The filtration time was 2 hours, so significant microbial growth was avoided. At a similar cell number, the resistance of the cell filter cake was five times less than that of the grown biofilm. The amount of EPS in the bacterial filter cake was small compared to the biofilm.

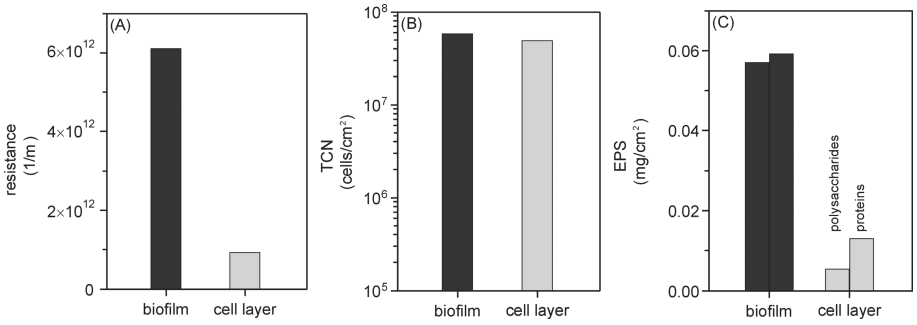

Figure 3.5: Comparison of effects of grown biofilm vs. filter cake of bacterial cells. Resistance (A), total cell numbers (B), and EPS of biofilm and cell layer (C).

3.3.3 Fouling effects

In a time series experiment, the influence of the biofouling layer was determined in more detail. Nutrient supply was offered as 1 mg L^{-1} acetate C in comparison to the control without added acetate.

Four flow cells were run in parallel for 4 days and after each day the membrane of one flow cell was sacrificed. The results are shown in Figure 3.6. At both fluxes (20 and 100 L m^{-2} h^{-1}), a clear increase of the total resistance was evident for the nutrient supplied flow cells (Figures 3.6a and b), with a higher resistance at higher flux. The cell density was approximately the same in the nutrient-supplied systems at both fluxes (Figures 3.6c and d). Thus, the cell density obviously was not the reason for the higher resistance observed at the higher flux. The cell density in the control was slightly higher at higher flux, not resulting in a significant increase of resistance (Figure 3.6b). With acetate dosage, the increase in TOC at both fluxes was significantly higher than in the control, reflecting that biomass accumulated as a growing biofilm (Figures 3.6e and f).

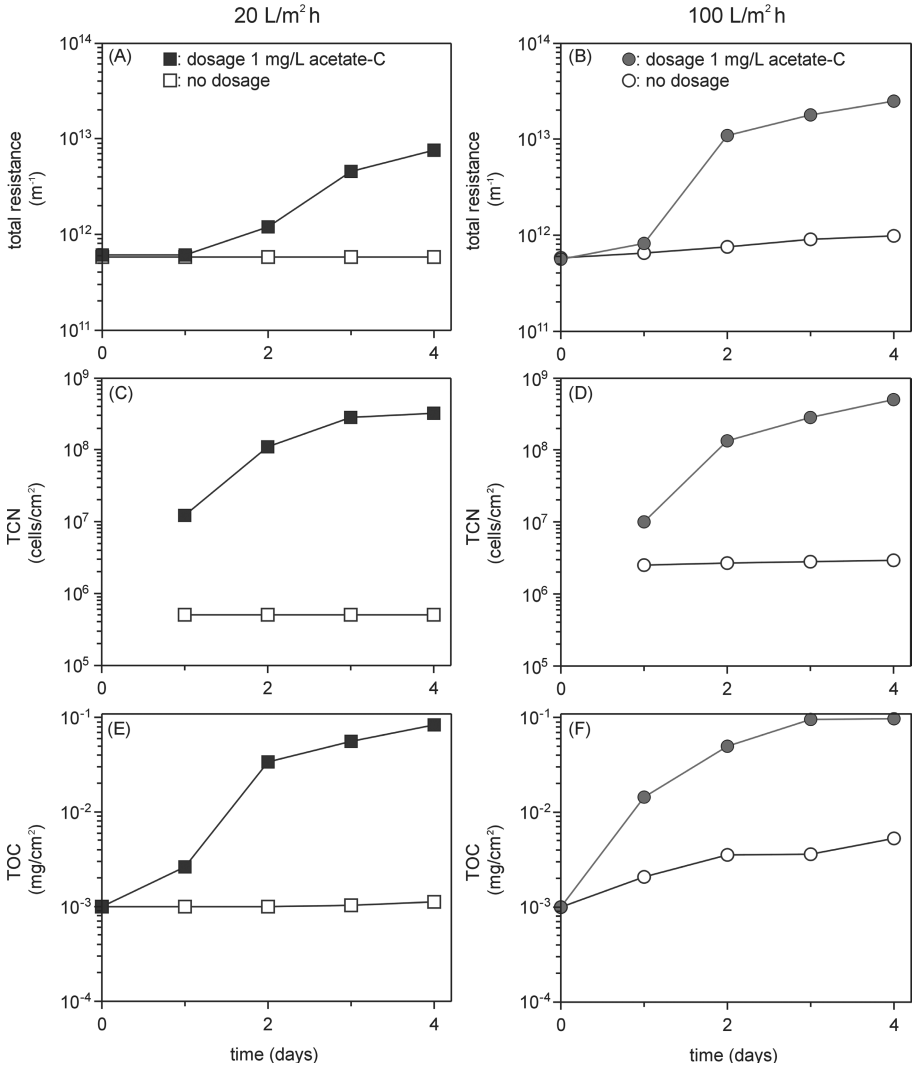

Figure 3.6: Development of total resistance (A, B), TCN (total bacterial cell numbers: C, D) and TOC (total organic carbon: E, F) during 4 days of operation at a flux of 20 (left) and 100 L m^{-2} h^{-1} (right) respectively. The data at time 0 were based on a virgin membrane.

3.3.4 Effect of flux variation on biofilm resistance

A relevant question is whether the resistance of a biofilm grown under given conditions changes when the flux changes. Is this a dynamic effect and, thus, reversible? In order to answer this question, two experiments were carried out:

i) a nutrient-supplied test cell at 20 L m^{-2} h^{-1} for 4 days, followed by a flux increase to 100 L m^{-2} h^{-1} for one hour and then a return to the original flux, and

ii) a nutrient-supplied test cell at 100 L m^{-2} h^{-1} for 4 days, followed by a flux decrease to 20 L m^{-2} h^{-1} and then a return to the original flux.

The results are shown in Figure 3.7. The response appeared dynamic. In case (i), the resistance increased with elevated flux and returned to the original resistance upon returning to the original flux, in case (ii) the opposite was observed.

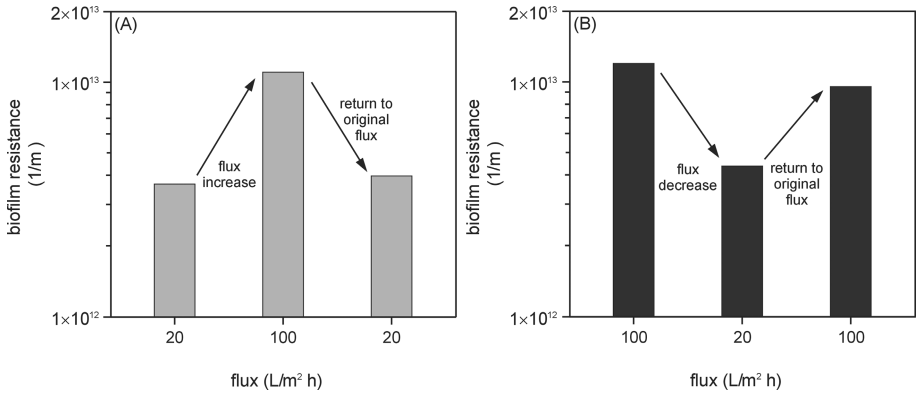

Figure 3.7: Influence of temporary change in flux regime after 4 days of operation. From 20 to 100 L m^{-2} h^{-1} for 1 hour and then back to 20 L m^{-2} h^{-1} (A) and from 100 to 20 L m^{-2} h^{-1} for 1 hour and then back to 100 L m^{-2} h^{-1} (B).

3.3.5 Effect of feed spacer presence on biofilm resistance

The role of the feed spacer has been demonstrated to be quite important in fouling (Vrouwenvelder et al., 2009b; Vrouwenvelder et al., 2009a). In the present study, the effect of the spacer was re-evaluated. Flow cells at 20 and 100 L m^{-2} h^{-1} were operated, with and without nutrients, and with and without a feed spacer (Figure 3.8). The TMP was monitored. After 4 days, the biofilm was analyzed (Figure 3.9).

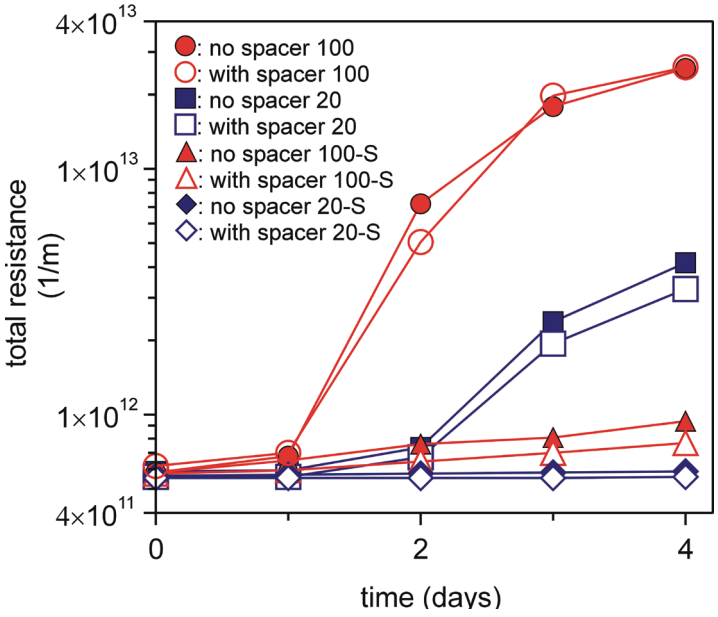

Figure 3.8: Development of total resistance with and without feed spacer during 4 days of operation at 20 and 100 L m^{-2} h^{-1}. Substrate was dosed to all flow cells except for the blanks: 20-S and 100-S. (-S: without substrate).

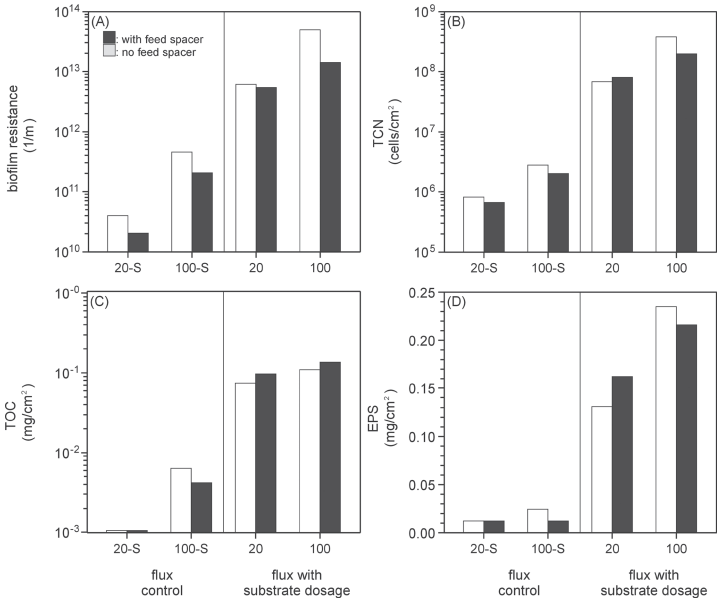

Figure 3.9: Influence of feed spacer. Total biofilm resistance (A), total bacterial cell number (B), TOC (C), and EPS concentration (D), analyzed after 4 days of operation. Substrate was dosed to all flow cells except for the

blanks: 20-S and 100-S. (-S: without substrate).

Regardless of the feed spacer presence, the same initial transmembrane resistance and the same increase of biofilm resistance in time was observed for a flux of 20 L m^{-2} h^{-1}. However, for a flux of 100 L m^{-2} h^{-1}, a lower biofilm resistance was observed in the presence of spacer and nutrient supply (Figure 3.9a). This was mirrored in the total cell numbers and the TOC (Figures 3.9a and c). In view of the hypothesis that the EPS play a key role in biofilm resistance, it is noteworthy that the EPS concentration (Figure 3.9d) at 20 L m^{-2} h^{-1} is higher in presence of the spacer, but this does not go together with a lower resistance (Figure 3.9a).

3.4. Discussion

Major objective of the study was to identify the impact of the intrinsic apparent hydraulic resistance of biofilms on the performance of membrane processes. The test system proved to be suitable for this kind of investigation; no fouling inside the membrane pores could be detected (Figures 3.2 and 3.3), which allowed for attributing the effects to biofilms growing on top of the membrane. For characterization of the biofilm, thickness, total cell numbers, TOC and EPS concentration were analyzed and their correlation to the resistance properties of the biofilms was determined. Furthermore, differentiation between the fouling mechanisms, cake formation by bacterial cells accumulated from the water phase and biofilm growth was possible: Our results clearly indicate biofilm growth (Figures 3.4 and 3.5). The contribution of bacterial cells to the overall hydraulic resistance is small compared to the resistance caused by biofilms: Calculations based on biofilm data from our monitor studies at 20 and 100 L m^{-2} h^{-1} showed that of the total biofilm volume less than 0.4% was occupied by bacteria. Also, without substrate addition the amount of filtered water had a negligible influence on the resistance compared with the effect of the same amount of water supplied with nutrients. The total volume filtered had only a very small effect on the increase of the biofilm (see Figure S3.4, in supplementary material). Table 3.2 summarizes the findings.

Table 3.2: Biofilm parameters obtained after 4 days of operation without feed spacer presence supplied with 1 mg L^{-1} acetate C and operated at crossflow velocity of 0.1 m s^{-1} and at flux 20 and 100 L m^{-2} h^{-1}.

Parameter	Unit	20 L m^{-2} h^{-1}		100 L m^{-2} h^{-1}	
Biofilm resistance	m^{-1}	6×10^{12}	$\pm 2 \times 10^{12}$	5×10^{13}	$\pm 2 \times 10^{13}$
Biofilm thickness	µm	114	± 20	97	± 22
Bacteria in biofilm	cells cm^{-2}	6×10^{7}	$\pm 6 \times 10^{6}$	4×10^{8}	$\pm 4 \times 10^{7}$
Volume of biofilm	cm^3 cm^{-2}	0.114	± 0.02	0.097	± 0.02
Volume of 1 cell	cm^3	10^{-12}		10^{-12}	
Total cell volume	cm^3	8.4×10^{-4}	$\pm 8.4 \times 10^{-5}$	2.8×10^{-3}	$\pm 2.8 \times 10^{-4}$
Ratio cells:total volume	%	0.1%	± 0.01	0.4%	± 0.07
Ratio EPS:total volume	%	99.9%	± 0.01	99.6%	± 0.07

The influence of nutrients on biofouling is evident and crucial. Substrate dosage caused a faster and stronger increase of total resistance and biofilm amount (Figures 3.6 and S3.2 in supplementary material). The concentration of biodegradable substrate in the feed water determined the biofilm growth. This observation is in agreement with NF and RO biofouling studies by Griebe and Flemming (1998) and Vrouwenvelder et al. (2009b). In summary, a higher feed water substrate concentration caused more biofilm growth and a higher biofilm resistance. Nutrients may be considered as potential biomass. This underlines the option of nutrient limitation as an alternative to biocide application in anti-fouling strategies which should be considered wherever applicable (Flemming, 2011); this option should not only include organic carbon but also bioavailable phosphorus (Vrouwenvelder et al., 2010a; Vrouwenvelder et al., 2010b). Herzberg et al. (2010) showed that MF pre-treatment for RO membranes led to a completely different microbial population composition on RO membranes, but the effects of the resulting biofilm on the membrane performance remained below the "threshold of interference" as suggested by Griebe and Flemming (1998).

An interesting factor is the influence of the feed spacer. Biofouling in NF and RO spiral-wound membrane modules is considered a feed channel (feed-concentrate) pressure drop problem (Vrouwenvelder et al., 2010a; Vrouwenvelder et al., 2010b; Vrouwenvelder et al., 2009b; Vrouwenvelder et al., 2009a). Baker et al. (1995) reported that initial deposits of fouling accumulated alongside the membrane feed channel spacer and in time these deposits encroached upon the remaining free membrane area. Van Paassen et al. (1998) observed an exponential increase of the feed channel pressure drop as a function of time caused by biofouling build up onto the feed spacer of the membrane modules. This proved to be related with impurities of chemicals dosed to the feed water. Tran et al. (2007) found that the vicinity of the feed spacer strands was most affected by fouling. Strategies

to reduce feed spacer biofouling have been addressed, e.g., periodic air/water flushing (Cornelissen et al., 2007) and applying thick feed spacers (Araújo et al., 2012; Majamaa et al., 2010). Feed spacers are considered important for membrane performance and play an important part in biofouling of membrane systems. In the present study, however, for a flux of 20 L m^{-2} h^{-1} the feed spacer presence had no effect on the development of the transmembrane biofilm resistance. Irrespective of spacer presence, the same initial resistance and increase of biofilm resistance were observed.

A higher flux caused more biofilm accumulation and a higher biofilm resistance (Figure 3.4). A higher biofilm resistance but a similar biofilm thickness was observed for a flux of 100 L m^{-2} h^{-1} compared to 20 L m^{-2} h^{-1} after 4 days of operation. A temporary flux increase raised the biofilm resistance, while a subsequent flux decrease re-established the original biofilm resistance (Figure 3.7). The biofilm resistance increased with the flux. The question is: What causes this increase of resistance in response to flux increase? As mentioned earlier, the volume of bacterial cells is small (ca. 0.4%) compared to the volume of hydrated EPS (ca. 99.6%: Table 3.2), suggesting that not the bacterial cells but the biofilm EPS is the dominant factor for biofilm resistance. The EPS is present as a highly hydrated gel which might be compacting under pressure, resulting in a higher resistance. The reversible nature of the effect suggests a dynamic behavior of the EPS matrix.
The determination of the intrinsic apparent hydrodynamic resistance of a biofilm as shown in this study allows for the assessment of the contribution of the biofilm to the overall resistance of a membrane system. NF and RO membrane biofilms may have a different fouling layer resistances compared to biofilms produced in our studies on a 0.05 µm pore size MF membrane, as many parameters influencing biofilm growth are significantly different, such as nutrient concentration, surface characteristics including roughness as well as concentration polarization.
The biofilm resistance represents the resistance of a pure biofilm which is free from any influences of concentration polarization or other fouling types. In MF and UF, the pure biofilm resistance dominates the intrinsic membrane resistance, while in NF and RO, the intrinsic membrane resistance is much higher than that of a biofilm. For these types of membrane processes, the contribution of biofilm resistance to transmembrane resistance is small (Figure 3.10), contrary to the findings of Lee et al. (2009). Therefore, in NF and RO systems, pure biofilm resistance cannot be the major factor in biofouling effects. It is suggested that biofilms formed in

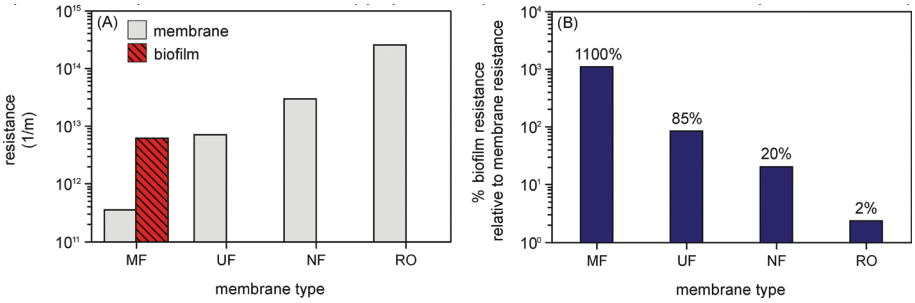

Figure 3.10: Comparison of biofilm resistance (for a biofilm grown at a flux of 20 L m^{-2} h^{-1}) to intrinsic resistance of microfiltration, ultrafiltration, nanofiltration and reverse osmosis membrane. Absolute values (A), ratio of biofilm to membrane resistance (B). The clean membrane resistances for UF, NF and RO were taken from Mulder (1996). The MF membrane resistance is the value measured in this research.

The transmembrane biofilm resistance is only 20% and 2% of the membrane resistance for NF and RO membranes (Figure 3.10). When applying the results of our MF studies to NF/RO systems the pure biofilm resistance (which is not influenced by concentration polarization) cannot explain the reduction in NF/RO installation performance observed in practice. Therefore, the combination of the pure biofilm with concentration polarization (Chong et al., 2008), feed-concentrate pressure drop (Ridgway & Flemming, 1996) and/or the influence of the feed spacer (Vrouwenvelder et al., 2009b; Vrouwenvelder et al., 2009c) are most likely predominant causes for performance declines in NF/RO systems.

An important question is: what causes the decline of membrane performance? It is evident that the EPS are responsible for this effect, but how? The main component of biofilms is hydrated EPS and the contribution of EPS to the resistance may be described as the "hair-in-sink-effect", Meaning, the EPS molecules represent a random coil system which includes practically no liquid flow channels leading from top to bottom right through the biofilm and therefore EPS is not showing convective transport (Stewart, 2012). Increased pressure will cause compaction of the gel. The effect may be based on the tortuosity of the EPS matrix which concerns the path of water molecules while penetrating such a matrix. A model describing these effects and providing a deeper understanding of the underlying mechanisms is currently in preparation, also addressing the question whether there is a possibility to develop "flux enhancers" (Drews, 2010; Iversen et al., 2009; McDonogh et al., 1994) on a solid theoretical background. For NF and RO systems the decline of membrane performance is not predominantly caused by an increase of biofilm resistance. Concentration polarization may play an important part (Chong et al., 2008; Herzberg & Elimelech, 2007).

Acknowledgements

This work was performed at Wetsus, Centre of Excellence for Sustainable Water Technology (www.wetsus.nl). Wetsus is funded by the Dutch Ministry of Economic Affairs, the European Union European Regional Development Fund, the Province of Fryslan, the city of Leeuwarden and by the EZ-KOMPAS Program of the "Samenwerkingsverband Noord-Nederland". The authors like to thank the participants of the research theme "Biofouling" and Evides waterbedrijf for the fruitful discussions and their financial support. In addition the authors would especially like to thank the students Judita Laurinonyte, Nathalie Juranek and Zhen Xiang for their great support with the experimental work in the laboratory and colleague Witold Michalowski for the help with the CLSM. The fruitful and inspiring discussions with Tony Fane (NTU Singapore), Christian Mayer (Essen), Wiebren Veeman (Essen) and Harry Ridgway (US) about the background for understanding the reasons for the hydraulic resistance by the EPS is greatly acknowledged. The graphic expression "hair-in-sink- effect" is owed to Yu Shiping (NTU Singapore).

Supplementary material Chapter 3

S3.1 Effect biofilm treatment with ultrasonic water bath and sonifier probe on plate count

Control experiments have been performed to evaluate the effect of pre-treatment with ultrasonic bath and sonifier probe on the plate count. The pre-treatment was applied to remove the biofilm from the microfiltration membrane as obtained after our 4 days studies. Heterotrophic plate counts were performed on R2A agar after incubation for 7 days at 25 °C. For samples of the same biofilm, colony counts were measured without pre-treatment (biofilm suspended in PBS) and the applied pre-treatment (as described in section 2.3). The number of colony forming units (CFU) was about the same for the biofilm sample treated by shaking and vortex use and the sample treated with the ultrasonic bath and probe (see Figure S3.1). The applied treatment had no significant effect of the CFU number.

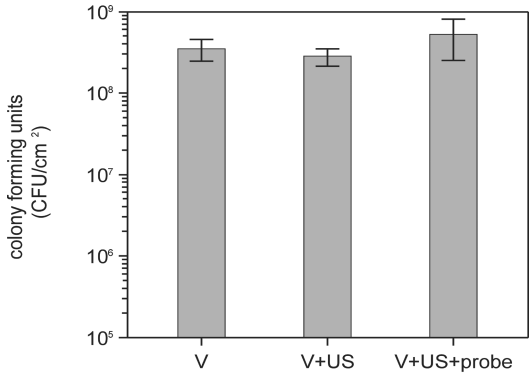

Figure S3.1: The number of colony forming units (CFU) on R2A media for a biofilm obtained in our studies without and with treatment with vortex (V), ultrasonic water bath (US) and sonifier probe (probe) under the conditions as described in section 2.3. The similar number of CFU was found with and without pre-treatment, suggesting that no cell lyses occurred during sample pre-treatment.

S3.2 Influence of substrate concentration

The biofilm resistance, TCN, TOC and EPS increase with an increasing substrate concentration in the feed water (Figure S3.2).

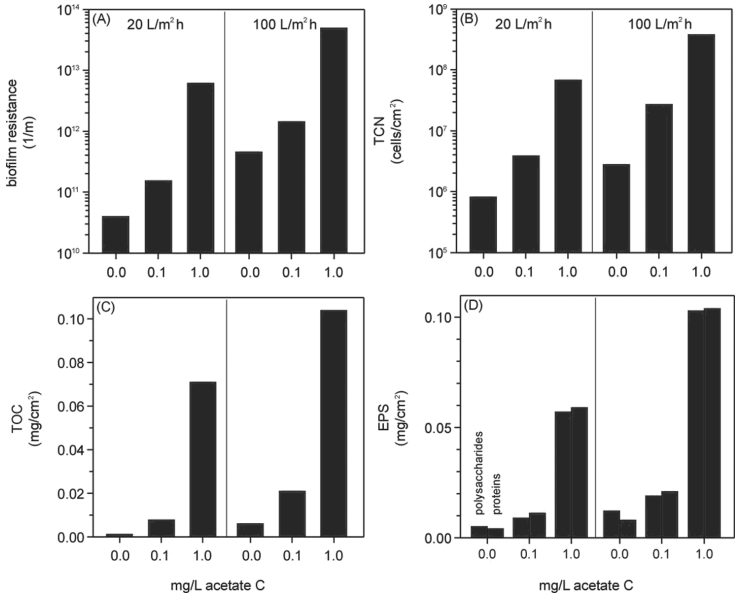

Figure S3.2: Biofilm and membrane resistance (A) and biofilm parameters: TCN (B), TOC (C), and EPS (D: left column = polysaccharides and right = proteins) in the monitor supplemented with 0.0, 0.1 and 1.0 mg L-1

acetate C equivalents and operated at constant flux (20 or 100 Lm-2 h-1) and constant cross flow velocity (0.1 m s-1) for 4 days.

S3.3 Reproducibility

The resistance and TOC measured in six independent experiments show the reproducibility of the development of resistance and biomass (Figure S3.3).

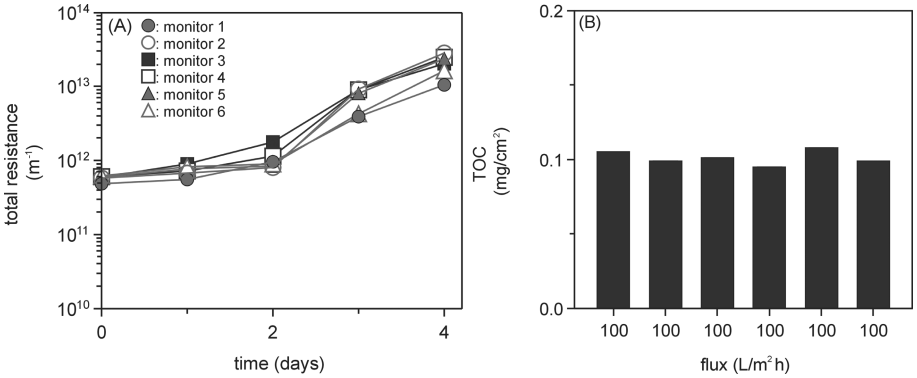

Figure S3.3: Development of total resistance measured in 6 different experiments operated with 100 L m^{-2} h^{-1} and with 1.0 mg L^{-1} acetate C equivalents in the feed water (A) and amount of accumulated biomass at the end of the research period (B).

S3.4 Resistances of virgin and mechanically cleaned membranes

In addition to the SEM analyses the possibility of adsorption of macromolecules to the pores of the membrane affecting the resistance was determined by experiments performed under the same conditions (substrate, flux and crossflow velocity). The total resistance was determined before (virgin membrane), during and after fouling followed by removal of the biofilm.

Experiments were performed in triplicate. Membranes were removed from flow cells for biofilm removal applied by scraping off the membrane surface. Subsequently, the membranes were replaced in the flow cell for resistance measurements. Removal and replacement of the membrane in the flow cell showed to cause a variation in the resistance up to 4%, the same order of magnitude as the difference between the cleaned and virgin membrane.

Scraping off the fouled membrane reduced the resistance to values similar to the virgin membrane resistance (Table S3.1). The scraped membrane had a resistance up to 5% higher than the virgin membrane probably mainly caused by not-removed biofilm on the membrane surface and possibly some internal fouling as well. The effect of internal membrane fouling on the resistance is therefore negligible compared to the effect of fouling on the membrane surface.

Table S3.1: Resistances of virgin, fouled and cleaned membranes (triplicate experiments). Biofouling was caused by biodegradable substrate dosage. The membranes were cleaned by scraping off the membrane surface.

Resistance (1/m)			
virgin membrane	fouled membrane	cleaned membrane	resistance change cleaned/virgin
3.8×10^{11}	1.8×10^{12}	4.0×10^{11}	+5%
3.9×10^{11}	5.4×10^{12}	4.1×10^{11}	+5%
3.6×10^{11}	7.2×10^{12}	3.7×10^{11}	+3%

S3.5 Influence of filtered water volume

The influence of filtered water volume was found to be very low (Figure S3.4). The effect of a growing biofilm due to nutrient supply is dominant over the effect of filtered water volume.

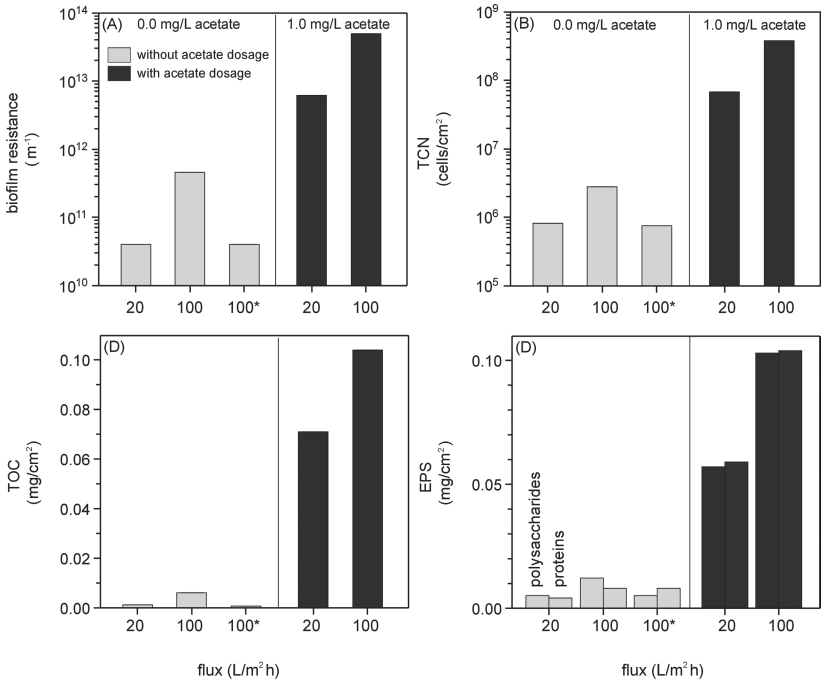

Figure S3.4: Biofilm resistance (A) and biofilm parameters: TCN (B), TOC (C) and EPS (D: left column = polysaccharides and right = proteins) in the monitor supplemented without and with 1.0 mg L^{-1} acetate C equivalents and operated at constant flux (20 or 100 L m^{-2} h^{-1}) and constant cross flow velocity (0.1 m s^{-1}) for 4 days. 100* was operated for 0.8 days at 100 L m^{-2} h^{-1}, equalling the total volume filtered after 4 day operation at 20 L m^{-2} h^{-1}.

References

Araújo, P. A., Kruithof, J. C., Van Loosdrecht, M. C. M., & Vrouwenvelder, J. S. (2012). The potential of standard and modified feed spacers for biofouling control. *Journal of Membrane Science, 403-404*(0), 58-70.

Araújo, P. A., Miller, D. J., Correia, P. B., van Loosdrecht, M. C. M., Kruithof, J. C., Freeman, B. D., Paul, D.R., & Vrouwenvelder, J. S. (2012). Impact of feed spacer and membrane modification by hydrophilic, bactericidal and biocidal coating on biofouling control. *Desalination, 295*(0), 1-10.

Baker, J., Stephenson, T., Dard, S., & Cote, P. (1995). Characterisation of Fouling of Nanofiltration Membranes used to Treat Surface Waters. *Environmental Technology, 16*(10), 977-985.

Chong, T. H., Wong, F. S., & Fane, A. G. (2008). The effect of imposed flux on biofouling in reverse osmosis: Role of concentration polarisation and biofilm enhanced osmotic pressure phenomena. *Journal of Membrane Science, 325*(2), 840-850.

Cornelissen, E. R., Vrouwenvelder, J. S., Heijman, S. G. J., Viallefont, X. D., Van Der Kooij, D., & Wessels, L. P. (2007). Periodic air/water cleaning for control of biofouling in spiral wound membrane elements. *Journal of Membrane Science, 287*(1), 94-101.

Drews, A. (2010). Membrane fouling in membrane bioreactors: characterisation, contradictions, cause and cures. *Journal of Membrane Science, 363*(1-2), 1-28.

Dubois, M., Gilles, K. A., Hamilton, J. K., Rebers, P. A., & Smith, F. (1956). Colorimetric Method for Determination of Sugars and Related Substances. *Analytical Chemistry, 28*(3), 350-356.

Flemming, H.-C., Ridgway, H. F. (2009). Biofilm control - conventional and alternative approaches. In H. C. Flemming, Venkatesan, R., Murthy, P.S., Cooksey, K. C. (Ed.), *Marine and Industrial Biofouling* (pp. 103 - 118). New York: Springer Heidelberg.

Flemming, H. C. (2000). Membranes and Microorganisms - love at first sight and the consequences. In P. Hillis (Ed.), *Membrane Technology in Water and Wastewater Treatment* (pp. 139 - 149): Lancaster University.

Flemming, H. C. (2002). Biofouling in water systems - Cases, causes and countermeasures. *Applied Microbiology and Biotechnology, 59*(6), 629-640.

Flemming, H. C. (2011). Microbial biofouling - unsolved problems, insufficient approaches and possible solutions. In H. C. Flemming, Wingender, J., Szewzyk, U. (Ed.), *Biofilm Highlights* (pp. 81 - 109). Heidelberg, New York: Springer Int.

Flemming, H. C., & Wingender, J. (2010). The biofilm matrix. *Nature Reviews Microbiology, 8*(9), 623-633.

Flemming, H. C., Wingender, J. (2003). Biofilms. In A. Steinbuechel (Ed.), *Biopolymers* (pp. 209 - 245). Weinheim: VCH Wiley.

Frølund, B., Palmgren, R., Keiding, K., & Nielsen, P. H. r. (1996). Extraction of extracellular polymers from activated sludge using a cation exchange resin. *Water Research, 30*(8), 1749-1758.

Griebe, T., & Flemming, H.-C. (1998). Biocide-free antifouling strategy to protect RO membranes from biofouling. *Desalination, 118*, 153-156.

Herzberg, M., Berry, D., & Raskin, L. (2010). Impact of microfiltration treatment of secondary wastewater effluent on biofouling of reverse osmosis membranes. *Water Research, 44*(1), 167-176.

Herzberg, M., & Elimelech, M. (2007). Biofouling of reverse osmosis membranes: Role of biofilm-enhanced osmotic pressure. *Journal of Membrane Science, 295*(1-2), 11-20.

Herzberg, M., & Elimelech, M. (2008). Physiology and genetic traits of reverse osmosis membrane biofilms: A case study with Pseudomonas aeruginosa. *ISME Journal, 2*(2), 180-194.

Iversen, V., Koseoglu, H., Yigit, N. O., Drews, A., Kitis, M., Lesjean, B., & Kraume, M. (2009). Impacts of membrane flux enhancers on activated sludge respiration and nutrient removal in MBRs. *Water Research, 43*(3), 822-830.

Kim, D., Jung, S., Sohn, J., Kim, H., & Lee, S. (2009). Biocide application for controlling biofouling of SWRO membranes â€" an overview. *Desalination, 238*(1-3), 43-52.

Klahre, J., & Flemming, H. C. (2000). Monitoring of biofouling in papermill process waters. *Water Research, 34*(14), 3657-3665.

Lee, J., Jung, J.-Y., Kim, S., Chang, I. S., Mitra, S. S., & Kim, I. S. (2009). Selection of the most problematic biofoulant in fouled RO membrane and the seawater intake to develop biosensors for membrane biofouling. *Desalination, 247*(1-3), 125-136.

Majamaa, K., Aerts, P. E. M., Groot, C., Paping, L. L. M. J., van den Broek, W., & van Agtmaal, S. (2010). Industrial water reuse with integrated membrane system increases the sustainability of the chemical manufacturing. *Desalination and Water Treatment, 18*(1-3), 17-23.

McDonogh, R., Schaule, G., & Flemming, H.-C. (1994). The permeability of biofouling layers on membranes. *Journal of Membrane Science, 87*(1-2), 199-217.

Miller, D. J., Araujo, P. A., Correia, P. B., Ramsey, M. M., Kruithof, J. C., van Loosdrecht, M. C. M., Freeman, B.D., Paul, D.R., Witheley, M., & Vrouwenvelder, J. S. (2012). Short-term adhesion and long-term biofouling testing of polydopamine and poly(ethylene glycol) surface modifications of membranes and feed spacers for biofouling control. *Water Research, 46*(12), 3737-3753.

Mulder, M. (1996). *Basic Principles of Membrane Technology* (2 ed.). Dordrecht: Kluwer Academic Publishers.

Ridgway, H. F. & Flemming, H. C. (1996). Biofouling of membranes. In J. Mallevialle, Odendaal, P. E., Wiesner, M. R. (Ed.), *Water treatment membrane processes* (pp. 629 - 640). New York: McGraw-Hill.

Smith, P. K., Krohn, R. I., Hermanson, G. T., Mallia, A. K., Gartner, F. H., Provenzano, M. D., Fujimoto, E.K., Goeke, N.M., Olson, B.J., & Klenk, D. C. (1985). Measurement of protein using bicinchoninic acid. *Analytical Biochemistry, 150*(1), 76-85.

Stewart, P. S. (2012). Mini-review: Convection around biofilms. *Biofouling, 28*(2), 187-198.

Stewart, P. S., & Franklin, M. J. (2008). Physiological heterogeneity in biofilms. *Nat Rev Micro, 6*(3), 199-210.

Stoodley, P., Sauer, K., Davies, D. G., & Costerton, J. W. (2002). Biofilms as complex differentiated communities. *Annual Review of Microbiology, 56*(1), 187-209.

Tran, T., Bolto, B., Gray, S., Hoang, M., & Ostarcevic, E. (2007). An autopsy study of a fouled reverse osmosis membrane element used in a brackish water treatment plant. *Water Research, 41*(17), 3915-3923.

van Paassen, J. A. M., Kruithof, J. C., Bakker, S. M., & Kegel, F. S. (1998). Integrated multi-objective membrane systems for surface water treatment: pre-treatment of nanofiltration by riverbank filtration and conventional ground water treatment. *Desalination, 118*(1-3), 239-248.

Vrouwenvelder, J. S., Bakker, S. M., Cauchard, M., Le Grand, R., Apacandie, M., Idrissi, M., Lagrave, S., Wessel, L.P., van Paassen, J.A.M., Kruithof, J.C., & van Loosdrecht, M. C. M. (2007a). The Membane Fouling Simulator: a suitable tool for prediction and characterisation of membrane fouling. *Water Sci Technology, 55*(55), 197 - 205.

Vrouwenvelder, J. S., Bakker, S. M., Wessels, L. P., & van Paassen, J. A. M. (2007b). The Membrane Fouling Simulator as a new tool for biofouling control of spiral-wound membranes. *Desalination, 204*(1-3), 170-174.

Vrouwenvelder, J. S., Beyer, F., Dahmani, K., Hasan, N., Galjaard, G., Kruithof, J. C., & Van Loosdrecht, M. C. M. (2010a). Phosphate limitation to control biofouling. *Water Research, 44*(11), 3454-3466.

Vrouwenvelder, J. S., Buiter, J., Riviere, M., van der Meer, W. G. J., van Loosdrecht, M. C. M., & Kruithof, J. C. (2010b). Impact of flow regime on pressure drop increase and biomass accumulation and morphology in membrane systems. *Water Research, 44*(3), 689-702.

Vrouwenvelder, J. S., Graf von der Schulenburg, D. A., Kruithof, J. C., Johns, M. L., & van Loosdrecht, M. C. M. (2009b). Biofouling of spiral-wound nanofiltration and reverse osmosis membranes: A feed spacer problem. *Water Research, 43*(3), 583-594.

Vrouwenvelder, J. S., Hinrichs, C., Van der Meer, W. G. J., Van Loosdrecht, M. C. M., & Kruithof, J. C. (2009a). Pressure drop increase by biofilm accumulation in spiral wound RO and NF membrane systems: role of substrate concentration, flow velocity, substrate load and flow direction. *Biofouling, 25*(6), 543-555.

Vrouwenvelder, J. S., Van Loosdrecht, M. C. M., & Kruithof, J. C. (2011). A novel scenario for biofouling control of spiral wound membrane systems. *Water Research, 45*(13), 3890-3898.

Vrouwenvelder, J. S., van Paassen, J. A. M., Kruithof, J. C., & van Loosdrecht, M. C. M. (2009c). Sensitive pressure drop measurements of individual lead membrane elements for accurate early biofouling detection. *Journal of Membrane Science, 338*(1-2), 92-99.

Vrouwenvelder, J. S., van Paassen, J. A. M., Wessels, L. P., van Dam, A. F., & Bakker, S. M. (2006). The Membrane Fouling Simulator: A practical tool for fouling prediction and control. *Journal of Membrane Science, 281*(1-2), 316-324.

Wingender, J., & Flemming, H.-C. (2001). Biofilms in drinking water and their role as reservoir for pathogens. *International Journal of Hygiene and Environmental Health, 214*(6), 417-423.

Wingender, J., & Flemming, H. C. (2004). Contamination potential of drinking water distribution network biofilms *Water Science and Technology* (Vol. 49, pp. 277-286).

Wingender, J., Strathmann, M., Rode, A., Leis, A., Flemming, H.-C., & Ron, J. D. (2001). Isolation and biochemical characterization of extracellular polymeric substances from Pseudomonas aeruginosa *Methods in Enzymology* (Vol. 336, pp. 302-314): Academic Press.

Winters, H., Isquith, I., Arthur, W. A., & Mindler, A. (1983). Control of biological fouling in seawater reverse osmosis desalination. *Desalination, 47*(1-3), 233-238.

Chapter 4

Impact of biofilm accumulation on transmembrane and feed channel pressure drop: effects of crossflow velocity, feed spacer and biodegradable substrate

This chapter is published as:
C. Dreszer, H.-C. Flemming, A. Zwijnenburg, J.C. Kruithof, J.S. Vrouwenvelder. Impact of biofilm accumulation on transmembrane and feed channel pressure drop: effects of crossflow velocity, feed spacer and biodegradable substrate. Water Research 50 (2014) 200-211.

Abstract

Biofilm formation causes performance loss in spiral-wound membrane systems. In this study a microfiltration membrane was used in experiments to simulate fouling in spiral-wound reverse osmosis (RO) and nanofiltration (NF) membrane modules without the influence of concentration polarization. The resistance of a microfiltration membrane is much lower than the intrinsic biofilm resistance, enabling the detection of biofilm accumulation in an early stage. The impact of biofilm accumulation on the transmembrane (biofilm) resistance and feed channel pressure drop as a function of the crossflow velocity (0.05 and 0.20 m s^{-1}) and feed spacer presence was studied in transparent membrane biofouling monitors operated at a permeate flux of 20 L m^{-2} h^{-1}. As biodegradable nutrient, acetate was dosed to the feed water (1.0 and 0.25 mg L^{-1} carbon) to enhance biofilm accumulation in the monitors. The studies showed that biofilm formation caused an increased transmembrane resistance and feed channel pressure drop. The effect was strongest at the highest crossflow velocity (0.2 m s^{-1}) and in the presence of a feed spacer. Simulating conditions as currently applied in nanofiltration and reverse osmosis installations (crossflow velocity 0.2 m s^{-1} and standard feed spacer) showed that the impact of biofilm formation on performance, in terms of transmembrane and feed channel pressure drop, was strong. This emphasizes the importance of hydrodynamics and feed spacer design. Biomass accumulation was related to the nutrient load (nutrient concentration and linear flow velocity). Reducing the nutrient concentration of the feed water enabled the application of higher crossflow velocities. Pretreatment to remove biodegradable nutrient and removal of biomass from the membrane elements played an important part to prevent or restrict biofouling.

4.1. Introduction

Water treatment by membrane filtration is commonly accepted to secure drinking water supply. However, all membrane filtration processes suffer from fouling, so the membrane elements have to be cleaned and eventually replaced. Biofouling has been identified as one of the major problems in membrane operation (Flemming et al. 1997, Gamal Khedr 2000, Paul 1991, Saeed et al. 2000, Tanaka et al., 1994, Winters & Isquith 1979). By definition biofouling occurs due to biofilm growth on the membrane, when it exceeds a threshold of interference (Flemming et al. 1997). Biofilm development is caused by the accumulation and growth of bacterial cells which are embedded in a highly hydrated matrix: extracellular polymeric substances (EPS) (Flemming 2007, Flemming & Wingender 2010). Biofouling causes an increase of operational costs; therefore solutions to extend cleaning intervals and membrane lifetime are required. Biofilm formation impacts the feed channel pressure drop (FCP) as well as the transmembrane pressure drop (TMP). It has been reported that an increase of FCP, one of the main parameters monitored in membrane systems, is the most serious problem caused by biofouling (Baker & Dudley 1998, Vrouwenvelder et al. 2009a). Crossflow velocity (CFV), feed spacer presence and biodegradable nutrient availability have a significant impact on biofilm formation. Theoretically, by increasing the CFV biofilm accumulation can be impacted in two ways. On the one hand increasing the nutrient load, enhances fouling while, on the other hand increasing the shear force reduces fouling by detachment of the biofilms (Horn 2003, Stoodley et al. 1999, Van Loosdrecht 1995). Both possibilities are described in literature. Vrouwenvelder et al., (2010) found an increase in biomass and FCP in fouling simulators operated at a CFV increasing from 0.041 to 0.245 m s^{-1} at a constant nutrient concentration in the feed water. Contradictory to these findings a restriction of fouling at increasing CFV was found as well. Li et al., (2012) and Suwarno et al., (2012) investigated biofouling in reverse osmosis (RO) systems and showed that a crossflow increase caused a reduction of the TMP rise and the flux decline. Also for microfiltration (MF) and ultrafiltration (UF) systems the application of high CFV had a positive effect on fouling reduction (Choi et al. 2005). By applying a mathematical model Radu et al., (2012) showed that by a CFV increase a higher shear force was achieved causing more detachment of biomass. The CFV also had an impact on biofilm structure. At high CFV compact, smooth biofilms were observed, while at low CFV thick, fluffy biofilms were formed (Tijhuis et al. 1996, Van Loosdrecht et al. 1995). In all presented research efforts on

the influence of the CFV on biofouling, several fouling types were observed at the same time. When applying nanofiltration (NF) and RO, concentration polarization is impacting the fouling layer. The influence of the CFV on biofouling, without other fouling types and concentration polarization has not been studied so far in a practical representative system with permeate production. Investigating the impact of pure biofilm formation can give an important insight in biofouling prevention and/or restriction.

The impact of feed spacer presence on the biofilm resistance was investigated but no clear trends were observed (Dreszer et al. 2013). Vrouwenvelder et al., (2009a) concluded that biofouling was a feed spacer problem, because spacers added an additional surface area for bacterial attachment. On the other hand, feed spacers increased the turbulence on the membrane surface, thereby decreasing fouling and concentration polarization (Radu et al. 2012, Suwarno et al. 2012). To provide more insight into these phenomena the influence of feed spacer presence in combination with various CFVs was studied. The experimental set-up applied in these studies gave the possibility to investigate biofilm accumulation at the same hydrodynamic conditions as applied in spiral-wound membrane elements. The possibility to operate the system with and without a feed spacer enabled investigation of the influence of feed spacers. The application of a MF membrane gives the opportunity to investigate biofouling without the influence of concentration polarization or other types of fouling while the biofilm resistance could be distinguished from the membrane resistance (Dreszer et al. 2013).

The main objective of this study was to determine the impact of biofilm accumulation on hydraulic biofilm resistance (transmembrane pressure drop) and feed channel pressure drop as a function of crossflow velocity and feed spacer presence in membrane systems operated at constant flux (20 L m^{-2} h^{-1}) adding a biodegradable substrate. To the authors knowledge this is the first study addressing the impact of biofilm formation on both hydraulic biofilm resistance (transmembrane pressure) and feed channel pressure drop as a function of crossflow velocity and feed spacer presence in membrane systems operated at constant flux.

4.2. Material and Methods

4.2.1 Feed Water and Nutrients

Drinking water prepared from anaerobic groundwater (subsequently treated by aeration, rapid sand filtration, deacidification, and softening at treatment plant Spannenburg in The Netherlands) is distributed without primary chemical disinfection or applying a residual. For all experiments this drinking water was used as the feed water source. Microscopical investigation showed a total bacterial cell number of 3×10^5 cells mL^{-1} in the feed water. The number of colony forming units (CFU) on R_2A media was 2×10^3 CFU mL^{-1} after 10 days incubation at 25 °C. From a nutrient container of 10 L, a concentrated nutrient solution was dosed into the feed water prior to the transparent membrane biofouling monitor at a flow rate of 0.12 L h^{-1}. The dosing was maintained using a peristaltic pump (Masterflex, Cole Palmer, Vernon Hills, USA). The dosage of the nutrient solution was checked periodically by measuring the weight of the nutrient container. The pH-value of the nutrient solution was set at 11 by adding sodium hydroxide, in order to restrict bacterial growth. Fresh nutrient solutions were prepared every 2 days. The dosing flow rate of the nutrient solution (0.12 L h^{-1}) was low compared to the feed water flow rate (12.1 L h^{-1}, at the lowest CFV). Therefore the high pH-value of the nutrient solution had no effect on the pH of the feed water of 7.8. A solution of sodium acetate, sodium nitrate and sodium dihydrogen orthophosphate in a mass ratio C:N:P of 100:20:10, respectively, was employed at different concentrations (Araujo et al. 2012, Creber et al. 2010, Dreszer et al. 2013, Miller et al. 2012, Vrouwenvelder et al. 2009b). All chemicals were purchased in analytical grade from Boom B.V. (Meppel, The Netherlands) and were dissolved in deionized water.

4.2.2 Experimental set-up

The test system was developed by Dreszer et al., (2014, 2013). The test system was comprised of four identical crossflow filtration cells, each with a permeate producing membrane area of 200 cm^2 and a flow channel height of 787 µm (31 mil). In essence, the design of the filtration cells was similar to the membrane fouling simulator (Vrouwenvelder et al., 2006, 2007a,b). Spatial dimensions and hydrodynamics were similar to spiral-wound NF and RO membrane elements. The 787 µm thick feed spacer consisted of polypropylene strings, arranged as a net structure with 90° angles and a porosity of about 0.85. This feed spacer is commonly applied in spiral-wound NF and RO modules for water treatment in

The Netherlands (Vrouwenvelder et al., 2011; Araujo et al., 2012a,b). The height of the flow channel inside the filtration cell was equal to the spacer thickness: 787 µm. The four flow cells were produced from poly methyl methacrylate (PMMA). The transparent material offered the possibility for direct non-destructive visual observations of the biofilm growth. Feed water was filtered through two 10 µm pore size cartridge filters and kept constant at 20 °C. The pressure reducer (V782, Vink Kunststoffen B.V., Didam, The Netherlands) enabled a stable feed pressure of 1.7 bar for all experiments performed during the studies described in this paper. Before entering the filtration cell, nutrients were added using a peristaltic pump (Masterflex L/S pumps, Cole-Palmer Instrument Company, Vernon Hills, Illinois, USA). The linear flow velocity of the feed water was monitored by a flow controller (8805/8905, Brooks Instrument, Hatfield, PA, USA) which was installed behind the outlet of the filtration cell. The permeation rate was maintained by a peristaltic pump (Masterflex L/S pumps, Cole-Palmer Instrument Company, Vernon Hills, Illinois, USA). Fouling development was monitored by measuring the pressure drop over the feed channel and over the membrane, using a differential pressure transmitter (Deltabar S PMD70, Endress + Hauser, Maulburg, Germany; Vrouwenvelder et al., 2009c). The pressures were measured at the monitor inlet and permeate and concentrate outlet.

The application of PES (polyethersulfone) microfiltration membranes (NadirMP005, Microdyn-Nadir GmbH Wiesbaden, Germany) with a pore size of 0.05 µm enabled the investigation of biofouling/biofilm accumulation without any influence of concentration polarization and other types of fouling. Furthermore, membrane resistance and biofilm resistance can be clearly distinguished (Dreszer et al., 2013). The hydrodynamic properties of the transparent membrane biofouling monitor were similar to those found in spiral-wound membrane modules and the use of microfiltration membranes enabled the research on such systems in a simplified way at low pressure conditions (Dreszer et al., 2014).

4.2.3 Biofilm analyses

4.2.3.1 Resistance

Biofilms were analyzed for their resistance based on TMP measurements in the filtration system.

TMP is the driving force for filtration. It is the average pressure difference between the feed and permeate:

$$TMP = ((P_{inlet} + P_{outlet}) / 2) - P_{permeate} \ [bar] \quad (1)$$

Experiments were performed at a constant flux. This leads to an increasing TMP during the growth of the biofilm. The resistance R is therefore TMP depending.

$$R_{total} = TMP / (\eta * J) \ [m^{-1}] \quad (2)$$

where η [Pa s] is the dynamic viscosity of water at a temperature of 20 °C and J is the permeate flux [$m^3\ m^{-2}\ h^{-1}$].
The total resistance in equation (2) is the sum of the membrane resistance and the resistance due to the biofilm formation:

$$R_{total} = R_{membrane} + R_{biofilm} \ [m^{-1}] \quad (3)$$

The total resistance measured at t=0 gives the clean water membrane resistance which is used to calculate the biofilm resistance:

$$R_{biofilm} = R_{total} - R_{membrane} = R_{total} - R_{total\ (t=0)} \ [m^{-1}] \quad (4)$$

4.2.3.2 ***Pre-treatment***

The biofilm was removed from the membrane with a cell scraper (TPP, St. Louis, MO, USA) and suspended in phosphate buffered saline. This solution was shaken for 30 minutes on a multivortex and afterwards subjected to ultrasonic treatment (Bransonic, Berlin, Germany: model 5510E-DTH, output 135 Watts, 42 kHz,) for 2 minutes. Then the solution was homogenized using an ultrasonic probe (Brandson Sonifier 250, G. Heinemann Ultraschall- und Labortechnik, Schwäbisch Gmünd, Germany) in a pulsating mode (20% sonification per time-unit) for 10 pulses with an output of 45 Watt. The obtained biofilm suspension was used for total organic carbon (TOC) determination and EPS isolation.

4.2.3.3 ***Biofilm thickness***

The thickness of the biofilm was calculated by the following equation:

$$Thickness = m/(\rho * A) \ [m] \quad (5)$$

In which m is the mass, ρ the density and A the area of the biofilm. For the calculation, a density equal to the density of water (1 g cm^{-3}) was assumed given that the water content within the analyzed biofilms was above 95%.
The biofilm weight was determined by the weight difference of the membrane including the biofilm and the membrane after mechanical removal of the biofilm. Both weights were determined within 10 minutes after removal of the membrane from the biofouling monitor, in order to minimize liquid evaporation.

4.2.3.4 ***Total organic carbon (TOC)***

To determine the total organic carbon content of the biofilm, an aliquot of the biofilm suspension was placed in a TOC-free glass tube. The sample was treated with the ultrasonic probe (Brandson Sonifier 250, G. Heinemann Ultraschall- und Labortechnik, Schwäbisch Gmünd, Germany) in a pulsating mode (20% sonication per time-unit) for 30 pulses with an output of 45 Watt. During the ultrasonic treatment, the sample was kept on ice for sample temperature control. The TOC was measured with a Shimadzu TOC analyzer (Shimadzu Scientific instruments, Kyoto, Japan).

4.2.3.5 ***EPS isolation***

For the EPS isolation, the biofilm sample was mixed with a cation exchange resin (CER) in the Na^+-form (Dowex, Sigma-Aldrich, Steinheim, Germany) in the ratio of 0.2 g resin per 1 mL sample and shaken for 2 hours at room temperature (Wingender et al. 2001). This suspension was centrifuged at 9000 *g* for 20 minutes at 4 ˚C to separate bacterial cells from the liquid. The supernatant was used for EPS analyses (of proteins and polysaccharides). The number of CFU and total cell number before and after cation exchange treatment was not influenced by the EPS isolation procedure. The CER method for EPS extraction has proven to be successful and mild for charged and non-charged biopolymers, avoiding cell lysis and still providing a good yield of EPS (Frølund et al. 1996).

4.2.3.6 ***Protein quantification in EPS***

Protein concentration was determined using the bicinchoninic acid (BCA) method (Smith et al. 1985) in the Pierce BCA Protein Assay Kit 23225 (Thermo Scientific, Rockford, IL, USA).

4.2.3.7 Polysaccharide quantification in EPS

Polysaccharides were quantified by the phenol/sulfuric acid method (Dubois et al. 1956). Glucose was used as standard. 0.5 ml of sample/standard was mixed with 0.5 mL of 5 % phenol solution and 2.5 mL of 96 % sulfuric acid. The absorption was measured at 490 nm with a microtiterplate reader (1420 Multilable counter Victor^3, PerkinElmer, Waltham, MA, USA).

4.2.4 Experiments and operational conditions

In order to investigate the influence of the CFV and feed spacer presence on biofilm resistance (TMP), FCP and biofilm parameters experiments were performed at low and high CFV: 0.05 and 0.2 m s^{-1}. All experiments were carried out at a permeate flux of 20 L m^{-2} h^{-1} and were performed with and without feed spacer. Duplicate parallel experiments including blank were conducted. Representative data are presented in the paper. In all cases the same trends were observed. Table 4.1 gives detailed information about the operational and nutrient conditions for all performed experiments.

Table 4.1: Nutrient conditions and operational parameters for all performed experiments.

Description	CFV	spacer	dosed carbon load in monitor	dosed carbon conc. in feed water	feed flow	flux	section
	m/s		mg/min	mg/L	mL/min	L/m²/h	
Intramembrane fouling?	0.1	no	0.48	1	472	20	4.3.1
Constant nutrient	0.05	yes	0.20	1	201	20	4.3.2
concentration with spacer	0.2	yes	0.80	1	804		
Constant nutrient	0.05	no	0.24	1	236		
concentration without	0.2	no	0.96	1	944	20	4.3.2
spacer							
Constant nutrient load with	0.05	yes	0.20	1	201	20	4.3.2
spacer	0.2	yes	0.20	0.25	804		
Constant nutrient load	0.05	no	0.24	1	236		
without spacer	0.2	no	0.24	0.25	944	20	4.3.2

4.3. Results

The impact of biofilm accumulation on the transmembrane (biofilm) resistance and FCP was determined as a function of CFV (0.05 and 0.20 m s^{-1}) and feed spacer presence at a constant nutrient concentration (section 4.3.1). Similar studies were performed at constant biodegradable nutrient load (section 4.3.2). The studies were carried out in transparent flow cells (membrane biofouling monitors) operated at constant flux (20 L m^{-2} h^{-1}) and a water temperature of 20 °C. The biofilm resistance was determined by applying a MF membrane (0.05 µm pore size), with a clean membrane resistance much lower than the resistance of a biofilm. Concentration polarization is avoided because of the pore size of the MF membrane.

4.3.1. Intramembrane fouling?

4.3.1.1. Scanning electron microscopy (SEM) observations

It is important to determine whether internal fouling occurs of the microfiltration membrane with a 0.05 mm pore size, adding to the transmembrane pressure drop. To evaluate this, a flow cell was operated at constant flux (20 L m^{-2} h^{-1}) and linear flow velocity (0.1 m s^{-1}), fed with tap water supplemented with a biodegradable nutrient (1 mg L^{-1} acetate C). During 4 days of operation accumulation of biomass on the membrane was observed visually in the transparent monitors. SEM examination (up to 10,000x magnification) of membrane samples taken from the monitors, after that period of operation, showed that fouling accumulated only on the membrane surface and not in the membrane pores (Figure 2.4 and 3.2, Dreszer et al., 2013, 2014). Clearly, the microorganisms (Figure 2.4 and 3.2) were retained by the membrane due to the small pore size of the membrane (0.05 µm). Visually no apparent fouling was observed in the pores of the membrane (Dreszer et al., 2013, 2014).

4.3.1.2. Resistance of virgin and mechanically cleaned membranes

In addition to the SEM analyses the possibility of adsorption of macromolecules in the pores of the membrane affecting the resistance was determined by experiments performed under the same conditions (nutrient, flux and crossflow velocity) as the SEM observations (Dreszer et al., 2013, 2014). The total resistance was determined before (virgin membrane), after fouling and after subsequent

mechanical cleaning by removal of the biofilm by scraping. Experiments were performed in triplicate. Scraping off the fouled membrane reduced the resistance to values similar to the virgin membrane resistance (Figure 2.5 and 3.3, Dreszer et al., 2013, 2014). The scraped membrane had a resistance up to 5% higher than the virgin membrane probably caused by residual biofilm on the membrane surface remaining after the scraping procedure. Therefore the effect of internal membrane fouling on the resistance is negligible compared to the effect of fouling on the membrane surface (Figure 2.5 and 3.3, Dreszer et al., 2013, 2014).

4.3.2 Experiments at constant nutrient concentration

To evaluate the impact of CFV and feed spacer presence on biofilm accumulation, biofouling monitor experiments were carried out at constant nutrient concentration (see Table 4.1).

4.3.2.1. Influence of crossflow velocity on performance

Transparent membrane biofouling monitors were operated at CFVs of 0.05 and 0.20 m s^{-1} with and without feed spacer presence at an acetate concentration of 1 mg L^{-1} acetate C in the feed water.

At the start of the experiment, a higher FCP was observed at a CFV of 0.2 m s^{-1} than at a CFV of 0.05 m s^{-1} (Figures 4.1B and 4.1D). In time, the biofilm resistance (Figures 4.1A and 4.1C) and FCP (Figures 4.1B and 4.1D) increased. At a linear CFV of 0.2 m s^{-1}, a stronger increase of both biofilm resistance and FCP was found (Figures 4.1, 4.2A and 4.2B). With feed spacer a stronger increase in time of biofilm resistance and FCP was observed than without feed spacer, especially at high CFV (0.2 m s^{-1}).

The highest CFV resulted in the initially highest FCP and the most rapid and strongest performance decline in terms of biofilm resistance and FCP.

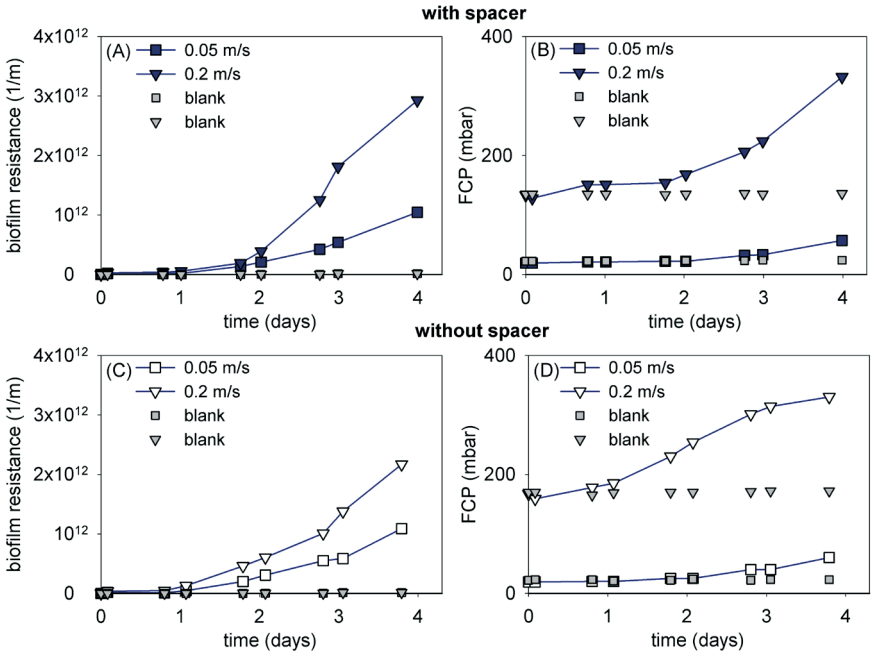

Figure 4.1: Biofilm resistance (A, C) and FCP (feed channel pressure drop, B, D) development over time at a crossflow velocity of 0.05 and 0.20 m s^{-1}. Experiments were performed with and without feed spacer. A constant nutrient concentration (1 mg L^{-1} acetate C) in the feed water was applied for each crossflow velocity. No nutrients were added in the blank measurements.

4.3.1.2 Influence of feed spacer presence on biofilm accumulation

Transparent membrane biofouling monitors were operated at CFVs of 0.05 and 0.20 m s^{-1} at the same acetate concentration (1 mg L^{-1} acetate C) in the feed water with and without feed spacer. After four days of operation the monitors were opened and biofilms were analyzed for thickness, TOC, extracellular proteins and extracellular polysaccharides.

For a CFV of 0.20 m s^{-1}, a stronger increase of biofilm resistance and FCP was observed with feed spacer than without feed spacer. For a CFV of 0.05 m s^{-1} the differences between presence and absence of feed spacer were insignificant (Figures 4.2A, 4.2B). For biofilm thickness, TOC and extracellular proteins and polysaccharides a stronger increase was observed with feed spacer than without feed spacer presence for both CFVs (Figures 4.2C, 4.2D, 4.2E, and 4.2F).

All biomass parameters showed an increased value in feed spacer presence especially when operated at the highest CFV.

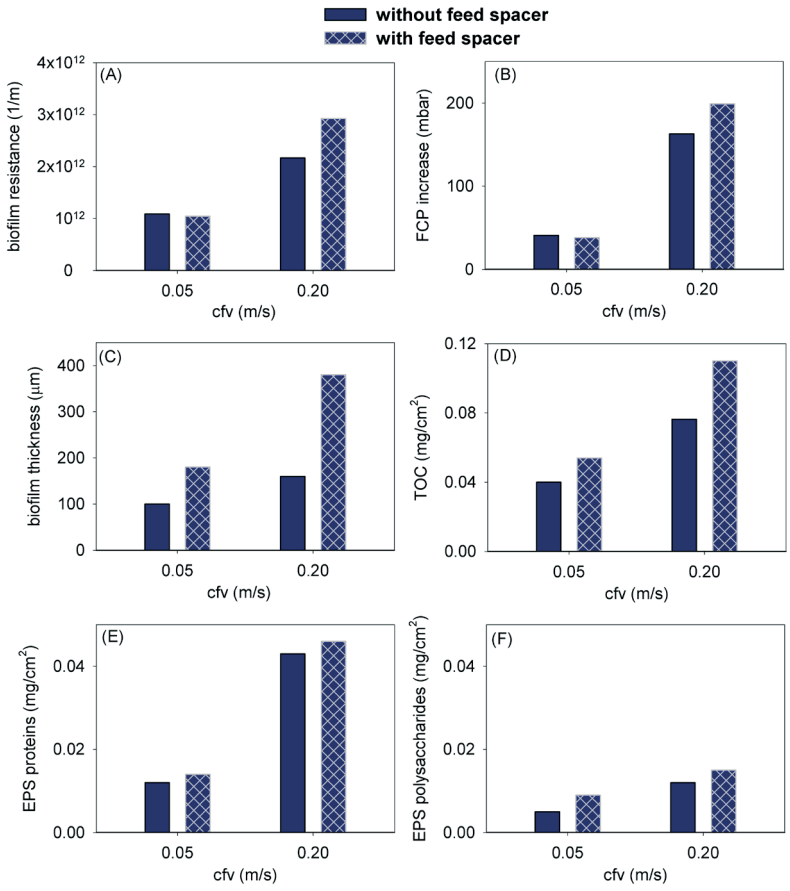

Figure 4.2: Biofilm resistance (A), FCP increase (B), biofilm thickness (C), TOC (D), extracellular proteins (E) and extracellular polysaccharides (F) for biofilms obtained at crossflow velocities of 0.05 and 0.2 m s^{-1}. Experiments were performed with and without feed spacer. A constant nutrient concentration (1 mg L^{-1} acetate C) in the feed water was applied for each crossflow velocity. These measurements refer to the data at the end of the experiments after 4 days.

4.3.2 Experiments at constant nutrient load

To evaluate the impact of the nutrient concentration on biofilm accumulation, biofouling monitor experiments were carried out at a constant nutrient load, in the absence and presence of a feed spacer. The nutrient conditions for these experiments are summarized in Table 4.1. A high nutrient concentration (1.0 mg L^{-1}) together with a low CFV (0.05 m s^{-1}) was compared with a low nutrient concentration (0.25 mg L^{-1}) and a high CFV (0.2 m s^{-1}).

4.3.2.1 Influence of crossflow velocity on performance

Transparent membrane biofouling monitors were operated with and without feed spacer presence at CFVs of 0.05 and 0.20 m s^{-1} at the same carbon load (~ 0.2 mg min^{-1} acetate C).

At the start of the experiment, a higher FCP was observed at a CFV of 0.2 m s^{-1} (Figures 4.3B and 4.3D). In time, the biofilm resistance (Figures 4.3A and 4.3C) and FCP (Figures 4.3B and 4.3D) increased. At a nutrient concentration of 1.0 mg L^{-1} combined with a CFV of 0.05 m s^{-1} a stronger increase in biofilm resistance and FCP was found than at a nutrient concentration of 0.25 mg L^{-1} combined with a CFV of 0.2 m s^{-1} (Figures 4.3, 4.4A and 4.4B). The only exception was observed in the presence of a feed spacer, where a combination of a lower substrate concentration and a higher CFV caused a stronger FCP increase (Figures 4.3B and 4.4B).

At a low nutrient concentration in the feed water combined with a high CFV less biofilm accumulation was observed than at a high nutrient concentration combined with a low CFV.

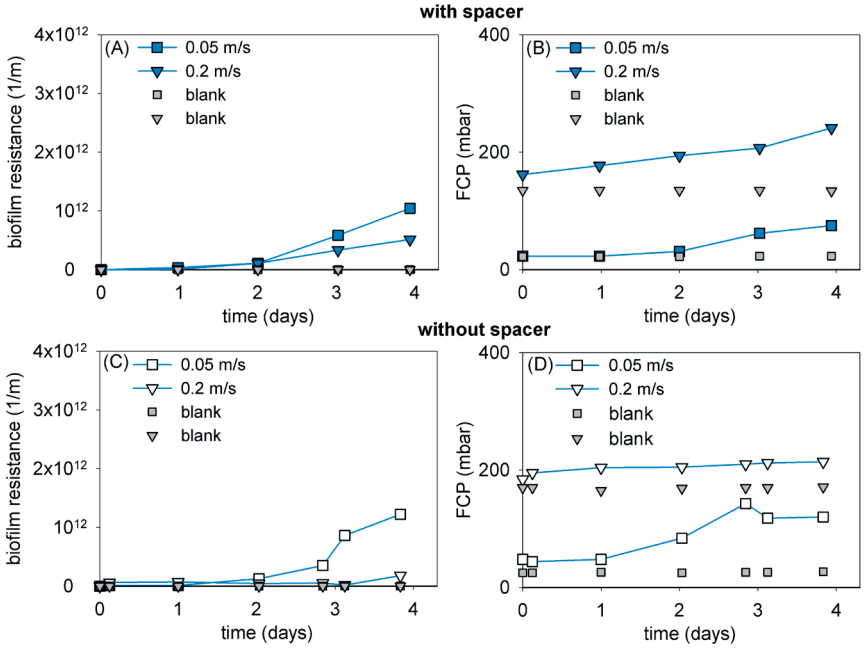

Figure 4.3: Biofilm resistance (A, C) and FCP (feed channel pressure drop, B, D) development over time at a crossflow velocity of 0.05 and 0.20 m s^{-1}. Experiments were performed with and without feed spacer. A constant nutrient load (~ 0.2 mg min^{-1} acetate C) in the fouling simulator was applied for each crossflow velocity. No nutrients were added in the blank measurements.

4.3.2.2 Influence of nutrient concentration on biofilm accumulation

Transparent membrane biofouling monitors were operated with a feed spacer at CFVs of 0.05 and 0.20 m s^{-1} at the same carbon load (~ 0.2 mg min^{-1} acetate C). Therefore, a high nutrient concentration (1.0 mg L^{-1}) together with a low CFV (0.05 m s^{-1}) was compared with a low nutrient concentration (0.25 mg L^{-1}) and a high CFV (0.2 m s^{-1}). After four days of operation the monitors were opened and biofilms were analyzed for thickness, TOC, extracellular proteins and extracellular polysaccharides.

Apart from the FCP increase all determined parameters showed lower values at a CFV of 0.2 m s^{-1} (lower nutrient concentration) compared to a CFV of 0.05 m s^{-1} (higher nutrient concentration) (Figure 4.4). Contrary to the constant nutrient concentration experiments, the constant load experiments showed less biofilm accumulation at the highest CFV. Lowering the nutrient concentration in the feed water (0.25 mg L^{-1} acetate C) decreased biofilm accumulation.

Experiments performed at a constant nutrient load emphasized the need for nutrient reduction to enable a high crossflow operation.

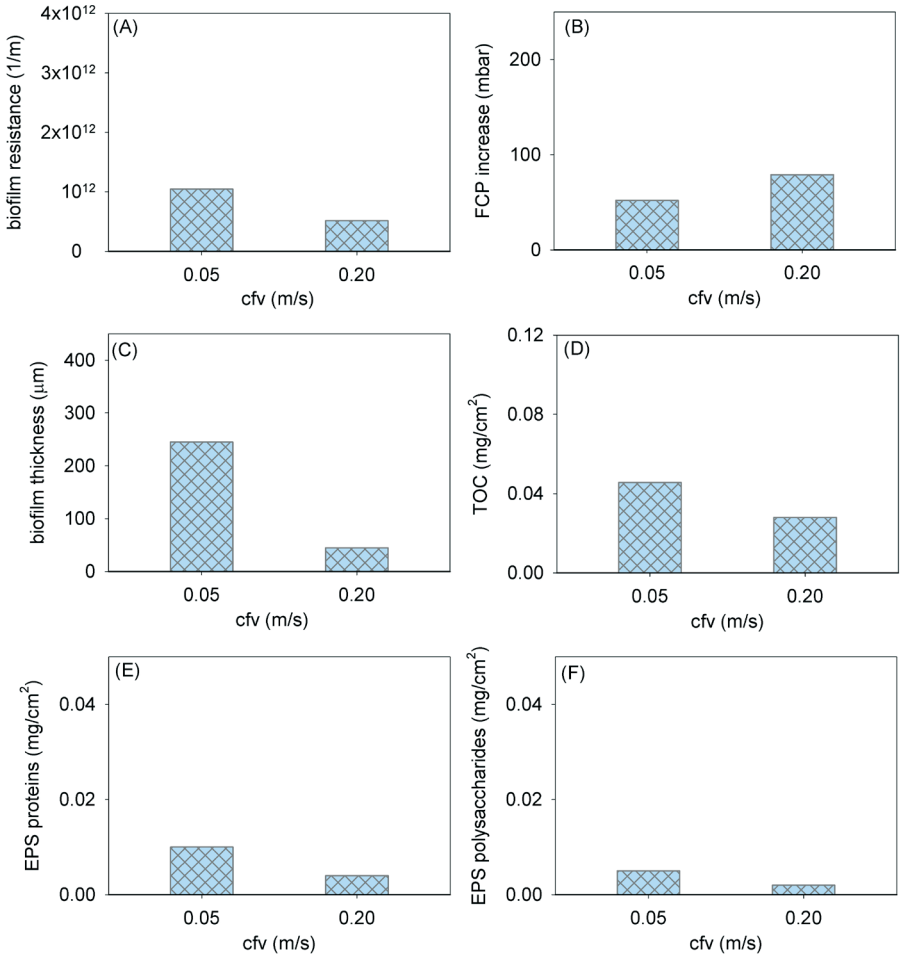

Figure 4.4: Biofilm resistance (A), FCP increase (B), biofilm thickness (C), TOC (D), extracellular proteins (E) and extracellular polysaccharides (F) for biofilms obtained at crossflow velocities of 0.05 and 0.2 m s^{-1}. Experiments were performed with feed spacer. A constant nutrient load (~ 0.2 mg min^{-1} acetate C) in the fouling monitor was applied for each crossflow velocity. These measurements refer to the data at the end of the experiments after 4 days.

4. Discussion

The main objective of this study was to determine the impact of biofilm accumulation on microfiltration (MF) membranes onto hydraulic biofilm resistance, feed channel pressure drop (FCP) and biofilm parameters. The impact of biofilm accumulation was determined as a function of the crossflow velocity (CFV) and feed spacer presence under constant flux (20 L $m^{-2}h^{-1}$) conditions and addition of a biodegradable nutrient. Herewith the conditions in spiral-wound nanofiltration and reverse osmosis membranes were simulated.

The impact of biofilm formation was determined by the increase in transmembrane (biofilm) resistance as well as the increase in FCP and by analyses of the obtained biomass.

It was shown that biofilm formation caused an increase in FCP as well as transmembrane (biofilm) resistance (Figures 4.1, 4.3). Biofilm formation has a strong impact on the FCP (Baker & Dudley 1998) but also the effect on transmembrane (biofilm) resistance cannot be neglected. The transmembrane pressure (TMP) is a direct measure for biofilm formation in a membrane filtration system.

A higher nutrient load was achieved by an increase in CFV at a constant nutrient concentration (Table 4.1). This increase in nutrient load caused a stronger biofilm formation in the monitors (Figures 4.1, 4.2). The smallest increase of all measured parameters was found at the lowest CFV (0.05 m s^{-1}), while the strongest effect of biofilm formation was observed at the highest CFV (0.2 m s^{-1}). An intermediate effect was observed at a CFV of 0.1 m s^{-1} (Supplementary material S4.1).

A feed spacer presence increased the effect of biofilm formation on process performance, especially at a high CFV (Figure 4.2). The surface area, provided by the spacer combined with a high nutrient load, caused a strong impact of biofilm formation on measured process and biofilm parameters (Figures 4.1 and 4.2).

Experiments with a constant nutrient load were applied for several CFVs (Table 4.1). The combination of a low nutrient concentration and a high CFV caused less impact of biofilm formation on all measured parameters than the combination of a high nutrient concentration and a low CFV (Figures 4.3 and 4.4). An exemption was the FCP increase in the presence of a feed spacer which was higher for a low nutrient concentration and a high CFV (Figures 4.3B and 4.4B). This may be caused by the influence of the feed spacer on the hydrodynamic conditions.

4.4.1 Effect of crossflow velocity

By a higher CFV both the nutrient load and the shear force in a filtration system are increased. In literature contradicting effects of CFV on process and biofilm parameters have been reported. In experiments without permeate production the strongest effect was found at the highest CFV (0.245 m s^{-1}) (Vrouwenvelder et al. 2010), while Li et al., (2012), Suwarno et al., (2012) and Radu et al., (2012) observed the lowest impact of the highest CFV in NF and RO systems. Choi et al., (2005) observed the same effect in MF and UF systems.

In this study pure biofilms were produced, so the effect of biofilm formation was not hampered by particle deposition and concentration polarization. Therefore, the impact of biofilm formation on all measured parameters could be studied. At a higher CFV the impact of biofilm formation increased. The net biofilm accumulation is determined by the balance between biofilm growth and biofilm detachment. If at a higher CFV the effect of biofilm formation is increasing, the biofilm growth must be stronger than the detachment. In our study, the effect of a higher nutrient load was predominant over a higher shear force effect: a higher CFV caused a stronger impact of biofilm formation on the measured process and biofilm parameters.

4.4.2 Effect of feed spacer

Feed spacers in spiral-wound membrane elements are used to separate the membrane sheets. Furthermore they cause turbulence close to the membrane surface, thereby restricting membrane fouling. A spacer commonly applied in water treatment, a 31 mil spacer, was also used in this study.

Literature shows that feed spacers reduce fouling by particle deposition and scaling by additional turbulence (Radu et al. 2012, Suwarno et al. 2012). However, also fouling enhancing effects have been reported (Vrouwenvelder et al. 2009a).

In the present study the impact of biofilm formation was increased by the presence of feed spacers, especially at high CFV and favorable nutrient conditions. At such nutrient conditions bacteria grow and produce a biofilm regardless of the turbulence caused by feed spacers.

To benefit to a larger extent from turbulence caused by feed spacers modifications may be necessary by making the structure and material of the spacer (and the membrane) less attractive for bacterial adhesion.

4.4.3 Effect of nutrient load

The fact that the nutrient load impacts biofilm formation and biofouling has been reported many times (Dreszer et al. 2013, Flemming et al. 1997, Griebe & Flemming 1998, Kamp et al. 2000, Speth et al. 2000, Suwarno et al. 2012, van der Hoek et al. 2000, Vrouwenvelder et al. 2009b; Ying et al., 2013).

This study has shown that an increase in nutrient load caused by an increase in CFV caused a stronger biofilm formation. At a constant nutrient load the combination low nutrient concentration / high CFV caused less biofilm formation than the combination high nutrient concentration / low CFV.

Recent studies (Vrouwenvelder et al., 2009a-c; Ying et al., 2013) show that the nutrient loading rate is a key determining parameter for biofilm growth, for the range of linear crossflow velocities (shear), currently applied in spiral-wound nanofiltration and reverse osmosis membrane systems. The effect of the same amount of accumulated biomass on the pressure drop increase was related to the linear flow velocity (Vrouwenvelder et al., 2009a-c).

These observations emphasize the need for nutrient removal by pretreatment to enable the application of high CFVs and to develop effective strategies for biomass removal from the membrane elements.

4.4.4 Concentration polarization

The use of a 0.05 µm pore size membrane, enables the accurate assessment of the pure hydraulic biofilm resistance in a simple set-up operated at low pressures, without the influence of concentration polarization of salts and biodegradable nutrients. However, in practical NF and RO systems concentration polarization can influence biofilm formation in several ways. Concentration polarization of salts may restrict biofilm development while concentration polarization of biodegradable nutrients may enhance biofilm development. The presence of a biofilm also contributes to concentration polarization and enhances osmotic pressure (Herzberg & Elimelech, 2007, 2008; Chong et al., 2008a,b; Radu et al., 2010, 2011). A high-pressure version of the low pressure monitor used in this study is being developed, enabling to further unravel the relationship between concentration polarization, biofouling and membrane performance.

4.4.5 Evaluation

In literature it is reported that a high CFV and a feed spacer application reduce biofilm formation and thereby biofouling (Choi et al. 2005, Li et al. 2012, Radu et al. 2012, Suwarno et al. 2012). However, the results presented in this paper on

biofilm formation without other fouling types and concentration polarization, are contradictory to these findings. The results in this study showed a stronger biofilm formation when the CFV increased. This effect was strongest in the presence of a feed spacer (Figure 4.5).

Combining the results of this research effort for intrinsic biofilm formation with results obtained in practice where organic fouling, scaling, and concentration polarization played a part as well (Choi et al. 2005, Li et al. 2012, Suwarno et al. 2012) the following hypothesis may be formulated:

High CFV and feed spacer presence decrease the effect of organic fouling, scaling and concentration polarization (Chong et al. 2008, Neal et al. 2003) but the effect of biofilm formation on process and biofilm parameters (and biofouling) is increased. Therefore it is crucial to reduce the nutrient concentration by pretreatment in order to benefit optimally from feed spacer presence and to enable a high CFV.

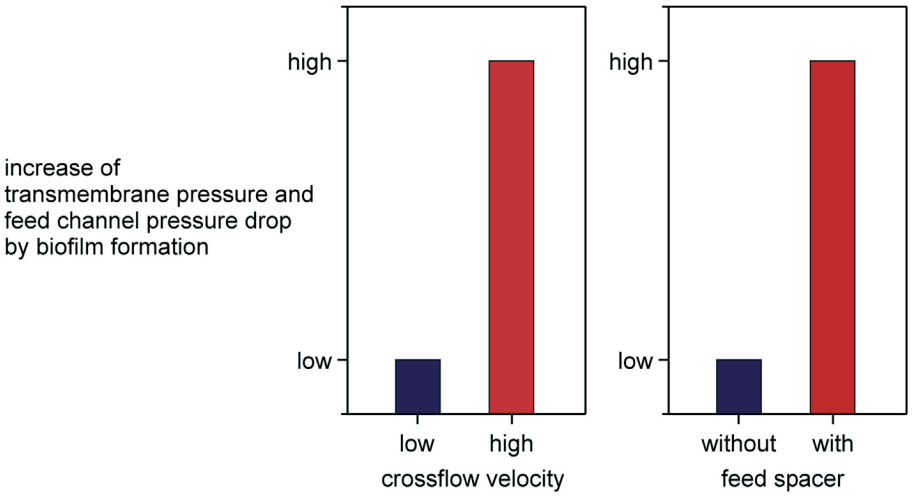

Figure 4.5: Impact of crossflow velocity (A), feed spacer presence (B) on the relative increase of transmembrane resistance and feed channel pressure drop by biofilm accumulation.

4.5. Conclusions

This study assessed the impact of biofilm accumulation on membrane performance varying the crossflow velocity and the feed spacer presence. Based on the results the following conclusions could be drawn:

- biofilm formation causes operational problems concerning both rate and extent of feed channel pressure drop and transmembrane (biofilm) resistance increase.
- biomass accumulation was related to nutrient load (nutrient concentration and linear flow velocity)
- problems are larger at higher crossflow velocity (more nutrient) and in feed spacer presence.
- nutrient removal by pretreatment enables the application of higher crossflow velocities.

Acknowledgements

This work was performed at Wetsus, Centre of Excellence for Sustainable Water Technology (www.wetsus.nl). Wetsus is funded by the Dutch Ministry of Economic Affairs, the European Union European Regional Development Fund, the Province of Fryslân, the city of Leeuwarden and by the EZ-KOMPAS Program of the "Samenwerkingsverband Noord-Nederland" and the King Abdullah University of Science and Technology (KAUST). The authors like to thank the participants of the research theme "Biofouling", KAUST and Evides waterbedrijf for the fruitful discussions and their financial support. In addition the authors would especially like to thank the students Małgorzata Nowak and Stanisław Wojciechowski for their great contribution to the experimental work.

Supplementary Material Chapter 4

S4.1 Initially all experiments were performed at three different crossflow velocities: 0.05, 0.1 and 0.2 m s^{-1}. For the convenience of the reader and to amplify the message of this paper results for 0.05 and 0.2 m s^{-1} are shown only. As shown in Figure S4.1 all the trends and messages in the presented research stay the same regardless the 0.1 m s^{-1} measurements.

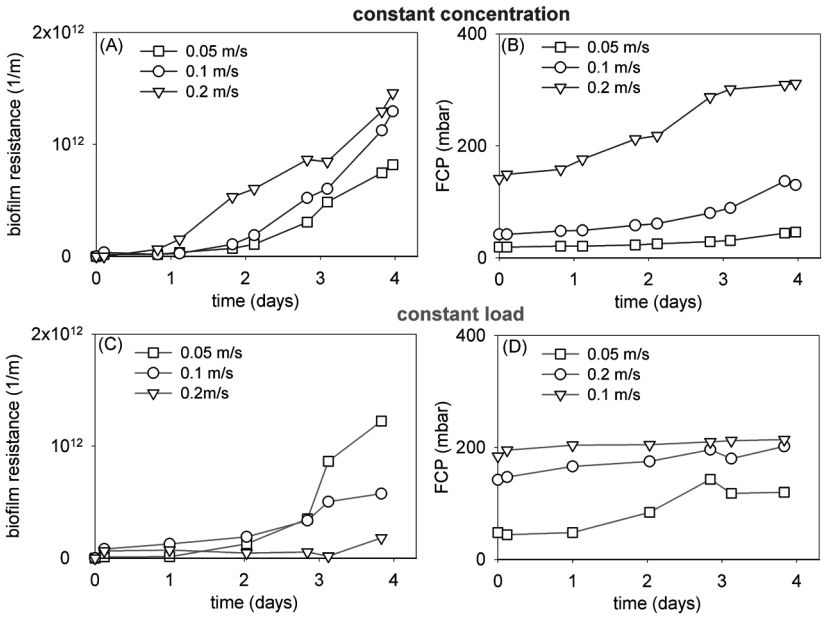

Figure S4.1: Biofilm resistance (A, C) and FCP (feed channel pressure drop B, D) development over time for biofilms obtained at 3 crossflow velocities with constant nutrient concentration in the feed water (1 mg L^{-1}, A, B) and constant nutrient load in the flow cell (0.2 mg min^{-1}, C, D). Experiments were performed without feed spacer.

References

Araújo, P.A., Miller, D.J., Correia, P.B., van Loosdrecht, M.C.M., Kruithof, J.C., Freeman, B.D., Paul, D.R. & Vrouwenvelder, J.S. (2012) Impact of feed spacer and membrane modification by hydrophilic, bactericidal and biocidal coating on biofouling control. *Desalination* 295(0), 1-10.

Araujo, P.A., Van Loosdrecht, M.C.M., Kruithof, J.C., & Vrouwenvelder, J.S. (2012b). The potential of standard and modified feed spacers for biofouling control. *Journal of Membrane Science* 403-404, 58-70.

Baker, J.S. & Dudley, L.Y. (1998) Biofouling in membrane systems - A review. *Desalination* 118(1-3), 81-89.

Choi, H., Zhang, K., Dionysiou, D.D., Oerther, D.B. & Sorial, G.A. (2005) Influence of cross-flow velocity on membrane performance during filtration of biological suspension. *Journal of Membrane Science* 248(1-2), 189-199.

Chong, T.H., Wong, F.S. & Fane, A.G. (2008) Implications of critical flux and cake enhanced osmotic pressure (CEOP) on colloidal fouling in reverse osmosis: Experimental observations. *Journal of Membrane Science* 314(1-2), 101-111.

Chong, T.H., Wong, F.S. & Fane, A.G. (2008b) The effect of imposed flux on biofouling in reverse osmosis: role of concentration polarization and biofilm enhanced osmotic pressure. *Journal of Membrane Science* 325(1-2), 840-850.

Creber, S.A., Vrouwenvelder, J.S., Van Loosdrecht, M.C.M., & Johns, M.L. (2010) Chemical cleaning of biofouling in reverse osmosis membranes evaluated using magnetic resonance imaging. *Journal of Membrane Science* 362(1-2), 202-210.

Dreszer, C., Vrouwenvelder, J.S., Paulitsch-Fuchs, A.H., Zwijnenburg, A., Kruithof, J.C. & Flemming, H.C. (2013a) Hydraulic resistance of biofilms. *Journal of Membrane Science* 429(0), 436-447.

Dreszer, C., Flemming, H.-C., Wexler, A.D., Zwijnenburg, A., Kruithof, J.C., & Vrouwenvelder, J.S. (2014) Development and testing of a transparent membrane biofouling monitor. *Desalination and Water Treatment* 52, 1807-1819.

Dubois, M., Gilles, K.A., Hamilton, J.K., Rebers, P.A. & Smith, F. (1956) Colorimetric Method for Determination of Sugars and Related Substances. *Analytical Chemistry* 28(3), 350-356.

Flemming, H.-C., Neu, T. R., & Wozniak, D. J. (2007) The EPS Matrix: The "House of Biofilm Cells". *Journal of Bacteriology* 189(22), 7945-7947.

Flemming, H.C., Schaule, G., Griebe, T., Schmitt, J. & Tamachkiarowa, A. (1997) Biofouling-the Achilles heel of membrane processes. *Desalination* 113(2-3), 215-225.

Flemming, H.C. & Wingender, J. (2010) The biofilm matrix. *Nature Reviews Microbiology* 8(9), 623-633.

Frølund, B., Palmgren, R., Keiding, K. & Nielsen, P.H.r. (1996) Extraction of extracellular polymers from activated sludge using a cation exchange resin. *Water Research* 30(8), 1749-1758.

Gamal Khedr, M. (2000) Membrane fouling problems in reverse osmosis desalination applications. *Desalination & Water Reuse* 10(3), 8–17.

Griebe, T. & Flemming, H.-C. (1998) Biocide-free antifouling strategy to protect RO membranes from biofouling. *Desalination* 118(1-3), 153-IN159.

Herzberg, M. & Elimelech, M. (2007) Biofouling of reverse osmosis membranes: role of biofilm-enhanced osmotic pressure. *Journal of Membrane Science* 295, 11-20.

Herzberg, M. & Elimelech, M. (2008) Physiology and genetic traits of reverse osmosis membrane biofilms: a case study with Pseudomonas aeruginosa. *International Society of Microbiological Engineering Journal* 2, 180-194.

Horn, H., Reiff, H., & Morgenroth, E. (2003) Simulation of growth and detachment in biofilm systems under defined hydrodynamic conditions. *Biotechnol. Bioeng.* 81(5), 607-617.

Kamp, P.C., Kruithof, J.C. & Folmer, H.C. (2000) UF/RO treatment plant Heemskerk: from challenge to full scale application. *Desalination* 131(1-3), 27-35.

Li, Z.-Y., Yangali-Quintanilla, V., Valladares-Linares, R., Li, Q., Zhan, T. & Amy, G. (2012) Flux patterns and membrane fouling propensity during desalination of seawater by forward osmosis. *Water Research* 46(1), 195-204.

Miller, D.J., Araújo, P.A., Correia, P.B., Ramsey, M.M., Kruithof, J.C., van Loosdrecht, M.C.M., Freeman, B.D., Paul, D.R., Whiteley, M. & Vrouwenvelder, J.S. (2012) Short-term adhesion and long-term biofouling testing of polydopamine and poly(ethylene glycol) surface modifications of membranes and feed spacers for biofouling control. *Water Research* 46(12), 3737-3753.

Neal, P.R., Li, H., Fane, A.G. & Wiley, D.E. (2003) The effect of filament orientation on critical flux and particle deposition in spacer-filled channels. *Journal of Membrane Science* 214(2), 165-178.

Paul, D.H. (1991) Reverse osmosis: scaling, fouling and chemical attack. *Desalination & Water Reuse* 1, 8–11.

Radu, A.I., Vrouwenvelder, J.S., van Loosdrecht, M.C.M. & Picioreanu, C. (2010) Modeling the effect of biofilm formation on reverse osmosis performance: flux, feed channel pressure drop and solute passage. *Journal of Membrane Science* 365(1-2), 1-15.

Radu, A.I., Vrouwenvelder, J.S., van Loosdrecht, M.C.M. & Picioreanu, C. (2011) Biofouling in membrane devices treating water with different salinities: a modeling study. *Desalination and Water Treatment* 34(1-3), 284-289.

Radu, A.I., Vrouwenvelder, J.S., van Loosdrecht, M.C.M. & Picioreanu, C. (2012) Effect of flow velocity, substrate concentration and hydraulic cleaning on biofouling of reverse osmosis feed channels. *Chemical Engineering Journal* 188(0), 30-39.

Saeed, M.O., Jamaluddin, A.T., Tisan, I.A., Lawrence, D.A., Al-Amri, M.M. & Chida, K. (2000) Biofouling in a seawater reverse osmosis plant on the Red Sea coast, Saudi Arabia. *Desalination* 128(2), 177-190.

Smith, P.K., Krohn, R.I., Hermanson, G.T., Mallia, A.K., Gartner, F.H., Provenzano, M.D., Fujimoto, E.K., Goeke, N.M., Olson, B.J. & Klenk, D.C. (1985) Measurement of protein using bicinchoninic acid. *Analytical Biochemistry* 150(1), 76-85.

Speth, T.F., Gusses, A.M. & Scott Summers, R. (2000) Evaluation of nanofiltration pretreatments for flux loss control. *Desalination* 130(1), 31-44.

Stoodley, P., Boyle, J.D., DeBeer, D. & Lappin-Scott, H.M. (1999) Evolving perspectives of biofilm structure. *Biofouling* 14(1), 75-90.

Suwarno, S.R., Chen, X., Chong, T.H., Puspitasari, V.L., McDougald, D., Cohen, Y., Rice, S.A. & Fane, A.G. (2012) The impact of flux and spacers on biofilm development on reverse osmosis membranes. *Journal of Membrane Science* 405-406(0), 219-232.

Tasaka, K., Katsura, T., Iwahori, H., & Kamiyama, Y. (1994) Analysis of RO elements operated at more than 80 plants in Japan. *Desalination* 96, 259–272.

Tijhuis, L., Hijman, B., Loosdrecht, M.C.M. & Heijnen, J.J. (1996) Influence of detachment, substrate loading and reactor scale on the formation of biofilms in airlift reactors. *Applied Microbiology and Biotechnology* 45(1-2), 7-17.

Van der Hoek, J.P., Hofman, J.A.M.H., Bonné, P.A.C., Nederlof, M.M. & Vrouwenvelder, H.S. (2000) RO treatment: selection of a pretreatment scheme based on fouling characteristics and operating conditions based on environmental impact. *Desalination* 127(1), 89-101.

Van Loosdrecht, M.C.M., Eikelboom, D., Gjaltema, A., Mulder, A., Tijhuis, L., & Heijnen, J.J. (1995) Biofilm structures. *Water Science and Technology* 32(8), 35-43.

Van Loosdrecht, M.C.M., Bereschenko, L.A., Radu, A.I., Kruithof, J.C., Picioreanu, C., Johns, M.L., & Vrouwenvelder, J.S. (2012) New approaches to characterizing and understanding biofouling od spiral wound membrane systems. *Water Science and Technology* 66(1), 88-94.

Vrouwenvelder, J.S., van Paassen, J.A.M., Wessel, L.P., van Dam, A.F., & Bakker, S.M. (2006) The membrane fouling simulator: a practical tool for fouling prediction and control. *Journal of Membrane Science* 281(1-2), 316-324.

Vrouwenvelder, J. S., Bakker, S. M., Wessels, L. P., & van Paassen, J. A. M. (2007a). The Membrane Fouling Simulator as a new tool for biofouling control of spiral-wound membranes. *Desalination, 204*(1-3), 170-174.

Vrouwenvelder, J. S., Bakker, S. M., Cauchard, M., Le Grand, R., Apacandie, M., Idrissi, M., Lagrave, S., Wessel, L.P., van Passen, J.A.M., Kruithod, J.C., & van Loosdrecht, M. C. M. (2007b). The Membane Fouling Simulator: a suitable tool for prediction and characterisation of membrane fouling. *Water Sci Technology, 55*(55), 197 - 205.

Vrouwenvelder, J.S., Graf von der Schulenburg, D.A., Kruithof, J.C., Johns, M.L. & Van Loosdrecht, M.C.M. (2009a) Biofouling of spiral-wound nanofiltration and reverse osmosis membranes: A feed spacer problem. *Water Research* 43(3), 583-594.

Vrouwenvelder, J.S., Hinrichs, C., Van der Meer, W.G.J., Van Loosdrecht, M.C.M. & Kruithof, J.C. (2009b) Pressure drop increase by biofilm accumulation in spiral wound RO and NF membrane systems: role of substrate concentration, flow velocity, substrate load and flow direction. *Biofouling* 25(6), 543-555.

Vrouwenvelder, J.S., Van Paassen, J.A.M., Kruithof, J.C., & Van Loosdrecht, M.C.M. (2009c) Sensitive pressure drop measurements of individual lead membrane elements for accurate early biofouling detection. *Journal of Membrane Science* 338(1-2), 92-99.

Vrouwenvelder, J.S., Buiter, J., Riviere, M., van der Meer, W.G.J., van Loosdrecht, M.C.M. & Kruithof, J.C. (2010) Impact of flow regime on pressure drop increase and biomass accumulation and morphology in membrane systems. *Water Research* 44(3), 689-702.

Vrouwenvelder, J.S., Van Loosdrecht, M.C.M., & Kruithof, J.C. (2011) A novel scenario for biofouling control of spiral wound membrane systems. *Water Research* 45(13), 3890-3898.

Wingender, J., Strathmann, M., Rode, A., Leis, A., Flemming, H.-C., & Ron, J.D. (2001) *Methods in Enzymology*, pp. 302-314, Academic Press.

Winters, H. & Isquith, I.R. (1979) In-plant microfouling in desalination. *Desalination* 30(1), 387-399.

Ying, W., Gitis, V., Lee, J., & Herzberg, M. (2013) Effects of shear rate on biofouling of reverse osmosis membrane during tertiary wastewater desalination. *Journal of Membrane Science* 427, 390-398.

Chapter 5

Discussion

5.1 Introduction

Membrane filtration processes such as nanofiltration (NF) and reverse osmosis (RO) can produce high-quality water from sources such as seawater and sewage. The demand for fresh water in the world is increasing and regulations on water quality become more stringent (Shannon et al., 2008). The effect of these developments and decreasing costs of membrane processes are illustrated by the increasing role of membrane filtration processes in advanced water treatment practice (Mallevialle et al., 1996; Shannon et al., 2008). A major drawback of NF and RO application is membrane fouling, resulting in an increase of the membrane performance parameters feed channel pressure drop and transmembrane pressure drop (Dreszer et al., 2014a; Vrouwenvelder et al., 2010a; Vrouwenvelder et al., 2009a). These problems strongly increase the operation costs of the membrane filtration system. The four major fouling mechanisms of NF and RO membranes are inorganic, particulate, organic fouling, and biofouling (Baker, 2012a). These types of fouling may occur simultaneously and can influence each other (Strathmann et al., 2013). Scaling by inorganic compounds is usually controlled by using a scale inhibitor, such as a polymer or an acid (Baker, 2012b). Particulate fouling is controlled by pretreatment, such as ultrafiltration (Baker, 2012c). All types of fouling, except biofouling, are controllable by pretreatment. Biofouling includes the presence of living organisms which can multiply and grow into dense fouling layers even if present only in small numbers initially (Flemming et al., 1997).

Biofouling - excessive growth of microbial biofilms impacting membrane performance - is one of the most serious problems in membrane applications (Baker & Dudley, 1998; Ridgway & Flemming, 1996; Ridgway et al., 1983; Schneider et al., 2005; Tasaka et al., 1994), influencing (i) the amount and quality of the treated water, (ii) reliability of water production, and (iii) operating costs. Numerous authors have described biofouling problems in membrane installations (Flemming et al., 1997; Gamal Khedr, 2000; Paul, 1991; Saeed et al., 2000; Tasaka et al., 1994; Van Loosdrecht et al., 2012; Winters & Isquith, 1979). In relation to membrane performance, the influence of various operational parameters such as permeate flux (rate of water transport through the membrane), crossflow velocity (rate of water flow along the membrane feed side), biodegradable substrate content ("food" for bacteria causing biofilm growth), and feed spacer presence (separating the membrane sheets in membrane modules) has been addressed (Griebe & Flemming, 1998; Vrouwenvelder et al., 2009b). Recently the study of membrane biofouling and its control has intensified.

Given the relevance of biofouling, it is surprising that no measured data exist about the intrinsic hydraulic resistance of biofilms and the impact on transmembrane and feed channel pressure drop. It is essential to investigate the hydraulic resistance of biofilms and to determine the contribution of biofilms to membrane performance losses. To measure the resistance of biofilms the influence of other fouling types and concentration polarization should be avoided. Concentration polarization is the accumulation of a solute in a thin layer at the membrane surface, caused by the membrane solute rejection properties. It can influence biofilm formation and membrane performance (e.g. Gutman et al., 2012). Concentration polarization occurs of e.g. biodegradable substrates and salts. Biodegradable substrate concentration polarization causes a higher food concentration at the membrane surface enhancing biofilm formation, while salt concentration polarization reduces the permeate flux by an increased osmotic pressure (Chong et al., 2008; Herzberg et al, 2010; Herzberg & Elimelech, 2007). Biofilm formation on the membrane and feed spacer can enhance concentration polarization of salts, increasing the performance losses (Chen et al., 2013; Chong et al., 2008; Herzberg et al., 2010; Herzberg & Elimelech, 2007).

The aim of this thesis was to investigate the intrinsic hydraulic resistance of biofilms and the relation of hydraulic biofilm resistance to operational parameters such as: permeate flux, crossflow velocity, biodegradable substrate content, and feed spacer presence.

At the start of this PhD study, no suitable membrane test system was available to study the hydraulic resistance of pure biofilms without the influence of concentration polarization or other types of fouling.

5.2 Objectives

The main objectives of this thesis on hydraulic resistance of biofilms were:

1. The development of a membrane monitor system to enabling the determination of biofilm resistance.
2. The determination of the hydraulic biofilm resistance, at average and high permeate flux.
3. The investigation of operational parameters influencing the biofilm resistance such as biodegradable nutrient concentration, crossflow velocity, and feed spacer presence.

5.3 Proof of objectives

1. **Objective: Development of a membrane monitor system enabling the determination of biofilm resistance**

A modified, transparent and permeate producing version of the membrane fouling simulator (MFS, Vrouwenvelder et al., 2006) was developed to assess (i) hydraulic biofilm resistance, (ii) performance parameters feed-channel pressure drop and transmembrane pressure drop, and (iii) in situ spatial visual and optical observations of the biofilm in the transparent monitor (Figure 2.1; page 44), e.g. using optical coherence tomography. The active surface area of the membrane was 200 cm^2 which enabled the production of sufficient biomass amounts for microbiological and chemical analysis. The flow channel height of the transparent membrane fouling monitor was equal to the feed spacer thickness enabling operation with and without feed spacer. The application of a microfiltration membrane with a pore size of 0.05 µm allowed operation at low pressures and prevented concentration polarization of salt and substrate, enabling accurate measurement of the intrinsic hydraulic biofilm resistance. Tests confirmed that the biofilm was present on the membrane surface only which enabled the separation of membrane and biofilm resistance (Figures 2.4, 2.5, 3.2, and 3.3; pages 51, 52, 77, and 78). Experiments at various operating conditions showed the suitability of the monitor to determine hydraulic biofilm resistance and for controlled biofouling studies. Validation tests on e.g. hydrodynamic behavior, flow field distribution, and reproducibility showed that the small-sized monitor was a representative tool for membrane processes applied in practice, such as spiral-wound NF and RO (section taken from Dreszer et al 2014b). The numbers obtained for biofilm resistance are characteristic for biofilms obtained during this research. Different biofilms may show different values for biofilm resistance because it is related to the filtration system and operational conditions. Therefore it is essential to characterize the filtration cell, its hydrodynamics and the operating conditions in order to obtain results which can be compared to other studies and translated to other systems and practice. A membrane monitor system for the determination of the intrinsic hydraulic resistance of biofilms was successfully developed. The designed system is suitable for performing experiments at various operating conditions representing membrane processes as applied in full scale filtration systems.

2. Objective: Determination of the hydraulic biofilm resistance, at average and high permeate flux

In the developed monitor system biofilms were generated at two fluxes (20 and 100 L m^{-2} h^{-1}) and constant crossflow velocity (0.1 m s^{-1}). To accelerate fouling acetate was added to the feed water (1.0 mg L^{-1} carbon) besides a control without acetate supply. Transmembrane pressure drop was monitored and biofilm resistance was calculated. The following biofilm parameters were determined: total cell number (TCN), total organic carbon (TOC), extracellular polymeric substances (EPS), and biofilm thickness. It was shown that no internal membrane fouling occurred (Figures 2.4, 2.5, 3.2, and 3.3; pages 51, 52, 77, and 78) and that the fouling layer consisted of a grown biofilm and was not a filter cake of accumulated bacterial cells. Membrane operation at a flux of 100 L m^{-2} h^{-1} caused higher cell numbers, more biomass, and higher biofilm resistance than at a flux of 20 L m^{-2} h^{-1} (Figure 3.4; page 79). The biofilm thickness was not increased by the high permeate flux; it was in the same order of magnitude as the thickness of a biofilm formed at average flux (Figure 3.4b; page 79). Biofilms showing a different hydraulic resistance had the same biofilm thickness, thus no correlation of biofilm resistance with biofilm thickness was found. The total cell number in the obtained biofilms was between 4×10^{7} and 5×10^{8} cells cm^{-2}, making up less than a half percent of the overall biofilm volume, therefore not hampering the water flow through the biofilm significantly. Tests were performed in which the resistance of a grown biofilm was compared to the resistance of a filter cake consisting of bacterial cells without an EPS matrix. In both cases the total cell count was the same but there was a difference in EPS content. The hydraulic resistance of the biofilm was much higher than the resistance of the filter cake (Figure 3.5; page 80). The biofilm resistance is mainly attributed to EPS, probably due to the tortuosity of the biopolymers to water molecules passing the biofilm. Herzberg et al. (2007, 2009) performed a similar study and also concluded that mainly the EPS of the biofilm contributes to the hydraulic resistance. They suggested that the lower resistance of the filter cake is related to its more porous structure (Herzberg & Elimelech, 2007).

The obtained data showed that intrinsic biofilm resistance (6×10^{12} m^{-1}) was high compared to the resistance of the employed microfiltration membrane (5×10^{11} m^{-1}). However, in NF (virgin membrane resistance ca. 2×10^{13} m^{-1}) and RO (virgin membrane resistance ca. 9×10^{13} m^{-1}) membrane systems, the hydraulic

resistance of the biofilm will not contribute significantly to the overall hydraulic resistance (Figure 3.10; page 87) (section taken from Dreszer et. al, 2013). But biofilm accumulation is still crucial for NF and RO membrane system performance. The presence of a biofilm enhances the accumulation of salts on the membrane due to "hindered back-diffusion of salt ions" through the biofilm and the lack of crossflow velocity within the biofilm which increases the transmembrane osmotic pressure (Gutman et al., 2012; Herzberg, 2010; Radu et al., 2010; Chong et al., 2008; Herzberg & Elimelech, 2007). As a result, the performance declines. Biofilm accumulation also impacts the performance of membrane filtration systems by reducing the crossflow velocity which causes a flux decline as well (Vrouwenvelder et al., 2009c; Baker & Dudley, 1998).The crossflow velocity is reduced by two different mechanisms. First: Biofilm accumulation blocks the feed channel and the crossflow velocity of the feed water is hampered. Second: Biofilms increase the friction resistance in the feed channel due to their surface roughness and three-dimensional vibration under the influence of crossflow velocity (Andrewartha et al., 2010; Picologlou et al., 1980). Biofilms in membrane filtration systems disturb the performance not only by the additional hydraulic (transmembrane) resistance but also by enhancing other types of fouling and reducing flow velocities.
The intrinsic hydraulic resistance of biofilms at average and high permeate flux was effectively determined and the obtained results were related to biofilm composition and membrane performance.

3. **Objective: Investigation of operational parameters influencing the biofilm resistance such as biodegradable nutrient concentration, crossflow velocity, and feed spacer presence**

The impact of biofilm accumulation on the transmembrane (biofilm) resistance and feed channel pressure drop as a function of the crossflow velocity (0.05 and 0.20 m s^{-1}) and feed spacer presence was studied in transparent membrane biofouling monitors operated at a permeate flux of 20 L m^{-2} h^{-1}. Acetate was dosed to the feed water (1.0 and 0.25 mg L^{-1} carbon) to enhance biofilm accumulation in the monitors. The obtained results showed that biofilm formation caused an increased transmembrane resistance and feed channel pressure drop. The effect was strongest at the highest crossflow velocity (0.2 m s^{-1}) in the presence of a feed spacer (Figures 4.1 and 4.2; pages 108 and 109). Simulating conditions currently applied in NF and RO installations (crossflow velocity 0.2 m s^{-1} and standard feed

spacer) showed that the impact of biofilm formation on performance, in terms of transmembrane and feed channel pressure drop, was strong. This emphasized the importance of modified plant operation in terms of hydrodynamics and feed spacer design. In the present thesis pure biofilms were produced, so the effect of biofilm formation was not hampered by particle deposition and concentration polarization. Therefore, the impact of biofilm formation on all measured parameters could be studied. At a higher crossflow velocity a stronger impact of biofilm formation was observed (Figures 4.2 and 4.5; pages 109 and 116) thus, the biofilm growth must dominate the detachment. In this study, the effect of a higher nutrient load was predominant over a higher shear force effect: a higher crossflow velocity caused a stronger impact of biofilm formation on the measured process and biofilm parameters. Reducing the nutrient concentration of the feed water enabled the application of higher crossflow velocities without an increase in biofilm formation.

As in many studies before (Flemming et al., 1997; Griebe & Flemming, 1998; Flemming, 2002; Vrouwenvelder et al., 2009a; Vrouwenvelder et al., 2010b; Chen et al., 2013) biomass accumulation was related to the nutrient load (nutrient concentration and linear flow velocity). At a higher crossflow velocity the nutrient load in the filtration system was increased but the shear force was increased as well. In literature contradicting effects of high crossflow velocity on process and biofilm parameters have been reported. Vrouwenvelder et al. (2010) found the most biofilm accumulation at the highest crossflow velocity (0.245 m s^{-1}), while Li et al. (2012), Suwarno et al. (2012) and Radu et al. (2012) observed the lowest fouling at the highest crossflow velocity in NF and RO systems. Choi et al. (2005) observed the same effect in microfiltration and ultrafiltration systems.

In spiral-wound membrane elements, feed spacers are used to separate the membrane sheets. Furthermore they cause turbulences close to the membrane surface, thereby restricting membrane fouling and concentration polarization. A 31 mil spacer commonly applied in water treatment, was also used in this study. The obtained results showed that the impact of biofilm formation was increased by the presence of feed spacers, especially at high crossflow velocities which again increased the nutrient load in the system (Figure 4.5; page 116). At high nutrient conditions bacteria grow and produce a biofilm regardless of the turbulence caused by feed spacers. In literature it can be found that feed spacers reduce particulate fouling and scaling by causing additional turbulences in the feed channel (Radu et al., 2012; Suwarno et al., 2012). The convective mass transport which is created

by the turbulences caused by the feed spacer reduces concentration polarization. This effect is essential for nanofiltration and reverse osmosis membrane processes. The geometry of the feed spacer has an influence on the shear stress and the turbulences in the feed channel (Radu et al., 2010). Also fouling enhancing effects have been reported due to the presence of a feed spacer (Vrouwenvelder et al., 2009b) (section taken from Dreszer et al., 2014a).
The influence of biodegradable nutrient concentration, crossflow velocity, and feed spacer presence on the intrinsic hydraulic resistance of biofilms was successfully determined and compared to results from literature.

All objectives of this thesis were achieved and the hydraulic resistance of biofilms was measured under various operating conditions and related to membrane performance.

5.4 Use of new insights

This thesis showed that biofilm formation in membrane systems increased both the feed-channel pressure drop and transmembrane pressure drop (Figure 4.1; page 108). The hydraulic biofilm resistance was increased by a (i) higher biodegradable substrate load, (ii) higher permeate flux, (iii) higher cross flow velocity, and (iv) feed spacer presence (Figure 5.1). Therefore, low permeate flux and low crossflow operation, modified feed spacers or feed spacer-less membrane modules, and (of course) the limitation of nutrients is recommended in order to prevent that biofilms turn into biofouling.

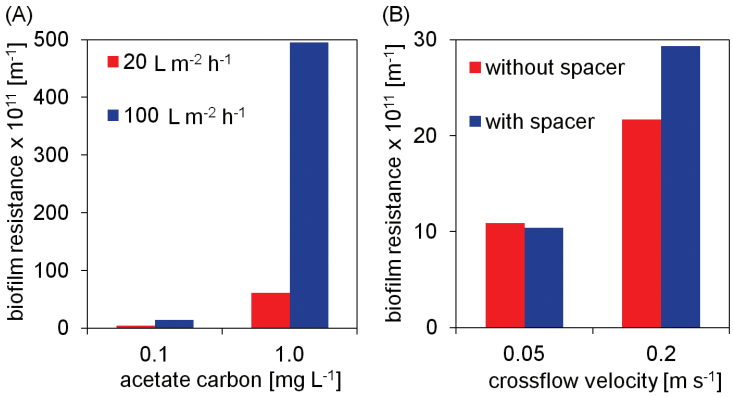

Figure 5.1: Biofilm resistance at average and high permeate flux and two different acetate carbon concentrations; the system was operated at a crossflow velocity of 0.1 m s^{-1} (A). Biofilm resistance at crossflow velocities of 0.05 and 0.2 m s^{-1} in the presence and absence of a feed spacer; the system was operated at an average permeate flux (20 L m^{-2} h^{-1}) (B).

5

An obvious approach in delaying biofilm development and even biofouling prevention is to reduce the concentration of biodegradable substrate in the water by pre-treatment. A large number of research papers (Flemming et al., 1997; Griebe & Flemming, 1998; Flemming, 2002; Vrouwenvelder et al., 2009a; Vrouwenvelder et al., 2010b; Chen et al., 2013) show that nutrient limitation lowers the biofouling rate. Pretreatment by biofiltration is a common approach (Chinu et al., 2009; Hallé et al., 2009; Mosqueda-Jimenez & Huck, 2009; Huck et al., 2011; Peldszus et al., 2012; Bar-Zeev et al., 2013).

In NF and RO membrane systems commonly applied permeate fluxes are about 15 to 20 L m^{-2} h^{-1}. Increasing the permeate flux has been proposed as an approach to reduce the footprint and production costs of the membrane installation (Mallevialle et al., 1996). The studies presented in this thesis clearly showed that a higher permeate flux caused a much higher biofilm resistance (e.g. Figure 3.4; page 79), suggesting that a higher flux will increase operation problems and costs. The impact of biofilm accumulation on membrane performance is reduced by lowering the flux. Thus, low flux operation can be preferred from a perspective of restricting the impact of biofouling and costs.

The studies presented in this thesis showed that performance losses were larger at a high crossflow velocity (due to an increased nutrient load caused by the higher crossflow velocity) and with feed spacer presence. In practice, most biofouling is observed in the lead membrane modules at the feed side of the membrane

installation (Baker, 2012d; Mallevialle et al., 1996). This location is characterized by a high crossflow velocity (~0.2 m s^{-1}) which was also applied in the monitor studies. A lower crossflow velocity and modified feed spacers could be an approach to reduce the impact of accumulated biomass on feed channel pressure drop in practice (Vrouwenvelder et al., 2009b, Araujo et al., 2012). Concentration polarization may be increased by the application of low crossflow velocity but reduced by a low permeate flux.

The experiments of this thesis showed that the intrinsic hydraulic resistance of biofilms is much lower than the resistance of a RO or NF membrane. Thus, hydraulic biofilm resistance alone is not responsible for performance losses in such membrane systems. It is rather the accompaniment of biofilms which leads to biofouling problems in NF/RO systems. Biofilm accumulation in a membrane system enhances the development of concentration polarization and increases the transmembrane osmotic pressure (Gutman et al., 2012; Herzberg, 2010; Radu et al., 2010; Chong et al., 2008; Herzberg & Elimelech, 2007). During crossflow filtration the accumulation of salt ions on the membrane surface is restricted by the crossflow velocity. The lack of crossflow velocity inside the biofilm and the hampered back diffusion of salt ions promote the accumulation of salts on the membrane surface within the biofilm (Figure 5.2); leading to concentration polarization, flux decline and membrane performance losses (Gutman et al., 2012; Herzberg, 2010; Radu et al., 2010; Chong et al., 2008; Herzberg & Elimelech, 2007). Flux decline can be caused by a reduced transmembrane driving force (as in the case of an increased transmembrane osmotic pressure) and also by decreased crossflow velocity (Vrouwenvelder et al., 2009c; Baker & Dudley, 1998). Biofilm development narrows the feed channel and therefore increases the feed channel pressure drop and decreases the crossflow velocity. The presence of biofilms inside filtration systems also increases the friction resistance in the feed channel which reduces the crossflow velocity as well. Biofilms do not have a smooth surface but a high variation in local biofilm thickness (see OCT observations in Figures 1.7 and 2.7; pages 24 and 54). This surface roughness of the biofilm increases the frictional drag which is directly related to performance losses (Andrewartha et al., 2010; Picologlou et al., 1980). The flow velocity in the feed channel causes a three-dimensional vibration of the biofilm which causes additional energy losses on the system (Andrewartha et al., 2010) This behavior can be related to the viscoelasticity of the EPS matrix (Flemming & Wingender, 2001).

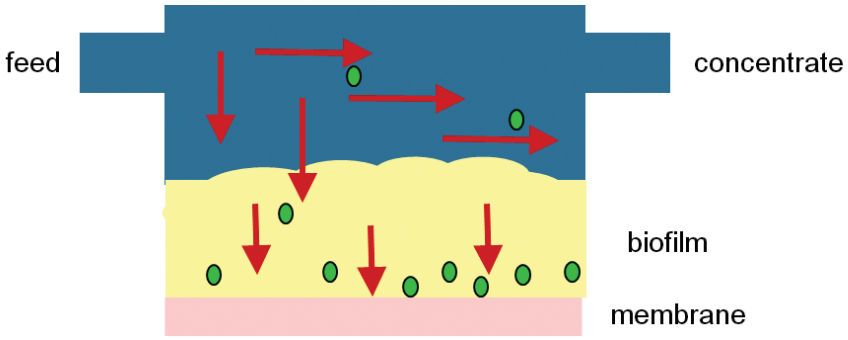

Figure 5.2: A membrane filtration system with biofilm accumulation. The different flow directions and accumulation of salts are indicated.

For obvious reasons it is desirable to keep the unavoidable biofilm accumulation as low as possible in a membrane filtration system. Besides the countermeasures mentioned above (low flux, low crossflow velocity, modified feed spacers, and nutrient limitation) the principle of biofilm management can be applied as well. Biofouling is an operational defined problem, as long as the biofilm accumulation stays below the threshold of interference it is possible to live with biofilms. Early warning system to detect biofilms in order to apply countermeasures and cleaning steps before the biofilm turns into biofouling as well as efficacy control of cleaning procedures, monitoring of relevant operational parameters, and limitation of access of microorganisms into the filtration system can help to manage the biofouling problem (Flemming, 2011; Flemming, 2002; Griebe & Flemming, 1998; Flemming .et al., 1997).

5.5 Recommendations for future research

This thesis showed that EPS presents the main reason for an increase in hydraulic biofilm resistance and not bacterial cells (Chapter 3). Based on this insight the preliminary and so far unsuccessful study of flux enhancer (section 1.5) could be resumed. The first part of this study should focus on the structure and bindings of the EPS, it should be determined which part of the EPS is responsible for the increase in hydraulic resistance. Is it the composition, binding forces, or the structure of the biopolymers of the EPS? After one or more targets have been defined the search for a flux enhancing substance can be reestablished. A quick screening of several substances can be performed in test tube experiments

for which a biofilm is transferred into a test tube and its reaction with the flux enhancer is observed visually. The most promising substances should be tested in the biofouling monitor at practice conditions.

The developed low pressure transparent membrane biofouling monitor has shown to be suitable for investigating the hydraulic resistance of biofilms without interference of other types of fouling and concentration polarization. A modified version of the monitor which can be operated a high pressure allowing the application of NF or RO membranes should be developed to study the impact of concentration polarization on biofouling development. It can be used to evaluate the hydraulic biofilm resistance, feed-channel pressure drop, transmembrane pressure drop and salt passage of NF and RO systems at varying conditions: (i) low and high feed pressure, (ii) with and without concentration polarization, (iii) various crossflow velocities, (iv) various fluxes and (v) various feed spacers designs. A modified feed spacer may reduce the impact of accumulated biofilm on membrane performance and may enable biomass removal from the membrane system by cleaning. Such studies will provide insight on the impact of biofilm formation and concentration polarization on biofouling and how this effect can be influenced.

The transparent sight window of the developed monitor enables to study *in-situ* spatially-resolved the biofilm thickness distribution and biofilm detachment over a large surface area as a function of flux distribution, and flux change in combination with membrane performance parameters. The compression of biofilms as a result of permeate flux increase can be targeted as well. Optical coherence tomography offers the possibility of generating 3D images without disruption of the flow velocities in a non-destructive manner. Such studies will increase the understanding of biofilm development and spatial variability and impact on performance.

All recommended studies should be carried out under well-controlled laboratory conditions and confirmed at full-scale NF and RO installations.

These recommended studies will help in understanding the biofilm phenomena better and help to target biofouling in membrane filtration systems.

References

Andrewartha, J., Perkins, K., Sargison, J., Osborn, J., Walker, G., Henderson, A., & Hallegraeff, G. (2010). Drag force and surface roughness measurements on freshwater biofouled surfaces. *Biofouling, 26(4),* 487-496.

Araújo, P. A., Kruithof, J. C., Van Loosdrecht, M. C. M., & Vrouwenvelder, J. S. (2012). The potential of standard and modified feed spacers for biofouling control. *Journal of Membrane Science, 403-404*(0), 58-70.

Baker, J. S., & Dudley, L. Y. (1998). Biofouling in membrane systems - A review. *Desalination, 118*(1-3), 81-89.

Baker, R. W. (2012a). Membrane Fouling Control *Membrane Technology and Applications* (3rd ed., pp. 231). West Sussex: John Wiley and Sons Ltd.

Baker, R. W. (2012b). Scale *Membrane Technology and Applications* (3rd ed., pp. 231-233). West Sussex: John Wiley and Sons Ltd.

Baker, R. W. (2012c). Silt *Membrane Technology and Applications* (3rd ed., pp. 233). West Sussex: John Wiley and Sons Ltd.

Baker, R. W. (2012d). Biofouling *Membrane Technology and Applications* (3rd ed., pp. 233). West Sussex: John Wiley and Sons Ltd.

Bar-Zeev, E., Belkin, N., Liberman, B., Berman-Frank, I., & Berman, T. (2013). Bioflocculation: Chemical free, pre-treatment technology for the desalination industry. *Water Research, 47*(9), 3093-3102.

Chen, X., Suwarno, S. R., Chong, T. H., McDougald, D., Kjelleberg, S., Cohen, Y., Fane, A. G., & Rice, S. A. (2013). Dynamics of biofilm formation under different nutrient levels and the effect on biofouling of a reverse osmosis membrane system. *Biofouling, 29(3), 319-330.*

Chinu, K. J., Johir, A. H., Vigneswaran, S., Shon, H. K., & Kandasamy, J. (2009). Biofilter as pretreatment to membrane based desalination: Evaluation in terms of fouling index. *Desalination, 247*(1-3), 77-84.

Choi, H., Zhang, K., Dionysiou, D. D., Oerther, D. B., & Sorial, G. A. (2005). Influence of cross-flow velocity on membrane performance during filtration of biological suspension. *Journal of Membrane Science, 248*(1-2), 189-199.

Chong, T. H., Wong, F. S., & Fane, A. G. (2008). The effect of imposed flux on biofouling in reverse osmosis: Role of concentration polarisation and biofilm enhanced osmotic pressure phenomena. *Journal of Membrane Science, 325*(2), 840-850.

Dreszer, C., Flemming, H. C., Zwijnenburg, A., Kruithof, J. C., & Vrouwenvelder, J. S. (2014a). Impact of biofilm accumulation on transmembrane and feed channel pressure drop: Effects of crossflow velocity, feed spacer and biodegradable nutrient. *Water Research, 50,* 200-211.

Dreszer, C., Flemming, H. C., Wexler, A. D., Zwijnenburg, A., Kruithof, J. C., & Vrouwenvelder, J. S. (2014b). Development and testing of a transparent membrane biofouling monitor. *Desalination and Water Treatment,* 52, 1807-1819.

Dreszer, C., Vrouwenvelder, J. S., Paulitsch-Fuchs, A. H., Zwijnenburg, A., Kruithof, J. C., & Flemming, H. C. (2013). Hydraulic resistance of biofilms. *Journal of Membrane Science, 429*(0), 436-447.

Flemming, H.C. (2011). Biofilm Highlights. *Microbial biofouling: Unsolved problems, insufficient approaches, and possible solutions*. Berlin Heidelberg. Springer Verlag

Flemming, H.-C., Tamachkiarowa, A., Klahre, J., & Schmitt, J. (1998). Monitoring of fouling and biofouling in technical systems. *Water Science and Technology, 38*(8-9), 291-298.

Flemming, H. C. (2002). Biofouling in water systems - Cases, causes and countermeasures. *Applied Microbiology and Biotechnology, 59*(6), 629-640.

Flemming, H. C., & Wingender, J. (2001). Relevance of microbial extracellular polymeric substances (EPSs) – Part II: Technical aspects. *Water Science and Technology, 43(6),* 9-16.

Flemming, H. C., Schaule, G., Griebe, T., Schmitt, J., & Tamachkiarowa, A. (1997). Biofouling - The Achilles heel of membrane processes. *Desalination, 113*(2-3), 215-225.

Gamal Khedr, M. (2000) Membrane fouling problems in reverse osmosis desalination applications. *Desalination & Water Reuse* 10(3), 8–17.

Griebe, T., & Flemming, H.-C. (1998). Biocide-free antifouling strategy to protect RO membranes from biofouling. *Desalination, 118*(1-3), 153-159.

Gutman, J., Fox, S., Gilron, J. (2012). Interactions between biofilms and NF/RO flux and their implications for control-A review of recent developments. *Jounal of Membrane Science*, 421-422, 1-7.

Hallé, C., Huck, P. M., Peldszus, S., Haberkamp, J., & Jekel, M. (2009). Assessing the performance of biological filtration as pretreatment to low pressure membranes for drinking water. *Environmental Science and Technology, 43*(10), 3878-3884.

Herzberg, M. (2010). Osmotic effects of biofouling in reverse osmosis (RO) processes: Physical and physiological measurements and mechanisms. *Desalination and Water Treatment, 15*(1-3), 287-291.

Herzberg, M., Kang, S. & Elimelech, M. (2009). Role of extracellular polymeric substances (EPS) in biofouling of reverse osmosis membranes. *Environmental Science and Technology, 43*(12), 4393-4398.

Herzberg, M., & Elimelech, M. (2007). Biofouling of reverse osmosis membranes: Role of biofilm-enhanced osmotic pressure. *Journal of Membrane Science, 295*(1-2), 11-20.

Huck, P. M., Peldszus, S., Halle, C., Ruiz, H., Jin, X., Van Dyke, M., Amy, G., Uhl, W., Theodoulou, M., & Mosqueda-Jimenez, D. B. (2011). Pilpt scale evaluation of biofiltration as an innovative pre-treatment for ultrafiltration membranes for drinking water treatment. *Water Science and Technology: Water Supply, 11(1), 23-29.*

Li, Z.-Y., Yangali-Quintanilla, V., Valladares-Linares, R., Li, Q., Zhan, T., & Amy, G. (2012). Flux patterns and membrane fouling propensity during desalination of seawater by forward osmosis. *Water Research, 46*(1), 195-204.

Mallevialle, J., Odendaal, P. E., & Wiesner, M. R. (1996). *Water Treatment Membrane Processes*. New York: Graw-Hill.

Mosqueda-Jimenez, D. B., & Huck, P. M. (2009). Effect of biofiltration as pretreatment on the fouling of nanofiltration membranes. *Desalination, 245*(1-3), 60-72.

Paul, D.H. (1991) Reverse osmosis: scaling, fouling and chemical attack. *Desalination & Water Reuse* 1, 8–11.

Peldszus, S., Benecke, J., Jekel, M., & Huck, P. M. (2012). Direct biofiltration pretreatment for fouling control of ultrafiltration membranes. *Journal - American Water Works Association, 104*(7), E430-E445.

Picologlou, B. F., Zelver, N., & Characklis, W. G. (1980). Biofilm growth and hydraulic performance. *Journal of Hydraulics Division, 106(5),* 733-746.

Radu, A. I., Vrouwenvelder, J. S., van Loosdrecht, M. C. M., & Picioreanu, C. (2012). Effect of flow velocity, substrate concentration and hydraulic cleaning on biofouling of reverse osmosis feed channels. *Chemical Engineering Journal, 188*, 30-39.

Radu, A.I., Vrouwenvelder, J.S., van Loosdrecht, M.C.M. & Picioreanu, C. (2010) Modeling the effect of biofilm formation on reverse osmosis performance: flux, feed channel pressure drop and solute passage. *Journal of Membrane Science* 365(1-2), 1-15.

Ridgway, H. F., Flemming, H. C. (1996). Biofouling of membranes. In J. Mallevialle, Odendaal, P. E., Wiesner, M. R. (Ed.), *Water treatment membrane processes* (pp. 629 - 640). New York: McGraw-Hill.

Ridgway, H. F., Kelly, A., Justice, C., & Olson, B. H. (1983). Microbial fouling of reverse-osmosis membranes used in advanced wastewater treatment technology: Chemical, bacteriological, and ultrastructural analyses. *Applied and Environmental Microbiology, 45*(3), 1066-1084.

Saeed, M. O., Jamaluddin, A. T., Tisan, I. A., Lawrence, D. A., Al-Amri, M. M., & Chida, K. (2000). Biofouling in a seawater reverse osmosis plant on the Red Sea coast, Saudi Arabia. *Desalination, 128*(2), 177-190.

Schneider, R. P., Ferreira, L. M., Binder, P., Bejarano, E. M., Góes, K. P., Slongo, E., . . . Rosa, G. M. Z. (2005). Dynamics of organic carbon and of bacterial populations in a conventional pretreatment train of a reverse osmosis unit experiencing severe biofouling. *Journal of Membrane Science, 266*(1-2), 18-29.

Shannon, M. A., Bohn, P. W., Elimelech, M., Georgiadis, J. G., Marinas, B. J., & Mayes, A. M. (2008). Science and technology for water purification in the coming decades. *Nature, 452*(7185), 301-310.

Strathmann, M., Mittenzwey, K.-H., Sinn, G., Papadakis, W., & Flemming, H.-C. Simultaneous monitoring of biofilm growth, microbial activity, and inorganic deposits on surfaces with an in situ, online, real-time, non-destructive, optical sensor. *Biofouling, 29*(5), 573-583.

Suwarno, S.R., Chen, X., Chong, T.H., Puspitasari, V.L., McDougald, D., Cohen, Y., Rice, S.A. & Fane, A.G. (2012) The impact of flux and spacers on biofilm development on reverse osmosis membranes. *Journal of Membrane Science* 405-406(0), 219-232.

Tasaka, K., Katsura, T., Iwahori, H., & Kamiyama, Y. (1994). Analysis of RO elements operated at more than 80 plants in Japan. *Desalination, 96*(1-3), 259-272.

Van Loosdrecht, M.C.M., Bereschenko, L.A., Radu, A.I., Kruithof, J.C., Picioreanu, C., Johns, M.L., & Vrouwenvelder, J.S. (2012) New approaches to characterizing and understanding biofouling od spiral wound membrane systems. *Water Science and Technology* 66(1), 88-94.

Vrouwenvelder, J. S., Buiter, J., Riviere, M., van der Meer, W. G. J., van Loosdrecht, M. C. M., & Kruithof, J. C. (2010a). Impact of flow regime on pressure drop increase and biomass accumulation and morphology in membrane systems. *Water Research, 44*(3), 689-702.

Vrouwenvelder, J. S., Beyer, F., Dahmani, K., Hasan, N., Galjaard, G., Kruithof, J. C., & Van Loosdrecht, M. C. M. (2010b). Phosphate limitation to control biofouling. *Water Research, 44*(11), 3454-3466.

Vrouwenvelder, J. S., Hinrichs, C., Van der Meer, W. G. J., Van Loosdrecht, M. C. M., & Kruithof, J. C. (2009a). Pressure drop increase by biofilm accumulation in spiral wound RO and NF membrane systems: role of substrate concentration, flow velocity, substrate load and flow direction. *Biofouling, 25*(6), 543-555.

Vrouwenvelder, J. S., Graf von der Schulenburg, D. A., Kruithof, J. C., Johns, M. L., & van Loosdrecht, M. C. M. (2009b). Biofouling of spiral-wound nanofiltration and reverse osmosis membranes: A feed spacer problem. *Water Research, 43*(3), 583-594.

Vrouwenvelder, J. S., van Paassen, J. A. M., Kruithof, J. C., & van Loosdrecht, M. C. M. (2009c). Sensitive pressure drop measurements of individual lead membrane elements for accurate early biofouling detection. *Journal of Membrane Science, 338*(1-2), 92-99.

Vrouwenvelder, J. S., van Paassen, J. A. M., Wessels, L. P., van Dam, A. F., & Bakker, S. M. (2006). The Membrane Fouling Simulator: A practical tool for fouling prediction and control. *Journal of Membrane Science, 281*(1-2), 316-324.

Winters, H., & Isquith, I. R. (1979). In-plant microfouling in desalination. *Desalination, 30*(1), 387-399.

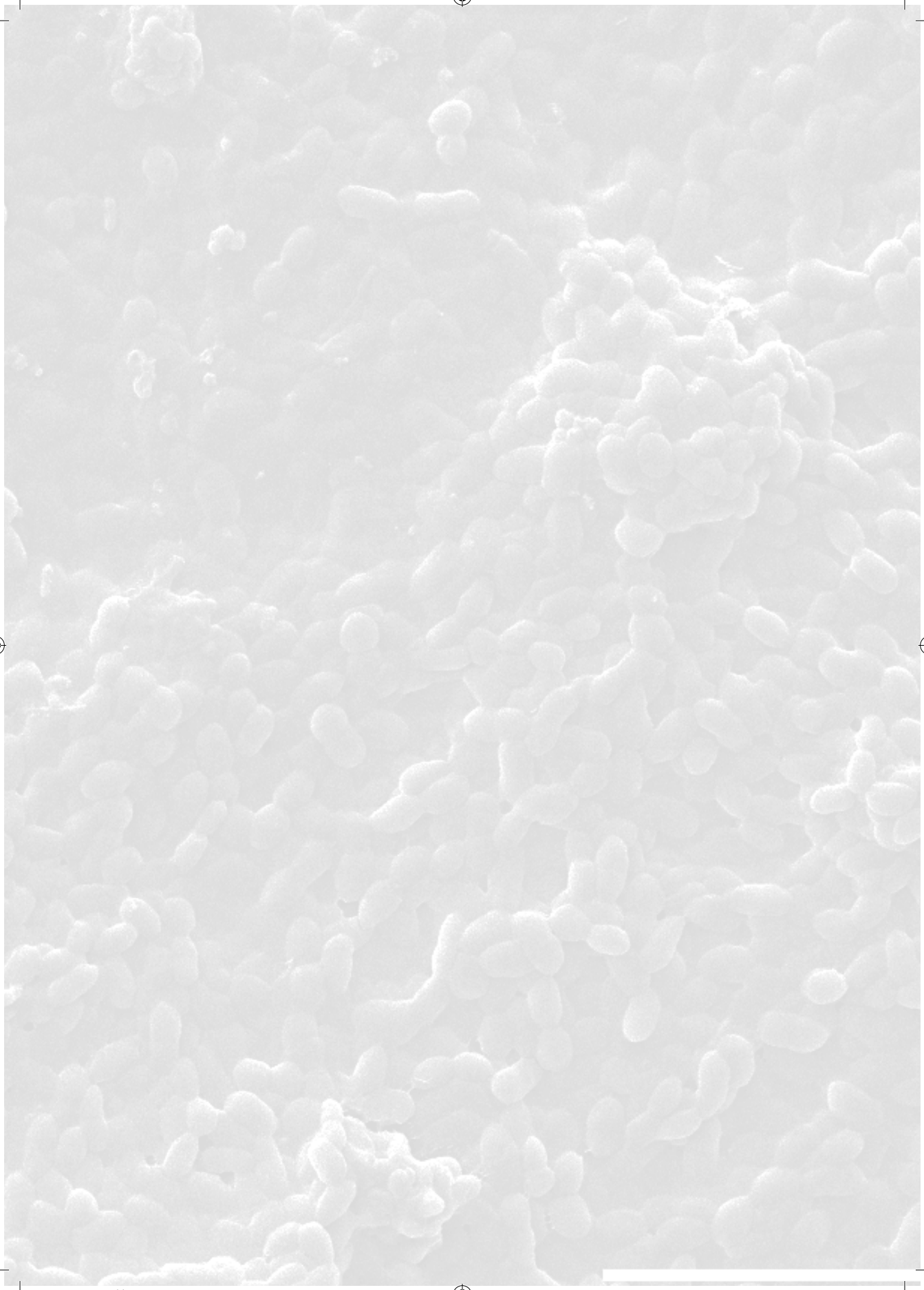

Abbreviations

Abbreviations

A	—	membrane area	(m^2)
BCA	—	bicinchoninic acid	(-)
CER	—	cationic exchange resin	(-)
CFU	—	colony forming units	(cells cm^{-2})
CFV	—	crossflow velocity	(m s^{-1})
CLSM	—	confocal laser scanning microscopy	(-)
dh	—	hydraulic diameter	(m)
EPS	—	extracellular polymeric substances	(-)
FCP	—	feed channel pressure drop	(bar)
J	—	permeate flux	(m^3 m^{-2} s^{-1}), (L m^{-2} h^{-1})
K	—	permeability	(L m^{-2} h^{-1} bar^{-1})
L	—	length	(m)
m	—	mass	(kg)
MBM	—	membrane biofouling monitor	(-)
MF	—	microfiltration	(-)
MFS	—	membrane fouling simulator	(-)
Mil	—	1 cm ¼ 0.00254 x mil	(mil)
NF	—	nanofiltration	(-)
OCT	—	optical coherence tomography	(-)
P	—	pressure	(bar)
P inlet	—	feed pressure	(bar)
P outlet	—	concentrate pressure	(bar)
P permeate	—	permeate pressure	(bar)
PBS	—	phosphate buffered saline	(-)
PES	—	polyethersulfone	(-)
PMMA	—	polymethylmethacrylate	(-)
R	—	resistance	(m^{-1})
Re	—	Reynolds number	(-)
RO	—	reverse osmosis	(-)
S	—	substrate	(-)
SEM	—	scanning electron microscopy	(-)
t	—	time	(h)
TCN	—	total cell number	(cells cm^{-2})
tMBM	—	transparent membrane biofouling monitor	(-)
TMP	—	transmembrane pressure drop	(bar)
TOC	—	total organic carbon	(mg cm^{-2})
UF	—	ultrafiltration	(-)
V	—	volume	(L)
η	—	dynamic viscosity	(Pa s)
λ	—	friction coefficient	(-)
v	—	linear velocity of water	(m s^{-1})
ρ	—	specific liquid density	(kg m^{-3})

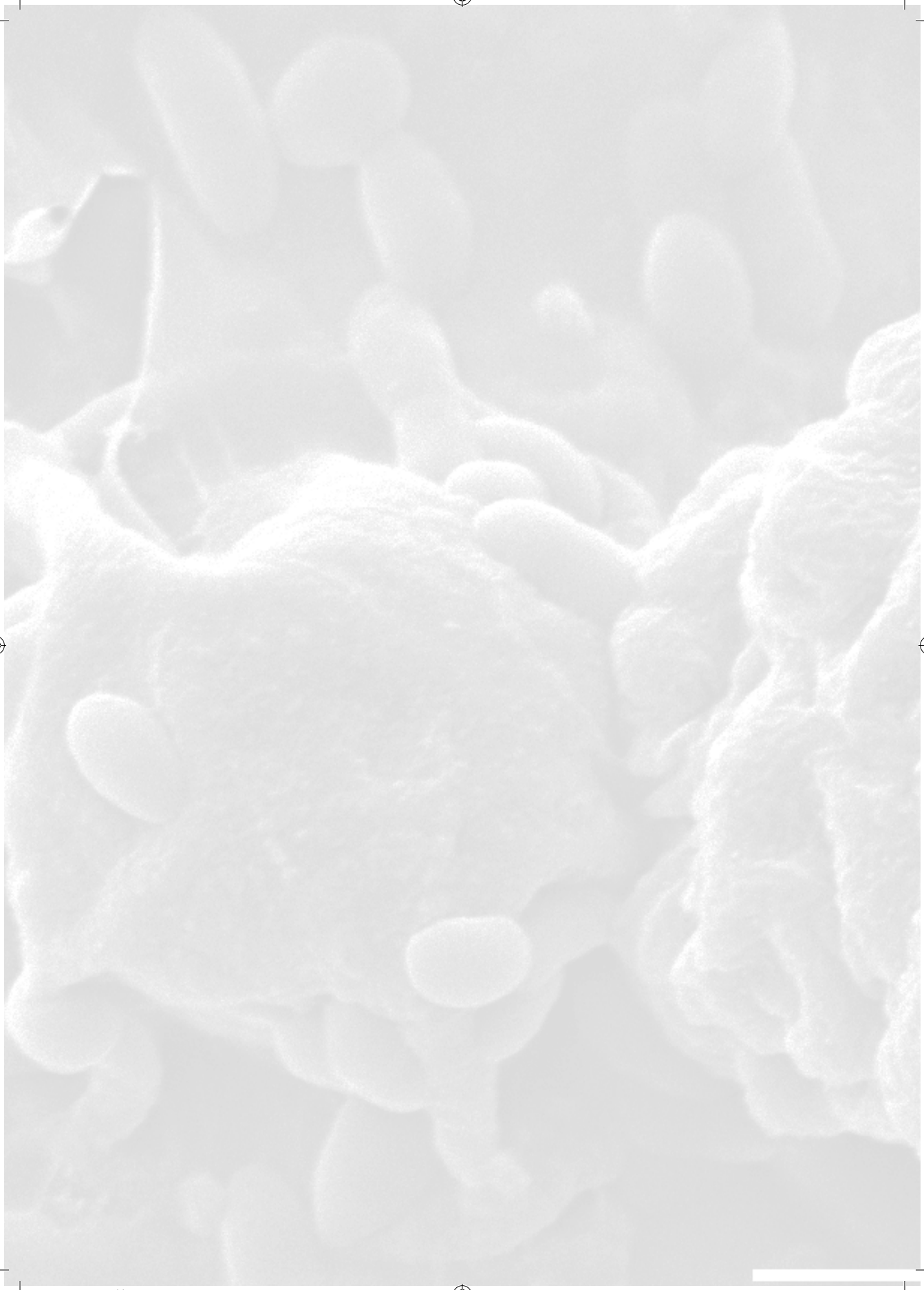

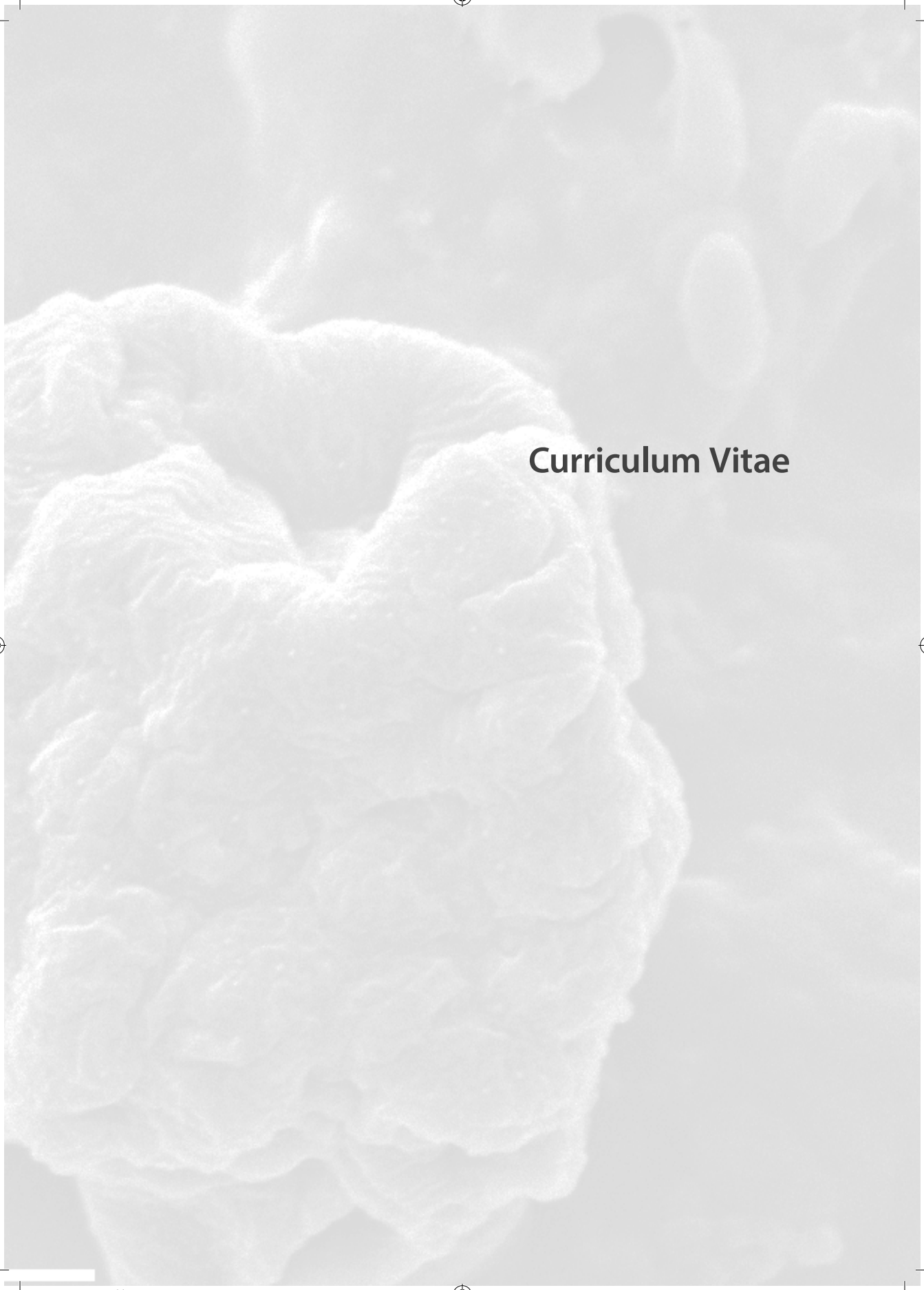

Curriculum Vitae

Claudia Dreszer was born in Bochum, Germany on April 6 1982. She graduated from high school in 2001 and started to study Environmental Engineering and Resource Management at the Ruhr-University Bochum, Germany in the same year. In 2003, after she heard about the quite new international study program 'Water Science' she switched universities and followed the water science course. She conducted her bachelor thesis at the Gulf Coast Research Laboratory, University of Southern Mississippi, USA in 2005. The topic of the thesis was 'Monitoring of Hydrology, Nutrients and Fecal Coliforms During Storm Events in the Back Bay of Biloxi, Mississippi, USA.' Her master thesis was conducted at the Marine Laboratory, University of Guam, USA in 2007. The topic of the thesis was 'Characterization of the Bacterial Community from the Marine Sponge Aplysinella rhax and Evaluation of its Antimicrobial Compounds Psammaplin A Sulfate and Psammaplin A.' In 2009 Claudia started her PhD work at Wetsus, centre of excellence for sustainable water technology within the biofouling theme in cooperation with the University Duisburg-Essen. The results and publications derived from this work are presented in this thesis.

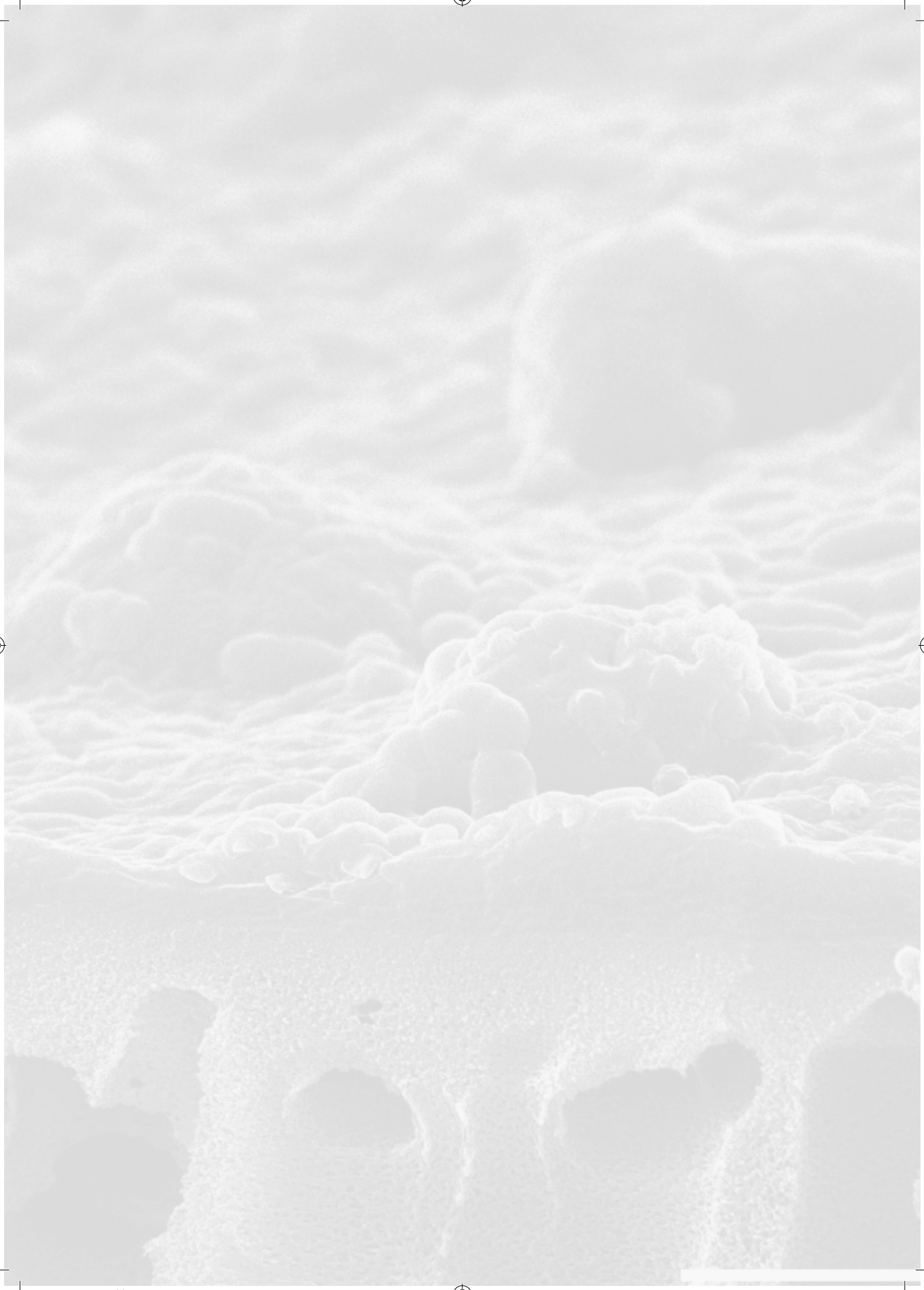

Publications

Publications

Dreszer, C., Flemming, H.-C., Zwijnenburg, A., Kruithof, J.C., Vrouwenvelder, J.S. (2014). Impact of biofilm accumulation on transmembrane and feed channel pressure drop: Effects of crossflow velocity, feed spacer and biodegradable nutrient. Water Research, Volume 50, Pages 200-211.

Dreszer, C., Flemming, H.-C., Wexler, A., Zwijnenburg, A., Kruithof, J.C., Vrouwenvelder, J.S. (2014). Development and testing of a transparent membrane biofouling monitor. Desalination and Water Treatment, Volume 52, Pages 1807-1819.

Dreszer, C., Vrouwenvelder, J.S., Paulitsch-Fuchs, A.H., Zwijnenburg, A., Kruithof, J.C., Flemming, H.-C. (2013). Hydraulic resistance of biofilms. Journal of Membrane Science, Volume 429, Pages 436-447

Dreszer, C., Vrouwenvelder, J.S., Paulitsch-Fuchs, A.H., Zwijnenburg, A., Kruithof, J.C., Flemming, H.-C. (2012). Hydraulic Biofilm Resistance. (Euromembrane conference abstract) Procedia Engineering, Volume 44, Pages 539-541

Conferences

Euromembrane 2012, London, UK, oral presentation 'Hydraulic Biofilm Resistance'

European Desalination Society 2012, Leeuwarden, The Netherlands, oral presentation 'Influence of various operational parameters on hydraulic biofilm resistance'

North American Membrane Society 2012, Louisiana, USA, oral presentation 'Influence of feed water, substrate concentration and permeate flux on biofilm resistance'

International Symposium on Membrane Biofouling 2010, Arizona, USA

Erklärung

Erklärung

Hiermit versichere ich, dass ich die vorliegende Arbeit mit dem Titel

„Hydraulic Resistance of Biofilms in Membrane Filtration Systems"

selbst verfasst und keine außer den angegebenen Hilfsmitteln und Quellen benutzt habe, und dass die Arbeit in dieser oder ähnlicher Form noch bei keiner anderen Universität eingereicht wurde.

Essen, Juni 2014

Claudia Dreszer

Acknowledgements

Acknowledgements

First and foremost I would like to thank my promoter and all my supervisors.
Thank you, Prof. Dr. Hans-Curt Flemming for advising me to apply for a PhD position at Wetsus and for being my promoter and supervising me along the way. Thank you very much Dr. Joop Kruithof and Prof. Dr. Hans Vrouwenvelder for your supervision, time and effort you spent while looking at data and correcting manuscripts. Thank you a lot Dr. Arie Zwijnenburg for your supervision and helping out in the experimental hall whenever the set up malfunctioned and for taking beautiful SEM pictures. Thank you very much Dr. Astrid Paulitsch-Fuchs for your supervision, always being there for me whenever problems occurred and teaching me new techniques in the lab.
I want to thank Cees Buisman and Johannes Boonstra for hosting my research at Wetsus, it is a great and innovative place.
Thank you to all my students: Zhen Xiang, Nathalie Juranek, Judita Laurinonyte, Malgorzata Nowak, Stanislaw Wojciechowski and Melvin Boelens. Your great support with the experimental work in the laboratory is highly acknowledged. I wish you all the best for your future career.
I would especially like to thank the Wetsus lab team for helping out wherever they can, analyzing samples and helping with building and fixing the set-up. Thank you for your great work.
I would like to thank all the PhD students of the Biofouling theme who accompanied me along the way. Florian Beyer (who is also very handy when it comes to rebuilding set-ups ;-)), Loreen Villacorte, Andrea Radu, Charu Chawla thanks for making the meetings interesting and fun.
I would also like to thank all my office mates, you made the time at Wetsus a lot of fun and go by very quickly: Philipp Kuntke, Luewton Lemos, Paula van de Brink, Lina Bachert, Nadine Boelee, Zlatica Novotna, Camile Janssen and Christina Kappel.
Thank you, Adam Wexler for your support and patience with the OCT work.
Thank you to everybody at Wetsus for making it such a special place.
NMR experiments with flow cells and artificial fouling layers were performed at Cambridge University, thank you to Dr. Mike Johns and Dr. Sarah Creber for their invitation and realization of the experiments. At the very beginning and the very end of this PhD work experiments on flux enhancer were conducted. I would like to thank Dr. Harry Ridgway for his input and ideas and Dr. Thomas Schwartz and Tanja Kleinschek for their supply of flux enhancer and knowledge on this topic.

Thanks to Wetsus and University Duisburg-Essen for making the whole PhD study possible.
Alexandra: Thank you, for always taking some extra time to read and check my manuscripts, for all the talks and laughs we had, for babysitting my dogs and for all the hours spent on horseback or carriage together.
Christina: Thank you, for making me feel at home far away from home. Thanks for all the nights we talked, all the photos you took and all the wine we drank. I do miss our lunch salad a lot.
Lena: Thank you, for always having an open ear for discussions about fouling and calculations but also for all the non-work related fun time spend. Meagan told me to say thank you as well.
Lina, Martina, Ingo, Phillip, Sandra: Thank you, for all the Dinners we had together, all the nice time spend and for always helping out when it was needed.

I am grateful to all my family and friends for their unconditional support and presence.
Norman, thank you for your love, patience and support and keeping up a long distance relationship for over 4 years. I am lucky to have you by my side.
Last but not least I would like to thank the two most important persons in my life: my mother and my grandmother. I am thankful and grateful for the support and love you spent and that you always believed in me throughout the whole way. Sadly my grandmother won´t be here to celebrate the finishing of the PhD with us. But I know you are watching from above.

Love,

Claudia

This work was performed in the cooperation framework of Wetsus, Centre of Excellence for Sustainable Water Technology (www.wetsus.nl). Wetsus is co-funded by the Dutch Ministry of Economic Affairs (IOP-TTI) and the Dutch Ministry of Infrastructure and the Environment, The European Community (European Fund for Regional Development and Seventh Framework Programme), Northern Netherlands Provinces (Peaks in the Delta), The City of Leeuwarden, the Province of Fryslân and University Campus Fryslân. The authors like to thank the participants of the research theme "Biofouling" for the fruitful discussions and their financial support.